



UNIVERSIDADE FEDERAL DE SANTA CATARINA
CENTRO TECNOLÓGICO
PROGRAMA DE PÓS-GRADUAÇÃO EM ENGENHARIA QUÍMICA

Davi Gustavo Lisboa Girardi

**High pressure phase equilibrium of the system containing carbon dioxide,
chloroform and globalide, and characterization of thermodynamic properties of
 ϵ -caprolactone, globalide and ω -pentadecalactone**

FLORIANÓPOLIS

2022

Davi Gustavo Lisboa Girardi

**High pressure phase equilibrium of the system containing carbon dioxide,
chloroform, and globalide, and characterization of thermodynamic properties
of ϵ -caprolactone, globalide and ω -pentadecalactone**

Dissertação submetida ao Programa de Pós-Graduação em Engenharia Química da Universidade Federal de Santa Catarina como requisito parcial para a obtenção do título de Mestre em Engenharia Química.

Orientador: Prof. Dr. José Vladimir de Oliveira
Coorientador: Dr. Evertan Antonio Rebelatto

Florianópolis

2022

Ficha de identificação da obra elaborada pelo autor,
através do Programa de Geração Automática da Biblioteca Universitária da UFSC.

Girardi, Davi Gustavo Lisboa

High pressure phase equilibrium of the system containing carbon dioxide, chloroform and globalide, and characterization of thermodynamic properties of γ -caprolactone, globalide and γ -pentadecalactone / Davi Gustavo Lisboa Girardi ; orientador, José Vladimir de Oliveira, coorientador, Evertan Antonio Rebelatto, 2022.

99 p.

Dissertação (mestrado) - Universidade Federal de Santa Catarina, Centro Tecnológico, Programa de Pós-Graduação em Engenharia Química, Florianópolis, 2022.

Inclui referências.

1. Engenharia Química. 2. Lactonas. 3. Equilíbrio de fases. 4. Fluidos supercríticos. 5. Pressão de vapor. I. Oliveira, José Vladimir de. II. Rebelatto, Evertan Antonio. III. Universidade Federal de Santa Catarina. Programa de Pós-Graduação em Engenharia Química. IV. Título.

Davi Gustavo Lisboa Girardi

**High pressure phase equilibrium of the system containing carbon dioxide,
chloroform and globalide, and characterization of thermodynamic properties of
 ϵ -caprolactone, globalide and ω -pentadecalactone**

O presente trabalho em nível de mestrado foi avaliado e aprovado, em 12 de dezembro de 2022 pela banca examinadora composta pelos seguintes membros:

Prof. Dr. José Vladimir de Oliveira
Presidente
Universidade Federal de Santa Catarina

Prof. Dr. Cristiano José de Andrade
Universidade Federal de Santa Catarina

Prof. Dr. Marcos Lúcio Corazza
Universidade Federal do Paraná

Certificamos que esta é a versão original e final do trabalho de conclusão que foi julgado adequado para obtenção do título de Mestre em Engenharia Química

Insira neste espaço a
assinatura digital

Coordenação do Programa de Pós-Graduação

Insira neste espaço a
assinatura digital

Prof. Dr. José Vladimir de Oliveira
Orientador

Florianópolis, 2022.

Este trabalho é dedicado a meus queridos avós, Antônio, Dino, Eunice e
Maria Therezinha.

AGRADECIMENTOS

Agradeço à minha família, em especial a meus pais, Fernando e Patrícia, por todo apoio, carinho e instrução que me deram, ao meu irmão Paulo, pela amizade que sempre tivemos nessa jornada que é a vida, e aos meus avós, Antônio, Dino, Eunice e Maria Terezinha, por todo exemplo e respeito que me ensinaram.

Aos meus orientadores, Prof. José Vladimir de Oliveira e Dr. Evertan Antonio Rebelatto, pela confiança, orientação, ensinamentos e oportunidades que me proporcionaram. Como também pela amizade e pelas boas músicas compartilhadas.

Ao colega e amigo Diego Alex Mayer, por todos os aprendizados e sugestões, e por todo apoio e paciência na realização deste trabalho.

Ao professor Papa Matar Ndiaye e à Camila Guindani, por me receberem com carinho e me apoiarem enquanto trabalhei nas instalações da UFRJ.

À toda equipe do LATESC/UFSC e do ATOMS/UFRJ, pela amizade e pelos momentos compartilhados. Em especial ao professor Marcelo Lanza pela confiança em mim depositada desde minha iniciação científica, e aos alunos de iniciação científica Aurora Lorini Letsch, Marcos Antônio Castiani e Thomas Philip Starucka, pela amizade, paciência e dedicação.

A todos os professores do departamento de Engenharia Química e Engenharia de Alimentos da UFSC. Especialmente a Adriano da Silva, Débora de Oliveira, Hugo Moreira Soares e Sergio Yesid Gómez González, não apenas pelos aprendizados e pela contribuição profissional, mas também pela amizade e pelas boas conversas em frente ao departamento.

Aos demais representantes discentes da Pós-Graduação em Engenharia Química, pela parceria e por todas as conquistas que alcançamos juntos.

Aos meus amigos mais próximos, Anelita Danetti, Bucky Anselmo Lencina, Eliana Weiss, Eric Junkes e Gabriel Gonçalves Mota, por todos os momentos, risadas e apoio em geral.

Aos diversos grupos de RPG, pelos momentos de descontração e pelas aventuras compartilhadas nas tardes de sábado e domingo.

Ao professor de arquearia Otávio de Azevedo, pelas instruções, amizade e conversas sobre músicas e pesquisa científica.

Ao professor de teatro Edécio Philippi, carinhosamente Deco, por todo apoio, confiança e mentoria de vida que pude receber junto ao NUCCA.

E a todos os demais que contribuíram de alguma forma e torceram por mim para a realização deste trabalho.

“I don’t know what I may seem to the world; but as to myself, I seem to have been only like a boy playing on the sea-shore, and diverting myself in now and then finding a smoother pebble or a prettier shell than ordinary, whilst the great ocean of truth lay all undiscovered before me.”
(Isaac Newton, 1727, apud SPENCE J., 1820, p. 158)

RESUMO

Globalide é uma macrolactona insaturada usada como fragrância em uma variedade de produtos de limpeza e cosméticos, bem como monômero na síntese de polímero e copolímeros biodegradáveis e biocompatíveis altamente funcionalizáveis. O produto polimérico pode ser obtido através da polimerização de abertura de anel de globalide em dióxido de carbono supercrítico. Para realizar essa reação de forma eficiente, é importante entender como as condições termodinâmicas do sistema, como temperatura, pressão e composição, afetam a miscibilidade dos componentes. Além disso, o efeito da adição de um cossolvente também é necessário, pois altera a pressão de transição de fase da mistura. Portanto, um objetivo deste trabalho é investigar o comportamento de fase do sistema ternário contendo dióxido de carbono, globalide e clorofórmio em diferentes proporções de massa de globalide para clorofórmio. Os experimentos foram conduzidos em uma célula de visualização de volume variável de alta pressão usando o método sintético-visual em uma faixa de temperatura de 313,15 a 343,15 K. Equilíbrio líquido-vapor com transição de ponto de bolha e com transição de ponto de orvalho, equilíbrio líquido-líquido e equilíbrio líquido-líquido-vapor foram observados em uma faixa de pressão de 5,17 a 20,25 MPa. Os resultados experimentais foram representados satisfatoriamente pela equação de estado de Peng-Robinson. Além disso, o clorofórmio mostrou ser um cossolvente eficaz para o sistema ternário, pois altas frações diminuíram a pressão de transição. Ademais, dados experimentais de pressão de vapor para globalide e duas outras lactonas, ϵ -caprolactona e ω -pentadecalactona, foram estudados em temperaturas de 297,8 a 333,7 K com boa repetibilidade e reprodutibilidade. Os resultados coletados foram usados para estimar os parâmetros de correlação de Antoine e os parâmetros de componentes puros da equação de estado PC-SAFT. Os dados apresentados neste trabalho são importantes para determinar as condições iniciais ótimas para a polimerização da globalide em altas pressões e são essenciais para a simulação, projeto e controle de sistemas contendo ϵ -caprolactona, ω -pentadecalactona e globalide.

Palavras-chave: Lactonas, Equilíbrio de fases, Fluidos supercríticos, Pressão de vapor.

RESUMO EXPANDIDO

Introdução

Globalide é uma macrolactona insaturada usada como fragrância em uma variedade de produtos de limpeza e cosméticos, bem como monômero na síntese de polímero e copolímeros biodegradáveis e biocompatíveis altamente funcionalizáveis. O produto polimérico pode ser obtido através da polimerização de abertura de anel de globalide em dióxido de carbono supercrítico. Para realizar essa reação de forma eficiente, é importante entender como as condições termodinâmicas do sistema, como temperatura, pressão e composição, afetam a miscibilidade dos componentes. Além disso, o efeito da adição de um cossolvente também é necessário, pois altera a pressão de transição de fase da mistura. Na literatura, encontram-se dados de equilíbrio de fases para o sistema binário contendo dióxido de carbono e globalide, e para o sistema ternário contendo dióxido de carbono, globalide e diclorometano. Entretanto, não existem trabalhos que estudam o comportamento de fases para o sistema ternário contendo dióxido de carbono, globalide e clorofórmio, enquanto para outras lactonas, como a ϵ -caprolactona e a ω -pentadecalactona, sistemas ternários contendo diclorometano ou clorofórmio como cossolvente já foram investigados. Ademais, para que a realização da simulação, do projeto e da operação de processos contendo ϵ -caprolactona, ω -pentadecalactona, ou globalide obtenha respostas significativas, é preciso que modelos termodinâmicos sejam capazes de descrever adequadamente os fenômenos. Dentre estes modelos, a equação de estado PC-SAFT é utilizada de modo satisfatório para sistemas contendo polímeros e necessita de parâmetros de componente puros, que podem ser calculados a partir de dados de pressão de vapor.

Objetivos

O objetivo deste trabalho é investigar o comportamento de fases do sistema ternário contendo dióxido de carbono, globalide e clorofórmio a altas pressões, além de estudar a pressão de vapor de globalide, ϵ -caprolactona e ω -pentadecalactona.

Metodologia

Para os dados de equilíbrio de fases, dióxido de carbono (0,999 fração de pureza em fase líquida) foi adquirido da White Martins S.A. (Brasil), clorofórmio (0,998 pureza da fração mássica) foi fornecido pela NEON (Brasil) e globalide foi adquirida da Symrise (Brasil). Para atingir o teor de água em fração mássica de 0,0032 com incerteza padrão de 0,0001, o monômero foi seco em estufa a vácuo a 373,15 K e 0,01 MPa durante 48 h e sua quantidade de água foi medida pelo Titulador Coulométrico Karl Fischer (HI-904 – HANNA). Para determinar a ocorrência de uma transição de fase, o método sintético-visual foi empregado durante a observação através de uma célula de visualização de volume variável de alta pressão. Este método consiste na observação visual de transições de fase em uma mistura com uma composição conhecida e precisa. Após a inserção dos componentes líquidos, a célula montada é conectada à aparelhagem de alta pressão e dióxido de carbono é inserido a pressão e temperatura constante de 10,0 MPa e 280,15 K. Para cada composição diferente, o comportamento das fases foi determinado sob temperaturas fixas de 313,15, 323,15, 333,15 e 343,15 K. Nessas condições, o sistema foi homogeneizado por aumentos de pressão e por agitação magnética, obtendo uma única fase. A partir daí, o sistema é exposto a um pequeno gradiente de pressão negativa, mantendo uma temperatura constante, de modo que uma transição de fase pudesse ser visualizada na iminência

de seu aparecimento. A pressão de transição foi observada em triplicata para cada temperatura e composição. A metodologia apresentada até então discute sobre o experimento de equilíbrio de fases. Já para os dados de pressão de vapor, ϵ -caprolactona e ω -pentadecalactona, ambas com pureza de fração de massa de 0,970, foram adquiridas da Sigma-Aldrich e globalide, com pureza de fração de massa de 0,998, foi fornecido pela Symrise. Além disso, o decano usado para verificar a precisão do procedimento experimental foi adquirido da Sigma-Aldrich. Os materiais foram usados sem purificação adicional, pois a desgaseificação da amostra é uma etapa do método. Cada medição foi realizada expondo ambas as entradas do transdutor de pressão ao vácuo, em seguida apenas uma das entradas se mantém sob vácuo, enquanto a outra fica sob a pressão de vapor da amostra. Este procedimento foi repetido três vezes com dez minutos entre cada medida para garantir a repetibilidade.

Resultados e Discussão

Para os dados experimentais de transição de fase dos sistemas na proporção mássica de globalide para clorofórmio de 0,5:1, 1:1 e 2:1 foram observadas transições de fases na faixa de temperatura de 313,15 a 343,15 K e pressões de 5,17 a 20,25 MPa. Para o equilíbrio líquido-vapor, tanto o ponto de bolha quanto o ponto de orvalho foram observados em condições distintas de pressão e de temperatura, enquanto os equilíbrio líquido-líquido e líquido-líquido-vapor foram relatados em diferentes pressões para a mesma composição e temperatura. Na proporção de 0,5:1 encontram-se maiores concentrações de cosolventes, o que leva a menores pressões de transição, pois o clorofórmio promove a solubilização do meio. Já para a proporção mássica de globalide para clorofórmio de 1:1, o aumento da fração globalide, quando comparado com a concentração anterior, causa um aumento na pressão. Em seguida, devido à baixa concentração de cosolvente na proporção de massa de globalide para clorofórmio de 2:1, as pressões de transição nessas composições são as mais altas coletadas, atingindo valores de até 20,25 MPa. Também é notável uma maior imiscibilidade entre as fases líquidas, pois as transições de equilíbrio líquido-líquido abrangem uma faixa mais ampla de concentrações. O modelo de Peng-Robinson com regra de mistura quadrática de van der Waals foi usado, para cada razão de massa distinta (0,5:1, 1:1 e 2:1), para estimar os parâmetros de interação binária k_{ij} e l_{ij} . O desempenho positivo destes cálculos pode ser verificado, através da visualização gráfica e pelos baixos valores dos parâmetros ajustados. Para todas as composições se observou o comportamento LCST (*Lower Critical Solution Temperature*), uma vez que se verifica o aumento da pressão para atingir um meio monofásico à medida que a temperatura é elevada. Além do apresentado, se observou que, para os dados experimentais de pressão de vapor, a precisão do procedimento experimental foi verificada pela medição da pressão de vapor do decano e pela comparação com dados da literatura, com correlação positiva. A boa repetibilidade foi alcançada conduzindo os experimentos em triplicata e uma reprodutibilidade positiva foi estabelecida conduzindo o experimento para três diferentes amostras preparadas de ϵ -caprolactona a 318,15 K. Com os dados experimentais, os parâmetros de correlação de Antoine foram calculados e, por fim, os parâmetros PC-SAFT foram calculados para os componentes puros.

Considerações Finais

Os dados apresentados neste trabalho são inéditos e importantes para determinar as condições iniciais ótimas para a polimerização da globalide em altas pressões e são

essenciais para a simulação, projeto e controle de sistemas contendo ϵ -caprolactona, ω -pentadecalactona e globalide.

Palavras-chave: Lactonas, Equilíbrio de fases, Fluidos supercríticos, Pressão de vapor.

ABSTRACT

Globalide is an unsaturated macrolactone used as a fragrance in a variety of cleaning and cosmetic products, as well as a monomer in the synthesis of highly functionalizable biodegradable and biocompatible polymer and copolymers. The polymeric product can be achieved through the ring-opening polymerization of globalide in supercritical carbon dioxide. In order to perform this reaction efficiently, it is important to understand how the thermodynamic conditions of the system, such as temperature, pressure and composition, affect the miscibility of the components. Furthermore, the effect of adding a cosolvent is also necessary as it changes the phase transition pressure of the mixture. Therefore, an objective of this work is to investigate the phase behavior of the ternary system containing carbon dioxide, globalide, and chloroform at different globalide to chloroform mass ratios. The experiments were conducted in a high pressure variable-volume view cell using the synthetic-visual method at a temperature range of 313.15 to 343.15 K. Vapor-liquid equilibrium with bubble point transition and with dew point transition, liquid-liquid equilibrium, and vapor-liquid-liquid equilibrium were observed at a pressure range of 5.17 to 20.25 MPa. The experimental results were satisfactorily represented by the Peng-Robinson equation of state. Moreover, chloroform has shown to be an effective cosolvent for the ternary system, as high fractions of it decreased the transition pressure. In addition, experimental vapor pressure data of globalide, and two other lactones, ϵ -caprolactone and ω -pentadecalactone, were studied at temperatures of 297.8 to 333.7 K with good repeatability and reproducibility. The collected results were used to estimate Antoine correlation parameters and the pure components parameters for the PC-SAFT equation of state. The data presented in this work are important to determine optimal initial conditions for polymerization of globalide at high pressure and are essential for the simulation, design, and control of systems containing ϵ -caprolactone, ω -pentadecalactone, and globalide.

Keywords: Lactones, Phase equilibrium, Supercritical fluids, Vapor pressure.

LIST OF FIGURES

Figure 1 – Classification of lactones.....	20
Figure 2 – Lactones and their derivatives applications in industrial processes	22
Figure 3 - ϵ -Caprolactone molecular structure.....	25
Figure 4 – Molecular structure of the repeating pattern of poly(ϵ -caprolactone).....	25
Figure 5 - ω -Pentadecalactone molecular structure.....	26
Figure 6 - Molecular structure of the repeating pattern of poly(ω -pentadecalactone).	27
Figure 7 – Globalide molecular structure.....	28
Figure 8 - Molecular structure of the repeating pattern of poly(globalide).	29
Figure 9 - A PT-diagram for a generic pure substance.....	30
Figure 10 – Two-dimensions VLE diagrams.....	33
Figure 11 – Three-dimensions VLE diagrams.	33
Figure 12 – Pxy-diagram for multiple isotherms.	34
Figure 13 – Retrograde condensation.	34
Figure 14 – Tx-diagram for liquid-liquid equilibrium.....	35
Figure 15- Pxy-diagram for binary mixtures with VLLE occurrence.....	37
Figure 16 - Classification of high-pressure phase equilibrium experimental methods.	38
Figure 17 - Procedure to form a molecule in SAFT-framework.	43
Figure 18 – High-pressure phase equilibrium apparatus.....	53
Figure 19 – Apparatus' valves.....	54
Figure 20 – Unassembled equilibrium cell.....	54
Figure 21- Synthetic-visual method.....	55
Figure 22 - Pressure - mass composition diagram for the system [CO ₂ (1) + GL (2) + CHCL ₃ (3)], in chloroform free-basis, at globalide to chloroform mass ratio of 0.5:1. 64	
Figure 23 - Pressure - mass composition diagram for the system [CO ₂ (1) + GL (2) + CHCL ₃ (3)], in chloroform free-basis, at globalide to chloroform mass ratio of 1:1. ...	65
Figure 24 - Pressure - mass composition diagram for the system [CO ₂ (1) + GL (2) + CHCL ₃ (3)], in chloroform free-basis, at globalide to chloroform mass ratio of 2:1. ...	66
Figure 25 – PT-diagram for the system [CO ₂ (1) + GL (2) + CHCL ₃ (3)], in chloroform free-basis, at globalide to chloroform mass ratio of 0.5:1.	68

Figure 26 – PT-diagram for the system [CO ₂ (1) + GL (2) + CHCl ₃ (3)], in chloroform free-basis, at globalide to chloroform mass ratio of 1:1.	68
Figure 27 – PT-diagram for the system [CO ₂ (1) + GL (2) + CHCl ₃ (3)], in chloroform free-basis, at globalide to chloroform mass ratio of 2:1.	69
Figure 28 – Pw'-diagram at 313.15 for the comparison between the ternary system [CO ₂ (1) + GL (2) + CHCl ₃ (3)], in chloroform free-basis, the pseudobinary system [CO ₂ (1) + GL (2)], and the binary system [CO ₂ (1) + CHCl ₃ (2)]......	70
Figure 29 - Pw'-diagram at 323.15 for the comparison between the ternary system [CO ₂ (1) + GL (2) + CHCl ₃ (3)], in chloroform free-basis, the pseudobinary system [CO ₂ (1) + GL (2)], and the binary system [CO ₂ (1) + CHCl ₃ (2)]......	70
Figure 30 – Pw'-diagram at 333.15 for the comparison between the ternary system [CO ₂ (1) + GL (2) + CHCl ₃ (3)], in chloroform free-basis, the pseudobinary system [CO ₂ (1) + GL (2)], and the binary system [CO ₂ (1) + CHCl ₃ (2)]......	71
Figure 31 – Pw'-diagram at 343.15 for the comparison between the ternary system [CO ₂ (1) + GL (2) + CHCl ₃ (3)], in chloroform free-basis, and the pseudobinary system [CO ₂ (1) + GL (2)]......	71
Figure 32 - Vapor pressure apparatus scheme.	75
Figure 33 - Vapor pressure of decane comparison with literature.	78
Figure 34 - Vapor pressure of ε-caprolactone and comparison with literature.....	80
Figure 35 - Vapor pressure of ω-pentadecalactone and comparison with literature..	81
Figure 36 - Vapor pressure of globalide and comparison with literature.....	81
Figure 37 - Experimental vapor pressure of ε-caprolactone and calculated vapor pressure with PC-SAFT.....	82
Figure 38- Experimental vapor pressure of ω-pentadecalactone and calculated vapor pressure with PC-SAFT.....	82
Figure 39 - Experimental vapor pressure of globalide and calculated vapor pressure with PC-SAFT.....	83

LIST OF TABLES

Table 1 – Parameters of cubic EoS.....	41
Table 2- Universal model constants in PC-SAFT EoS.	45
Table 3- Overview of the existing works in the literature about phase equilibrium data of ϵ -caprolactone, ω -pentadecalactone, globalide, chloroform, and dichloromethane in high pressures.....	47
Table 4 - Chemical name, molecular formula, provenance, purification method and purity of the materials.	52
Table 5 - Characteristics of pure compounds.....	57
Table 6 - Cosolvent free-basis mass fractions and overall mass fraction.	59
Table 7- Phase equilibrium results for the system [CO ₂ (1) + GL (2) + CHCL ₃ (3)], in chloroform free-basis, at globalide to chloroform mass ratio of 0.5:1.	60
Table 8 - Phase equilibrium results for the system [CO ₂ (1) + GL (2) + CHCL ₃ (3)], in chloroform free-basis, at globalide to chloroform mass ratio of 1:1.	61
Table 9 - Phase equilibrium results for the system [CO ₂ (1) + GL (2) + CHCL ₃ (3)], in chloroform free-basis, at globalide to chloroform mass ratio of 2:1.	62
Table 10 – Estimated binary interaction parameters.	67
Table 11 - Chemical name, molecular formula, provenance, purification method and purity of the materials.	75
Table 12 - Experimental vapor pressure data for decane, ϵ -caprolactone, ω -pentadecalactone, and globalide.....	78
Table 13 - Constants for the Antoine Equation.....	79
Table 14 - Characteristics of pure compounds for PC-SAFT calculated from the collected vapor pressure data.	83

LIST OF ABBREVIATIONS AND SYMBOLS

a^{assoc}	Helmholtz energy association contribution
a^{chain}	Helmholtz energy chain formation contribution
a^{disp}	Helmholtz energy dispersion contribution
a^{hs}	Helmholtz energy hard-sphere reference
a^{res}	Residual Helmholtz energy
a^{seg}	Helmholtz energy of the segment
$a(T)$	Attraction term
AD	Absolute deviation
APACT	Associated Perturbed Anisotropic Chain Theory
b	Repulsion term
CALB	<i>Candida Antarctica Lipase B</i>
CAS	Chemical Abstracts Service
CO ₂	Carbon dioxide
CPA	Cubic Plus Association
d_{ij}	Temperature-dependent diameter
EC	Equilibrium cell
EoS	Equation of State
eROP	Enzymatic
ESD	Elliot-Suresh-Donohue
e.g.	Exempla given
F	Number of degrees of freedom
g_{ij}	Radial distribution function
GL	Globalide
i	indicates the first substance
j	indicates the second substance
k_{ij}	Attraction binary interaction parameters
l_{ij}	Repulsion binary interaction parameters
m_i	Number of segments in a molecule
LCST	Lower critical solution temperature
LLE	Liquid-liquid equilibrium
LS	Light source

M_i	Number of association sites on molecule i
MS	Magnetic stirrer
N	Number of componentes
n	Number of components in the mixture
$noobs$	Number of experimental observations
OF	Objective function
P	Pressure
P_c	Critical Pressure
PC-SAFT	Perturbed Chain Statistical Associating Fluid Theory
PI	Pressure Indicator
PR	Peng-Robinson
PT	Pressure Transducer
R	Ideal gas constant
RB	Recirculation bath
RK	Redlich-Kwong
$rmsd$	root-mean-square-deviation
ROP	Ring-Opening Polymerization
SAFT	Statistical Associating Fluid Theory
sd	Standard deviation
SP	Syringe Pump
SR	Solvent reservoir
SRK	Soave-Redlich-Kwong
T	Temperature
TC	Thermocouple
T_c	Critical Temperature
TI	Temperature indicator
T_r	Reduced Temperature
UCST	Upper critical solution temperature
v	Molar volume
vdW	van der Waals
vdW2	van der Waals quadratic mixing rule
VLE	Vapor-liquid equilibrium
VLE-BP	Vapor-liquid equilibrium bubble point

VLE-DP	Vapor-liquid equilibrium dew point
VLLE	Vapor-liquid-liquid equilibrium
w_1	Mass fraction
w'_1	Mass fraction at cosolvent free-basis
X^{A_i}	Fraction of molecules i not bonded at site A
x_1	Molar liquid fraction
y_1	Molar vapor fraction
$\Delta^{A_i B_j}$	Association strength between two sites A and B from molecules i and j .
$\epsilon^{A_i B_i}$	Energy of association
ϵ -CL	ϵ -Caprolactone
ϵ_i/k	Segment energy
$\kappa^{A_i B_j}$	Volume of association
π	Number of phases
ρ_j	Molar density of j
σ_i	Segment diameter
ω	Acentric factor
ω -PDL	ω -Pentadecalactone

CONTENTS

1	INTRODUCTION	16
1.1	OBJECTIVES	18
1.1.1	General Objective	18
1.1.2	Specific Objectives	18
2	LITERATURE REVIEW.....	19
2.1	LACTONES	19
2.1.1	Lactone-based polymers	22
2.1.2	ϵ-Caprolactone.....	24
2.1.3	ω-Pentadecalactone	26
2.1.4	Globalide	27
2.2	SUPERCRITICAL FLUIDS	29
2.2.1	Supercritical carbon dioxide in eROP	30
2.3	PHASE EQUILIBRIUM	31
2.3.1	Vapor-liquid equilibrium	32
2.3.2	Liquid-liquid equilibrium.....	35
2.3.3	Vapor-liquid-liquid equilibrium.....	36
2.4	EXPERIMENTAL METHODS.....	37
2.5	THERMODYNAMIC MODELS	38
2.5.1	Cubic equations of state	40
2.5.2	Association models.....	42
2.5.3	The SAFT equations	42
2.6	STATE OF THE ART.....	46
3	HIGH PRESSURE PHASE EQUILIBRIUM DATA FOR THE TERNARY SYSTEM CONTAINING CARBON DIOXIDE, CHLOROFORM AND GLOBALIDE.	48
3.1	INTRODUCTION	49
3.2	MATERIAL AND METHODS	51
3.2.1	Materials	51
3.2.2	Phase equilibrium apparatus and procedure.....	52
3.2.3	Thermodynamic models	56
3.3	RESULTS AND DISCUSSION	57
3.4	PARTIAL CONCLUSIONS	72

4	EXPERIMENTAL VAPOR PRESSURE DATA FOR E-CAPROLACTONE, Ω-PENTADECALACTONE, AND GLOBALIDE, AND PREDICT PC-SAFT PARAMETERS	73
4.1	INTRODUCTION	73
4.2	MATERIAL AND METHODS	74
4.2.1	Materials	74
4.2.2	Apparatus and experimental procedure	75
4.2.3	Thermodynamic model	76
4.3	RESULTS AND DISCUSSION	77
4.4	PARTIAL CONCLUSIONS	83
5	CONCLUSION REMARKS	84
5.1	SUGGESTIONS FOR FUTURE RESEARCHES.....	84
	REFERENCES.....	86

1 INTRODUCTION

In almost all industrial sectors, plastics, or polymeric materials, are found playing important roles. However, as most polymers have a petrochemical origin and take a long time to decompose, their use becomes limited to not all applications when fast degradation and biocompatibility are necessary. Therefore, new biodegradable products are being developed from renewable sources and present suitable thermal, chemical and mechanical properties (WILSON, et al., 2019).

Lactone-based polymers has drawn great attention throughout the 1970s, during the resorbable-polymer-boom, the 1990s, as tissue engineering was being developed, and more recently, as new advances have been made in biomedical, food packaging, and pharmaceutical applications (THAKUR et al., 2021). These products are highly customizable, through copolymerization and functionalization, their mechanical and thermal properties can be adjusted, and therefore, also the biodegradation rates (BIŃCZAK et al., 2021; HEGE et al., 2014).

A variety of lactones is used as monomers at polymerization and copolymerization. Among those substances ϵ -caprolactone, ω -pentadecalactone, and globalide are utilized for the synthesis of exceptional polymers and copolymers for biomedical applications, as controlled drug delivery systems, and for tissue engineering.

Different techniques can be applied for the synthesis of these materials, from conventional condensation polymerization to ring-opening polymerization, from metallic catalysts to enzymes, and from toluene media to the use of supercritical carbon as solvent. Recently, new studies on enzymatic ring-opening polymerization under supercritical media have been performed due to the lack of toxic initiators and metallic catalysts, the controllable reaction mechanism, the mild temperature conditions, and the ease of recovering and separating the enzymes and solvent from the final product (SZELWICKA et al., 2020; WILSON, et al., 2019; POLLONI, et al., 2017).

Carbon dioxide is said to be at the supercritical state of matter when it is not possible for it to exist in a vapor-liquid equilibrium, at conditions above its critical temperature and critical pressure. Under these conditions, the fluid properties become highly suitable for its usage as a solvent, as its diffusion coefficient and density increase while its viscosity achieves lower values. Another great advantage is the

possibility to vary and control the supercritical solvent density through small changes in pressure and temperature (SMITH, VAN NESS, ABBOTT, 2018; COOPER, 2000).

Although supercritical carbon dioxide presents itself as an exceptional solvent, it may not be able to dissolve high molar mass polymers at desirable pressures. Therefore, the addition of chloroform or dichloromethane in small quantities as a cosolvent for the polymerization reaction have shown positive results for systems containing polymeric materials under supercritical media. Furthermore, as these organic compounds have low boiling temperatures, they can be easily separated as the system depressurizes (REBELATTO, 2018; NASCIMENTO, 2019, MAYER, 2020).

Variations in temperature and pressure not only vary the density of supercritical carbon dioxide, but also change the solubility of the materials dissolved by it. Also, during the polymerization, the overall chemical composition of the system changes, as reagents turn into products, which might require pressure increments to achieve higher molecular weights (TU et al., 2002; NUNES DA PONTE, 2009). Consequently, the understanding of how these properties behave is extremely important and can be accomplished by the study of phase equilibrium.

In the literature, the phase behavior of binary systems containing carbon dioxide and ϵ -caprolactone (XU et al., 2003; BERGEOUT et al., 2004; BENDER et al., 2010), ω -pentadecalactone (REBELATTO et al., 2018a), or globalide (REBELATTO et al., 2020) have already been reported, as well as ternary systems of carbon dioxide, ϵ -caprolactone, and chloroform (GIRARDI et al., 2021) or dichloromethane (MAYER et al., 2019), ternary systems of carbon dioxide, ω -pentadecalactone, and chloroform (REBELATTO et al., 2018a) or dichloromethane (REBELATTO et al., 2018B), and the ternary system of carbon dioxide, globalide, and dichloromethane (DE QUADROS et al., 2022). However, there is not a study of the high-pressure phase equilibrium of the ternary system {carbon dioxide + globalide + chloroform}.

Furthermore, the design and operation of polymerization processes under supercritical carbon dioxide media requires the use of appropriate models to correctly predict the operational conditions. The PC-SAFT equation of state has been used to estimate thermodynamic properties and conditions of polymeric materials and mixtures. Moreover, its pure component parameters can be obtained from experimental vapor pressure data (KONTOGEOORGIS; FOLAS, 2010; GROSS; SADOWSKI, 2002).

It has been reported the vapor pressure data for ϵ -caprolactone (BIAZUS et al., 2008; EMEL'YANENKO et al., 2010) and for ω -pentadecalactone (EMEL'YANENKO et al., 2011), although no work has studied the vapor pressure of globalide.

Therefore, the investigation of high-pressure phase equilibrium of the ternary system {carbon dioxide + globalide + chloroform} and the study of vapor pressure of globalide are essential to the development of the synthesis of poly(globalide) and copolymers at high pressure.

1.1 OBJECTIVES

1.1.1 General Objective

The general objective of this work was to investigate the high-pressure phase behavior of the ternary system containing carbon dioxide, globalide, and chloroform, and to study the vapor pressure of globalide, ϵ -caprolactone, and ω -pentadecalactone.

1.1.2 Specific Objectives

- a) Study the phase equilibrium of the ternary system containing carbon dioxide, globalide, and chloroform, with the different mass ratios of globalide to chloroform of 0.5:1, 1:1, and 2:1, at a temperature range of 313.15 to 343.15 K.
- b) Represent the phase equilibrium data for the ternary system containing carbon dioxide, globalide, and chloroform using the Peng-Robinson equation of state with the quadratic van der Waals mixing rule.
- c) Evaluate the effects of adding chloroform to the phase transition pressure of the ternary system containing carbon dioxide, globalide, and chloroform.
- d) Investigate the vapor pressure of ϵ -caprolactone, ω -pentadecalactone, and globalide at a temperature range of 297.8 to 333.7 K.
- e) Determine values for Antoine correlation parameters and pure components parameters of PC-SAFT equation of state.

2 LITERATURE REVIEW

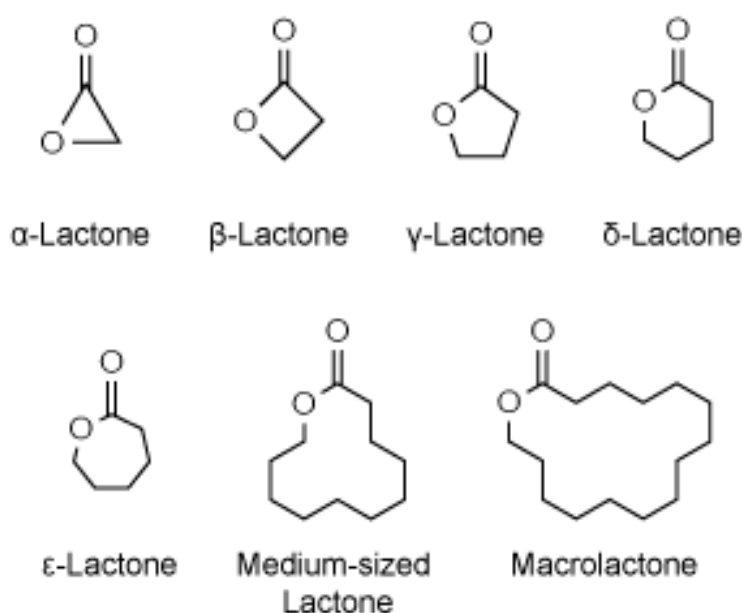
2.1 LACTONES

Lactones constitute a group of aliphatic or α,β -unsaturated cyclic esters of hydroxylated fatty acids, described with a 1-oxacycloalkan-2-one structure, as defined by IUPAC (IUPAC, 2014). They are volatile organic compounds and secondary metabolites, derived from the lipid metabolism of plants, bacteria, fungi, marine sponges, and other organisms (SILVA et al., 2021; TAKAMURA, 2018; REDDY et al., 2018). The term was first used between 1219 and 1227 by the french chemist J. Pelouze, to name a new compound isolated from lactic acid. This denomination was extended in 1880 by the german chemist W. Fitting to characterize all cyclic carboxylic esters derived from intramolecular esterification (BIŃCZAK et al., 2021). These compounds are commonly found in fruits, vegetables and wine, as well as in lipid-rich foods as meat, milk and vegetable oils, contributing to the flavor and aroma normally described as peach-, creamy-, coconut-, or oily-like, among others (BURDOCK, 2009; DASTAGER, 2009; SILVA et al., 2021).

Classification of lactones is based on the size of the cyclic ring. Their names receive a greek letter prefix to indicate the number of the carbon that is attached to the oxygen of the carboxyl group (BIŃCZAK et al., 2021; SILVA et al., 2021). α -Lactones, which cannot be found in nature, and β -lactones are less stable due to high tension in the ring and contain 3- and 4-membered rings, respectively. γ -Lactone represents one of the most abundant lactone classes, with more than three thousand different molecules, they contain 5-membered rings and can possess potent herbicidal, insecticidal, anti-tumor, and antifouling activity. δ -Lactone, with a cyclic ring made of six atoms, is also widely common in nature, being more present as α - β -unsaturated molecules; they have a wide range of biological activities, as HIV protease inhibition, apoptosis induction, antileukemic, antitumor, leishmanicidal, trypanocidal, antifungal, antibacterial and anti-inflammatory. ϵ -Lactones get their names due to the attachment of the oxygen of the carboxyl group at the sixth carbon of their 7-membered ring; the aliphatic member of this class known as ϵ -caprolactone will be described later in this work. Lactones containing rings with eight to eleven members are classified as medium-sized lactones, they have anti-tumor, antibiotic, antifungal, and phytotoxic activities, and a few of the largest molecules within this category are used by insects

as pheromones. Cyclic esters with at least twelve members within their rings are named macrolactones, or macrocyclic lactones, and can be further classified as olides or diolides; they can be obtained from vegetable oils or from animal sources and are used as fragrances, pheromones, insecticides, pharmaceuticals (antifungal, antiviral and anti-tumor), and phytotoxic agents (SARTORI et al., 2021; WILSON, et al., 2019). A representative scheme for lactones is presented in Figure 1.

Figure 1 – Classification of lactones

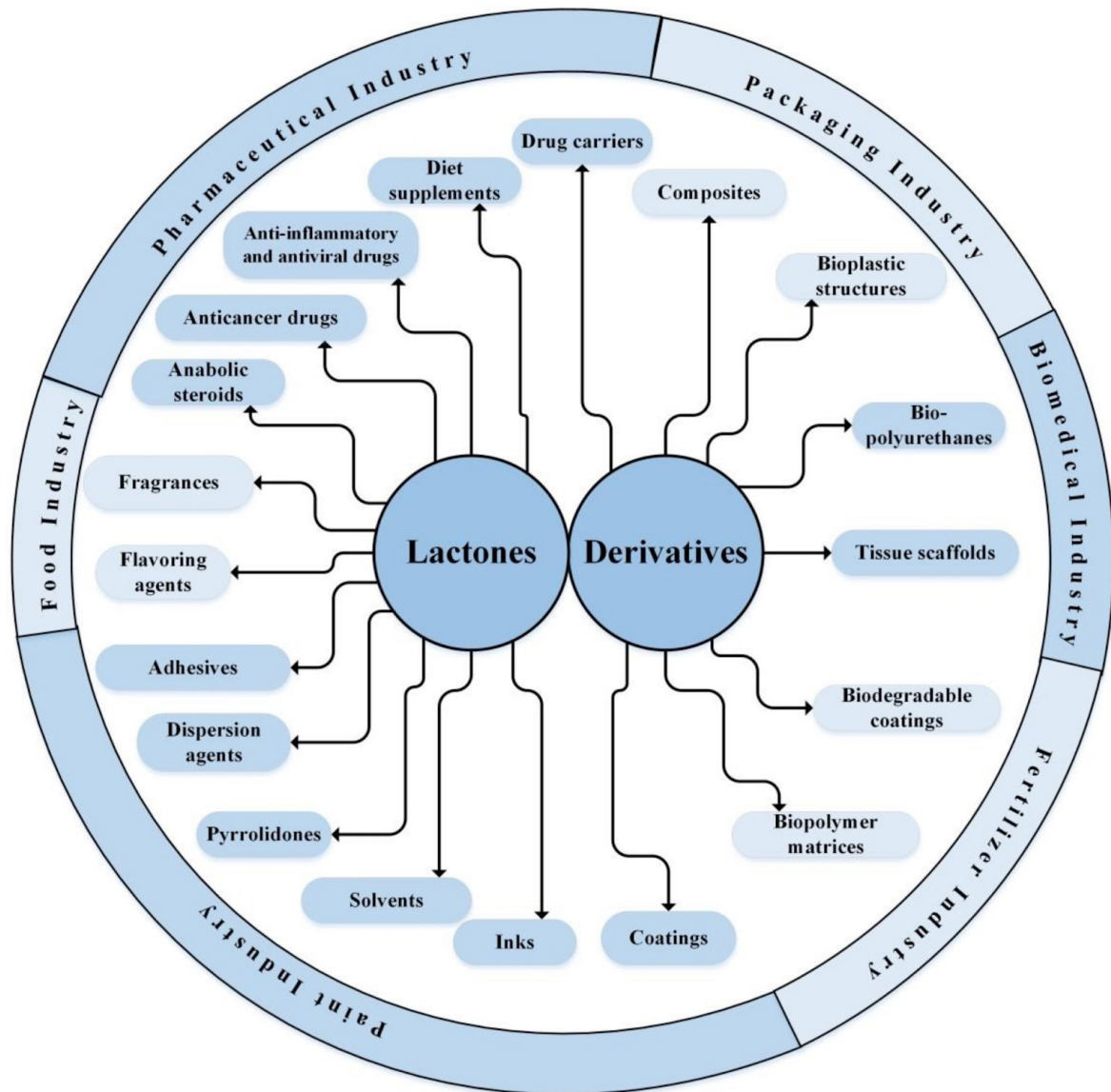


Source: the author.

Due to their aromas and flavors, lactones receive a high commercial interest in the cosmetic and food industries (SILVA et al., 2021). In 2020, this product achieved a total trade of USD 2.07 billion and had a market volume of 134.6 thousand tons, with an annual decrease of price per kilogram and an increase in market importance as research on the production and use of lactones develops (OEC, 2020; NOGUEIRA et al., 2022; BIŃCZAK et al., 2021). The lactone extraction from natural sources is generally economically unfeasible, as this product is found in small quantities in nature. Therefore, two main pathways are available and used for the production of lactones, biotechnological processes, which are more expensive and more environmentally friendly, and the traditional chemical synthesis (MAŁAJOWICZ et al., 2020). As sustainability is promoted by conscious market and legislation, a drop in cost for the biotechnological production route is expected (BIŃCZAK et al., 2021).

In addition to the cosmetic and food industries, a variety of other services uses lactones and their derivatives in different processes, as shown in Figure 2. It is been reported the use in pharmaceutical applications, for the production of antihypertensive, antifungal, antiparasitic, anti-tumor, dermatological, and antibiotic drugs, anabolic steroids and synthetic musks (BIŃCZAK et al., 2021; SARTORI et al., 2021). Among these antibiotic drugs, great emphasis has been made recently on azithromycin and hydroxychloroquine, due to preliminary studies declaring useful applications for the treatment of the pandemic of coronavirus disease 2019 (SARTORI et al., 2021). Lactones are also employed as green solvents and fuel precursors in the production of hydrocarbons used in jet fuel, gasoline, and biodiesel (ALONSO et al., 2013; KOURIST et al., 2015; BIŃCZAK et al., 2021). Other industries that have applications for this family of compounds include the agrochemical industry, the packaging industry, the biomedical industry and the paint industry (SARTORI et al., 2021; BIŃCZAK et al., 2021; CHEN et al., 2006). Among the main lactone derivatives are biodegradable polyesters, which are the subject of many studies dedicated into the production and application of lactone-based polymers and copolymers (BIŃCZAK et al., 2021).

Figure 2 – Lactones and their derivatives applications in industrial processes



Source: BIŃCZAK et al., 2021

2.1.1 Lactone-based polymers

Due to suitable thermal, chemical and mechanical properties, polyesters synthesized from lactones are mostly used for the pharmaceutical and biomedical industries. These polymers are also desirable since they are biocompatible and biodegradable, being appropriate to be applied as drug carriers, and as bone and muscle structure in tissue engineering (WILSON, et al., 2019; TSUTSUMI et al., 2019). Similarly to the biotechnological synthesis of lactones, legislation has pushed the production of environmentally friendly plastics, and, since lactone-based polymers can

be functionalized to receive additional properties, these materials have been implemented for fertilizer, automotive, and packaging applications. It has been reported that both mechanical and thermal properties, and biodegradation rates can be adjusted by modifying the polymer's crystalline phase by copolymerization, which is the reaction between two distinct monomers. Nevertheless, the production of these polymers must be carefully planned, as incorrect choices of solvents, catalysts, and initiators can impede medical, pharmaceutical, and food application, due to possible toxic components among those options (HEGE et al., 2014).

Different techniques can be applied for the synthesis of lactone-based polyesters. Catalysts can be chosen from metallic complexes, organic compounds, enzymes, or zeolites, the last two avoiding the need of initiators based on heavy metals. Furthermore, in a few cases, under dilute phosphoric acid medium, a catalyst-free reaction can be carried out with an increase in temperature and reaction time. Recently, the enzymatic reaction with *Candida Antarctica Lipase B* (CALB) as a catalyst has attracted attention due to lower temperature and pressure conditions required, and the lack of toxic initiators and metallic catalysts (LIN, 1999; SZELWICKA et al., 2020; BIŃCZAK et al., 2021; WILSON, et al., 2019).

In the last few decades, the controllable ring-opening polymerization (ROP) has become the most common reaction mechanism, replacing the condensation polymerization method that required rigorous purification step due to unwanted side reactions (WILSON, et al., 2019; FLORY, 1946). For small and medium-sized lactones, ROP releases energy as angular strains are undone. Since macrolactones lack this potential energy due to its wider bond angles, for macrocyclic lactones, the ROP is driven by the entropic gain obtained with lesser chain rotation (LEBEDEV et al., 1984). For this reaction mechanism, the molecular weight of the product is directly related to the amount of catalyst, and to the ratio of monomer to initiator in the starting solution (WILSON, et al., 2019).

The commercially available lipase Novozyme-435 is an acrylic resin with immobilized CALB that yields high conversion rates and have great selectivity degrees. It is a non-toxic catalyst that can be easily removed by filtration and can be reused in further reactions. This catalyst is used in enzymatic ring-opening polymerization (eROP), a reaction that can use water as an initiator, and is temperature dependable, achieving faster reaction rates and higher molecular mass when operating in elevated temperatures within a certain range (KUNDYS et al., 2018). For both the

polymerization of ϵ -caprolactone, a small lactone, and for the polymerization of ω -pentadecalactone, a macrolactone, exceptional operational results have been reported around 70 °C to 80 °C, and increases in temperature beyond that value would lead to enzyme denaturation (WILBERTH, et al., 2015; BISHT et al., 1997).

Another important planning step in conducting eROP is the polymer purification, which depends on the type of reactor, and on the solvent that must be separated from the final product. To reduce the amount of solvent consumed during purification, a packed-bed reactor with immobilized enzymes can be used (WILSON, et al., 2019). Furthermore, as reported by Polloni (2018), most works conduct the polymerization and copolymerization of ω -PDL through toluene solution. Due to the central nervous system damage, that toluene can cause, and the difficulty in separating it from the final polymerization product, new solvents must be sought so that these polymers can be safely applied in biomedicine and pharmaceutical uses (WIN-SHWE et al., 2010; POLLONI, 2018). A viable solution to this step is the use of supercritical carbon dioxide as solvent for the reaction, since it turns possible to recover both the solvent and the enzyme as the process ends (POLLONI, et al., 2017; GUINDANI et al., 2017; GUALANDI et al., 2010).

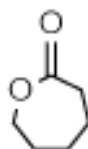
2.1.2 ϵ -Caprolactone

ϵ -Caprolactone (ϵ -CL), CAS Registry Number 502-44-3, is also named 2-oxepanone, hexanoic acid 6-hydroxy-lactone, or 6-hexanolactone, is a saturated small-sized lactone with a cyclic ring with seven members, its molecular formula is $C_6H_{10}O_2$ and it has a molecular weight of 114.14 (CAS COMMON CHEMISTRY, c2022; TGSC, c2021c). It appears as a colorless to pale yellow clear liquid and has a melting point of 18.00 °C and a boiling point of 215.00 °C (CAS COMMON CHEMISTRY, c2022). Figure 3 represents the molecular structure of ϵ -CL.

This chemical is mainly used as a monomer for the synthesis of biodegradable polyesters, but its use in pharmaceutical, paint, and chemical industries, as intermediate in adhesives, as a solvent, as coatings, as a diluent for epoxy resins, as elastomers, and as the precursor for the production of caprolactam has also been reported (LARRAÑAGA et al., 2016; BIŃCZAK et al., 2021). According to the Organisation for Economic Co-operation and Development in its Screening Information Dataset Initial Assessment Report, conducted in 2005, the annual production of ϵ -CL

was estimated to be from 40000 to 60000 tonnes worldwide (OECD, 2005). Furthermore, its predominant manufacture pathway is through a Bayer-Villager reaction, as peracetic acid is used to oxidize cyclohexanone (OECD, 2005).

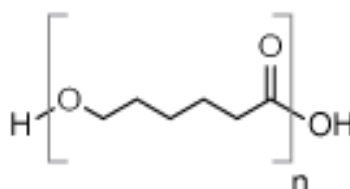
Figure 3 - ϵ -Caprolactone molecular structure.



Source: the author.

The ϵ -CL polymer, poly(ϵ -caprolactone), is a bioresorbable aliphatic semi-crystalline polyester with a glass transition temperature of $-60\text{ }^{\circ}\text{C}$ and a melting temperature between 58 and $65\text{ }^{\circ}\text{C}$ (THAKUR et al., 2021). It has high solubility in organic solvents such as benzene, chloroform, dichloromethane and toluene (SINHA et al., 2004). Moreover, both the degree of crystallinity and the molar weight has high impacts on the biodegradability and biocompatibility of this material and these properties can be manipulated by copolymerization and functionalization (BIŃCZAK et al., 2021; THAKUR et al., 2021). At present, poly(ϵ -caprolactone) is used in artificial blood vessels, long-term contraceptive devices, drug-delivery devices, nerve and bone regeneration, prosthetics, scaffolds for tissue engineering, long-lasting absorbable sutures, long-term vaccines, and in water purification (WOODRUFF et al., 2010; MOHAMED et al., 2015; BIŃCZAK et al., 2021; THAKUR et al., 2021). Figure 4 represents the molecular structure of the repeating pattern of poly(ϵ -caprolactone).

Figure 4 – Molecular structure of the repeating pattern of poly(ϵ -caprolactone).

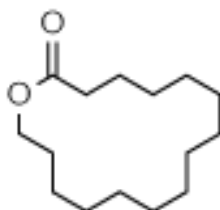


Source: the author.

2.1.3 ω -Pentadecalactone

ω -Pentadecalactone (ω -PDL), CAS Registry Number 106-02-5, also known as angelica lactone, cyclopentadecanolide, exaltex, exaltolide, 15-hydroxypentadecanoic acid ω -lactone, macrolide, muskalactone, oxacyclohexadecan-2one, pentadecanolide, pentalide, or thibetolide, is a saturated macrolactone with a 16-membered ring, molecular formula of $C_{15}H_{28}O_2$, and molecular weight of 240.387 (TGSC, c2021a; MCGINTY et al., 2011; API et al., 2020). It is a white to pale yellow solid with needle-like crystals that has a melting point of 34.00 °C and a boiling point of 364.47 °C. Its strong odor is commonly described as musk animal powdery natural fruit, tobacco, or coumarin, and it tastes like vanilla bean, creamy, and licorice, although it is harmful if swallowed. (TGSC, c2021a; API et al., 2020). Figure 5 represents the molecular structure of ω -PDL.

Figure 5 - ω -Pentadecalactone molecular structure.



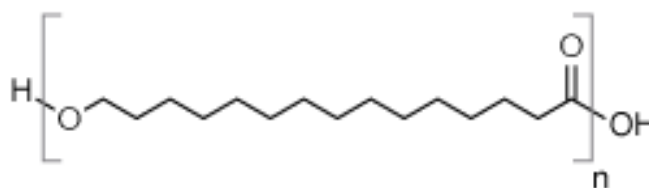
Source: the author.

This fragrance ingredient is mainly used for cosmetic and cleaning applications, being found in aerosol air fresheners, body lotions, decorative cosmetics, detergents, face moisturizers, fine fragrances, hand creams, household cleaners, lipsticks, shampoos, and soaps (MCGINTY et al., 2011; API et al., 2020). According to the latest International Fragrance Association survey in 2015, the worldwide volume consumption of ω -PDL ranges from 100 to 1000 tonnes yearly (API et al., 2020). Although it has been reported the natural occurrence of ω -PDL in angelica root oil in significant amounts, new synthetic forms of production have been the main production route in the recent years, due to development in scientific research (PANTEN et al., 2008; MCGINTY et al., 2011).

Another contemporary application for ω -PDL is the polymerization and copolymerization of this material, replacing fossil source monomers in the production

of polyesters at the medical, the packaging, and the pharmaceutical industries (DE GEUS et al., 2010; BIŃCZAK et al., 2021). Poly(ω -pentadecalactone) is a thermoplastic mainly synthesized by lipase catalysis, it is an aliphatic polyester with 14 methylene units and ester group in each repeating unit that can be decomposed through enzymatic hydrolysis (CAI et al., 2010; NASCIMENTO, 2019). The thermal and mechanical properties of this polymer, as well as the crystallinity and hydrophobicity, which are directly related to the biodegradability and biocompatibility, can be adjusted and controlled by copolymerization and/or functionalization (REBELATTO, 2018; POLLONI, 2018; BIŃCZAK et al., 2021). The poly(ω -pentadecalactone) can be applied in biomedicine as controlled drug delivery, suture, and tissue engineering (ALBERTSSON et al., 2003). Figure 6 represents the molecular structure of the repeating pattern of poly(ω -pentadecalactone).

Figure 6 - Molecular structure of the repeating pattern of poly(ω -pentadecalactone).

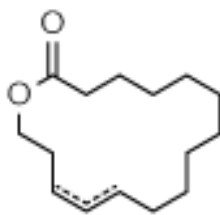


Source: the author.

2.1.4 Globalide

Globalide (GL), CAS Registry Number 34902-57-3, also known as cyclopentadecenolide, habanolide, musk decenone, 11/12-pentadecen-15-olide, 15-pentadecenolide, or (3E)-oxacyclohexadec-3-en-2-one, is a saturated macrolactone with a 16-membered ring that contains one unsaturated bond, molecular formula of $C_{15}H_{26}O_2$, and molecular weight of 238.366 (VAN DER MEULEN et al., 2008; TGSC, c2021b; API et al., 2022; GUINDANI, 2018). It is a colorless to pale yellow liquid that has a melting point of 26.06 °C and a boiling point of 357.00 °C. Its strong odor is commonly described as sweet musk waxy, woody, or herbal.. (TGSC, c2021b; API et al., 2022). Figure 7 represents the molecular structure of GL.

Figure 7 – Globalide molecular structure.



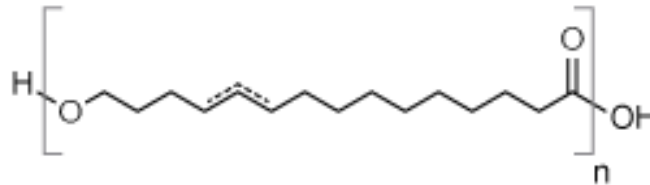
Source: the author.

This non-toxic and biodegradable substance can be found in a variety of cleaning and cosmetic products, being present in small amounts in baby oil, body lotions, face moisturizers, fine fragrances, hand creams, lipsticks, shampoos, and tampons, and in slightly higher concentrations in aerosol air fresheners, hand dishwashing detergents, and soaps (TGSC, c2021b; API et al., 2022). It has a volume of use higher than 1000 tonnes per year, as registered on the most recent International Fragrance Association volume of use survey in 2015. Furthermore, the presence of this compound in nature has not been discovered, as stated by the Volatile Compounds in Food Database (API et al., 2022).

A search in databases of scientific articles shows that research on globalide is recent, with only 28 works being presented by Semantic Scholar, 24 by Scopus, and 21 by Google Scholar (SEMANTIC SCHOLAR, c2021; SCOPUS, c2022; GOOGLE SCHOLAR, c2022). It is also clear that almost all of these works involve the polymerization and copolymerization of the globalide, as well as the functionalization of its polymer, poly(globalide), and of some of its copolymers. Van der Meulen et al. (2008), Chiaradia et al. (2018), Polloni et al. (2018), and Guindani et al. (2022) conducted polymerization of globalide with different conditions; Guindani et al. (2017) conducted copolymerization of globalide and ϵ -caprolactone in supercritical media; Tinajero-Díaz et al. (2020) conducted copolymerization of globalide and ω -pentadecalactone; Tinajero-Díaz et al. (2019) conducted copolymerization of globalide and α -amino acid l-alanine; Rebelatto et al. (2020), and De Quadros et al. (2023) conducted phase equilibrium data for polymerization in supercritical media; Ates et al. (2014), Chiaradia et al. (2019), Polloni et al. (2020), Amaral et al. (2021), and Oliveira et al. (2022) functionalized the poly(globalide) for medical use; Claudino et al. (2012), Guindani et al. (2019a), Guindani et al. (2019b), Guindani et al. (2020), and Beltrame et al. (2021) functionalized the copolymer poly(globalide-co- ϵ -caprolactone) for

different applications. Figure 8 represents the molecular structure of the repeating pattern of poly(globalide).

Figure 8 - Molecular structure of the repeating pattern of poly(globalide).



Source: the author.

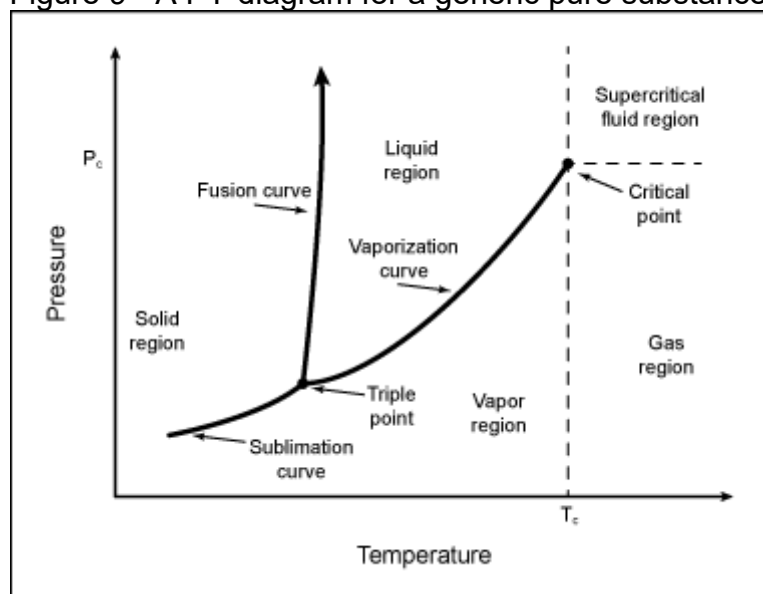
2.2 SUPERCRITICAL FLUIDS

Supercritical fluids are pure chemical species under conditions above its critical point. The critical point is defined by its two coordinates, the critical temperature (T_c) and the critical pressure (P_c), above these values it is not possible for a pure substance to exist in vapor-liquid equilibrium (SMITH, VAN NESS, ABBOTT, 2018). A PT-diagram for a generic pure substance is represented in Figure 9, where the critical point can be identified.

The use of supercritical fluids as solvents is related to their density, diffusion coefficient, and viscosity. It is highly advantageous for a solvent to have higher diffusion coefficient and lower viscosity values, coming close to the values of gases, as these conditions facilitate transport phenomena. It is also preferable to a solvent to have higher densities, as it occurs in liquids, which is directly related to its solvating power (BENDER, 2008). Another highlight about supercritical fluids is the possibility to vary their density through small changes in pressure and temperature (COOPER, 2000).

A reliable supercritical fluid for industrial processes is carbon dioxide (CO_2), as its critical point is easily achievable, having a critical temperature of 31.04 °C and a critical pressure of 7.38 MPa (NIST, 2021c). It is a low cost, non-flammable, inert solvent with low toxicity available in high purity that can be easily separated at ambient temperature and pressure from the final reaction product and be recycled in the process (LEITNER, 2000; COMIM et al., 2013).

Figure 9 - A PT-diagram for a generic pure substance.



Source: adapted and modified from SMITH; VAN NESS; ABBOTT, 2018.

2.2.1 Supercritical carbon dioxide in eROP

The use of supercritical CO₂ in eROP with ϵ -CL, ω -PDL, and/or GL as monomers has shown similar results when working with the organic solvent toluene (GUINDANI, 2018; POLLONI, 2018). Standard eROP uses toluene due to its high boiling point of 111 °C, being able to operate as a solvent within the optimal temperature range of CALB enzymatic activity, which spans from 60 to 80 °C. It is also due to its high boiling temperature that it becomes difficult to isolate the final polymer from this solvent (BISHT et al., 1997; WIN-SHWE et al., 2010). Therefore, working with supercritical CO₂ as a solvent allows the synthesis of suitable and safe polyesters for biomedical and food applications.

Although it may seem contradictory, recent studies investigated the effect of toxic organic compounds, such as chloroform and dichloromethane, as cosolvents for eROP under supercritical CO₂ media. Those cosolvents have lower boiling temperatures than toluene, 61.2 °C and 40.0 °C respectively, thus they can be more easily pulled apart from the polymer as the system depressurizes and CO₂ turns from a supercritical fluid into a gas (REBELATTO, 2018; NASCIMENTO, 2019, MAYER, 2020).

Just as the density of a supercritical fluid varies as temperature and pressure change, the solubility of a monomer in supercritical CO₂ can be adjusted as variation

on these conditions occurs (TU et al., 2002). Moreover, as the polymerization takes place the chemical composition of the system changes, and higher pressures are needed to solvate the developed polymer and to achieve higher molecular weights (NUNES DA PONTE, 2009; NASCIMENTO, 2019). Therefore, to better comprehend how these properties behave, and to achieve a single phase medium, as multi-phase systems disturbs the efficiency of eROP through mass transfer interfacial resistance between solvent phases, the study of phase equilibrium of systems containing the reaction compounds becomes indispensable (BENDER, 2008).

2.3 PHASE EQUILIBRIUM

Smith, Van Ness and Abbot (2018) define equilibrium as “a condition in which no changes occur in the macroscopic properties of an isolated system with time”. In other words, to an isolated non-reacting system be at equilibrium, its temperature, pressure, and phase composition must remain unchanged, which means that molecules can pass from one phase to another, although their average interfacial transport rate must be equal in both directions. Furthermore, phase can be defined as an homogeneous region of matter (SMITH; VAN NESS; ABBOT, 2018).

The study of phase equilibrium is the investigation on how distinct phases behave under changes in temperature, pressure, and system composition, as new conditions for equilibrium are established. This analysis is crucial for separation and purification methods, such as extraction with pressurized fluids, crystallization of pharmaceutical compounds, distillation of petroleum, and reactions under high pressure (SMITH; VAN NESS; ABBOT, 2018; DE QUADROS, 2022). For high pressure polymerization processes, it is by the understanding of phase behavior that essential information such as solubility, solidification, supersaturation, and solvent vaporization can be obtained and subsequently used to establish the ideal operating conditions. (PÉREZ DE DIEGO et al., 2005).

Phase equilibrium data can be obtained experimentally through analytical, or synthetic methods, or numerically through thermodynamic modeling (PEPER; FONSECA; DOHRN, 2019). For thermodynamic modeling, binary interaction parameters and pure substances properties can be attained by adjusting to experimental phase equilibria data, and by vapor pressure, density, and/or speed of sound data, respectively (NDIAYE et al., 2005; MAYER et al. 2020).

A variety of phase transitions can be studied with a high range of temperatures, pressure, and system composition. This work investigated vapor-liquid equilibrium (VLE), liquid-liquid equilibrium (LLE), and vapor-liquid-liquid equilibrium (VLLE).

2.3.1 Vapor-liquid equilibrium

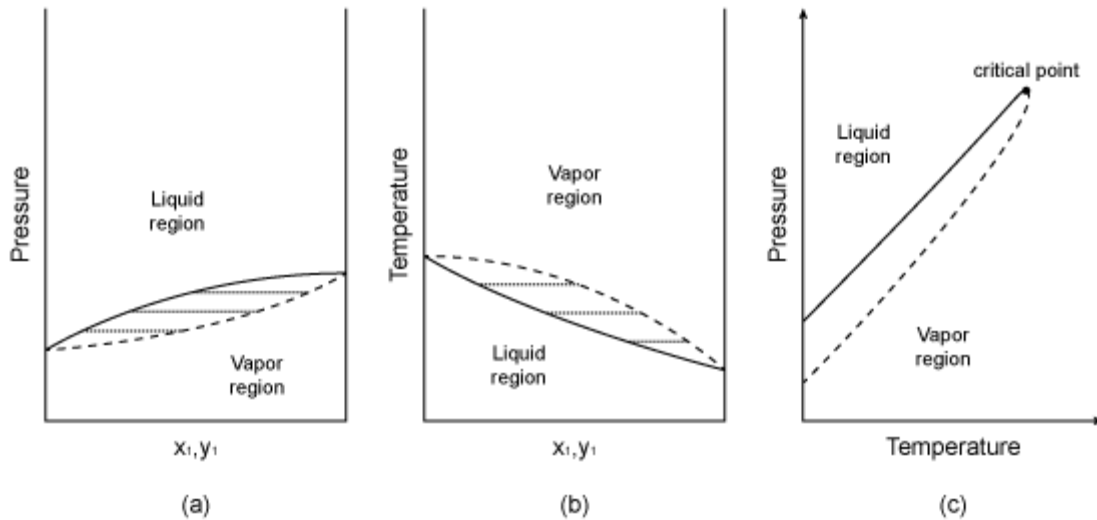
Vapor-liquid equilibrium, as defined by Smith, Van Ness and Abbot (2018), “is a state of coexistence of liquid and vapor phases”. For binary mixtures, constituted of two different substances, VLE is usually represented by two-dimensional diagrams with a fixed value of temperature, pressure, or system composition (mass or molar composition). These diagrams are represented in Figure 10, in which the continuous curve is the saturated liquid, the dashed curve is the saturated vapor, and the dotted lines are tie lines. The region between the saturated liquid and saturated vapor curves is the liquid-vapor region, where tie lines connect the liquid fraction (x_1) and vapor fraction (y_1) of the system at fixed temperature and pressure. Figure 10a represents a Pxy-diagram, where temperature is constant; Figure 10b represents a Txy-diagram, where pressure is constant; and Figure 10c represents a PT-diagram, where composition of the system is constant (SMITH; VAN NESS; ABBOT, 2018; PRAUSNITZ; LICHTENTHALER; AZEVEDO, 1999). Similarly to Txy and Pxy-diagrams, which contains information about molar fractions, Tw- and Pw-diagrams can also be used to display information regarding mass fractions (w_1).

It is important to understand that for binary mixture, all of these two-dimensional diagrams, including Pxy, Txy, and PT-diagrams, are within the same three-dimensional diagram as displayed in blue at Figure 11a, Figure 11b, Figure 11c, respectively.

Two phase transitions can occur when there are changes in pressure or in temperature. As the system’s conditions reach the saturated liquid curve, a transition called bubble point happens, as a small bubble of vapor appears inside the system as vaporization takes place. The second transition is named dew point, as small droplets of liquid appear as the vapor condenses, and occurs when the system’s conditions reach the saturated vapor curve. Therefore, whenever conditions at the saturated liquid curve do not change, it is said that the system is at a vapor-liquid bubble point equilibrium (VLE-BP). The same can be extrapolated for conditions at saturated vapor

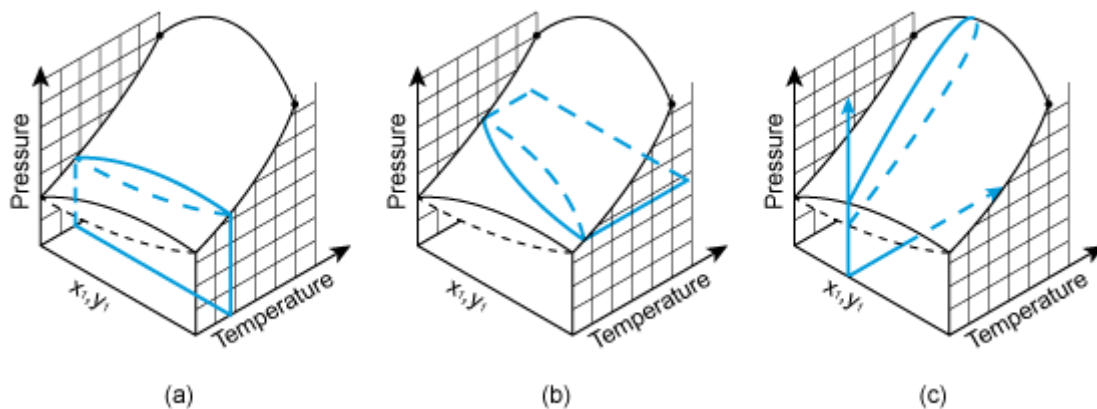
curve, and the system would be at a vapor-liquid dew point equilibrium (VLE-DP) (SANDLER, 2006; SMITH; VAN NESS; ABBOT, 2018).

Figure 10 – Two-dimensions VLE diagrams.



Source: adapted and modified from SMITH; VAN NESS; ABBOTT, 2018.

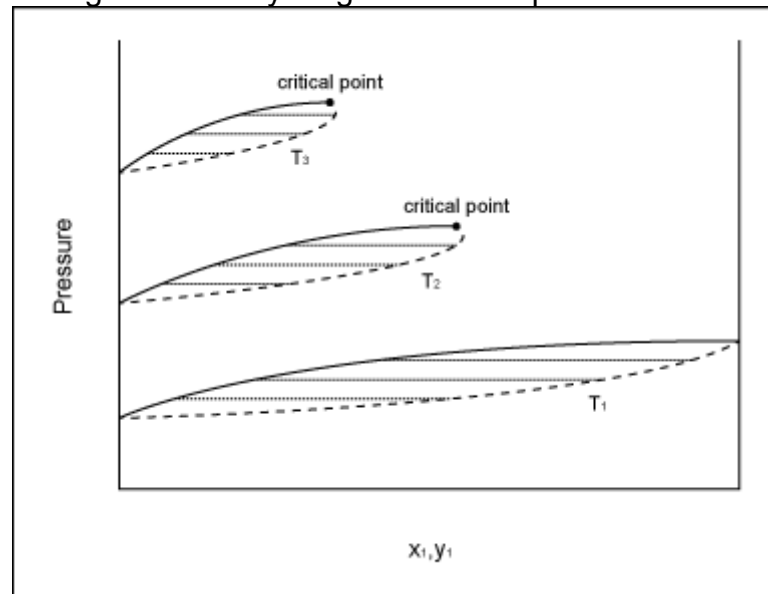
Figure 11 – Three-dimensions VLE diagrams.



Source: the author.

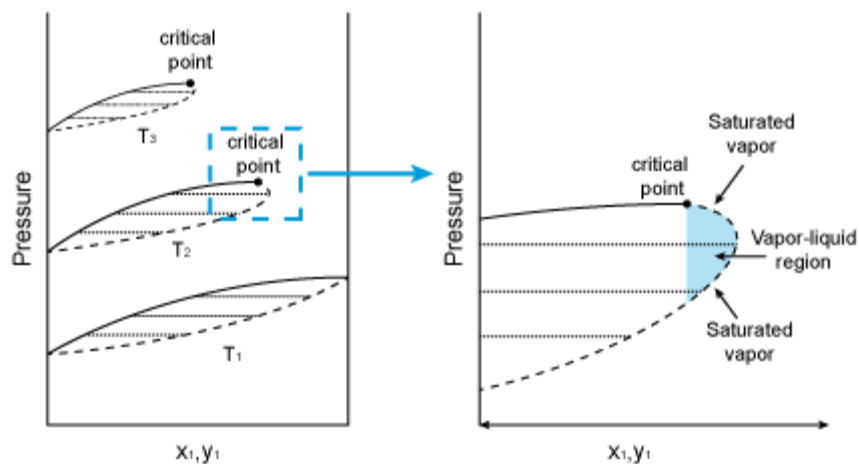
In order to compare changes in temperature (e.g. T_1 , T_2 , and T_3) for a Pxy-diagram, it is usual to represent multiple diagrams, as shown in Figure 12, and describe each pair of saturated liquid and saturated vapor curves as an isotherm, a line where all points are at a constant temperature.

Figure 12 – Pxy-diagram for multiple isotherms.



Source: adapted from SMITH; VAN NESS; ABBOTT, 2018.

Figure 13 – Retrograde condensation.



Source: the author.

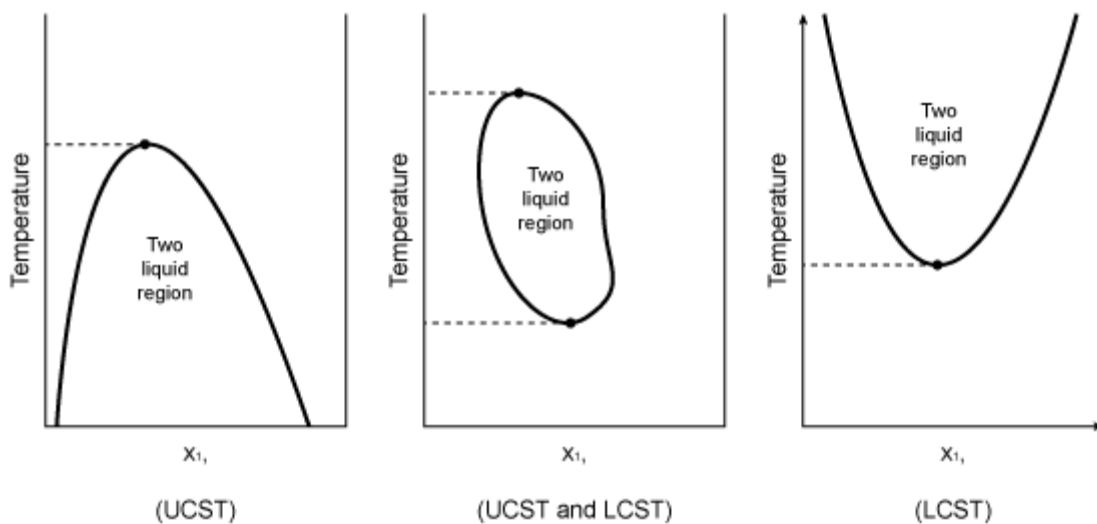
As shown in Figure 12, the critical point of a mixture can change as temperature varies. A close inspection near the critical point of a mixture allows the verification of an interesting phenomena, called retrograde condensation, which can occur in asymmetric mixtures. At a small region, for compositions close the critical point of the mixture, a dew point phase transition can occur as pressure values decrease, as the saturated vapor curve “envelops” around itself. This region is schematically represented in blue Figure 13. Within this region, the occurrence of vapor-liquid equilibria is expected, although significant pressure variations, both positive and

negative, cause the liquid phase to disappear (PRAUSNITZ; LICHTENTHALER; AZEVEDO, 1999; SMITH; VAN NESS; ABBOTT, 2018). This knowledge is crucial for this work, since retrograde condensation happens in the investigated ternary system.

2.3.2 Liquid-liquid equilibrium

Similarly to VLE, two stable phases of distinct composition are present in the liquid-liquid equilibrium, although it only occurs over specific temperature and pressure ranges. The highest temperature at which this phase transition happens is classified as upper critical solution temperature (UCST) and above it, the solution is completely miscible. Likewise, the lowest temperature at which two liquid phases are immiscible is called lower critical solution temperature (LCST) and below it, the mixture appears in a single phase. Figure 14 shows Tx-diagrams for a system with a LLE region. A system with a liquid-liquid region should exhibit at least one of the critical solution temperatures, although it could be obscured by the occurrence of vaporization, for UCST, or freezing, for LCST, of the mixture (SANDLER, 2006; ATKINS, DE PAULA, 2006).

Figure 14 – Tx-diagram for liquid-liquid equilibrium.



Source: adapted from SANDLER, 2006.

A system is also said to have UCST behavior if, as temperature decreases, an increase in pressure is necessary to achieve a single phase, that is $(\partial P / \partial T)_x < 0$.

Otherwise, if $(\partial P / \partial T)_x > 0$, the system can be characterized by LCST behavior (PRAUSNITZ; LICHTENTHALER; AZEVEDO, 1999).

2.3.3 Vapor-liquid-liquid equilibrium

When a system with vapor in equilibrium with one liquid phase presents another liquid phase in a coexisting equilibrium, it is said to occur a VLLE. For binary mixtures, there's only one temperature for each pressure at which VLLE can be observed. This statement can be verified through the Gibbs phase rule of nonreacting systems in equation 1.

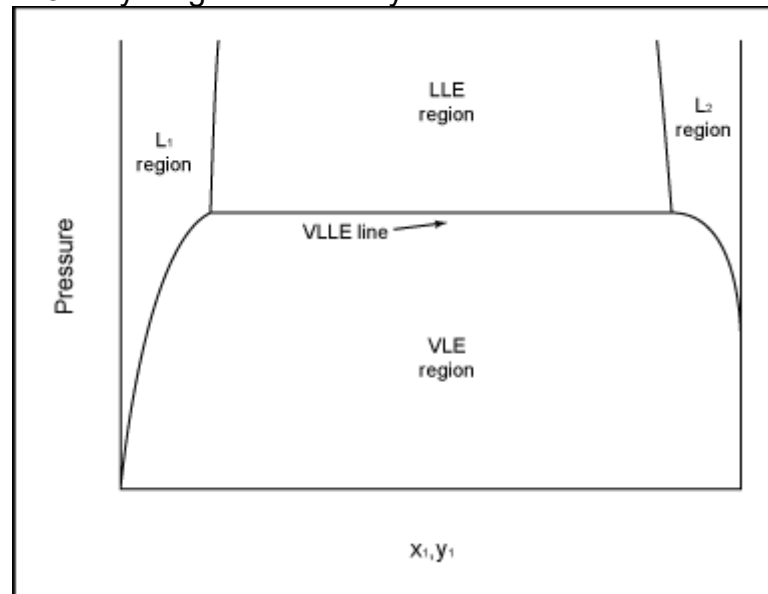
$$F = 2 - \pi + N \quad 1$$

where F is the number of degrees of freedom, π is the number of phases and N is the number of components. The degree of freedom is defined as the number of independent variables that must be given to establish the intensive state of the system. Among those variables are pressure, temperature, and the mass or molar composition of each phase.

A binary system at a three-phase equilibrium ($N = 2$ and $\pi = 3$) must have its degree of freedom to be equal to one ($F = 1$). Therefore, for any given temperature it is possible to determine the value of pressure for a system at VLLE, unaffected by the composition, as shown in Figure 15. Because of this, the determination of vapor-liquid-liquid transitions in binary mixtures may present some difficulties to be obtained experimentally. For ternary and multicomponent systems the number of degrees of freedom increases ($F \geq 2$) and this phenomena can be more easily observed (SANDLER, 2006; SMITH; VAN NESS; ABBOT, 2018).

For this work, a ternary system ($F = 2$) was investigated with a mass ratio that was arbitrarily determined and fixed between the two less volatile compounds. This choice was made in order to reduce by one the number of degrees of freedom, as any given fraction of the most volatile compound would be satisfactory to determine the overall system composition, which can be verified in equations 2 to 7. Therefore, for each studied isotherm, vapor-liquid-liquid equilibrium was observed at a fixed value of pressure.

Figure 15- Pxy-diagram for binary mixtures with VLLE occurrence.



Source: adapted from SANDLER, 2006.

$$\frac{w_2}{w_3} = C \quad \text{where } C \text{ is any arbitrarily determined constant} \quad 2$$

$$w_2 = C \cdot w_3 \quad 3$$

$$1 = \sum_{i=1}^N w_i \quad 4$$

$$1 = (w_1 + w_2 + w_3) \quad 5$$

$$w_1 = 1 - (w_2 + w_3) \quad 6$$

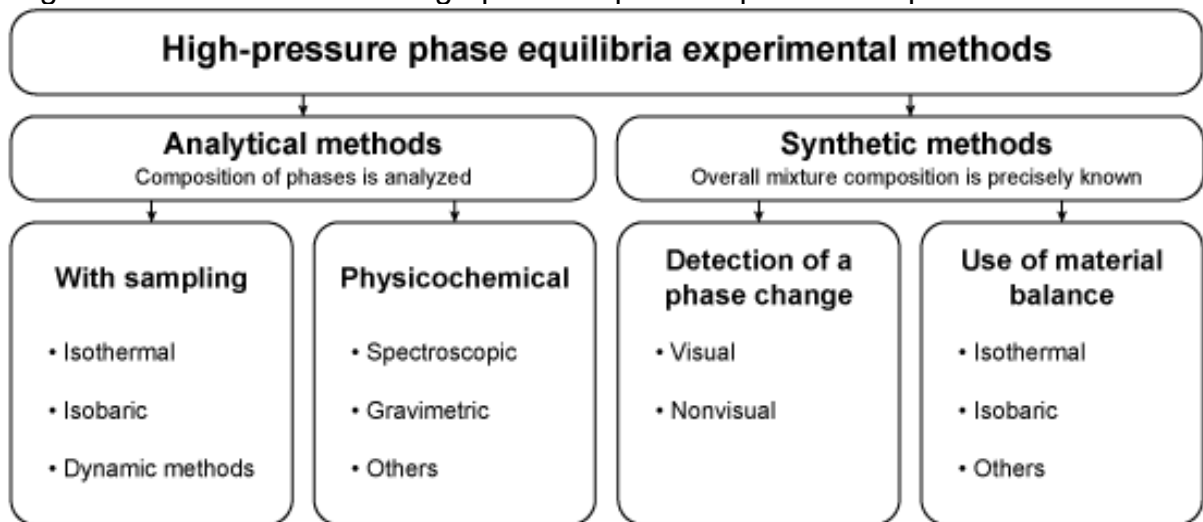
$$w_1 = 1 - w_3(1 + C) \quad 7$$

2.4 EXPERIMENTAL METHODS

High pressure phase equilibrium experiments can be performed using a variety of methods, which each one is recommended for specific situations, according to their advantages and disadvantages. Methods are classified as analytical, if the compositions of the coexisting phases are measured during the experiment, or as

synthetic, if the overall composition is previously and accurately known. These two major classes can be further divided as shown in Figure 16 (PEPER; FONSECA; DOHRN, 2019). Detailed information for those method and an overview of the experimental results published in the last five decades are carefully described by Deiters and Schneider (1986), Fornari, Alessi, and Kikic (1990), Dohrn and Brunner (1995), Christov and Dohrn (2002), Dohrn, Peper, and Fonseca (2010), Fonseca, Dohrn, and Peper (2011), Dohrn, Fonseca, and Peper (2012) and Peper, Fonseca, and Dohrn (2019).

Figure 16 - Classification of high-pressure phase equilibrium experimental methods.



Adapted from (PEPER et al. 2019)

Synthetic methods, when compared to analytical methods, are better applied to mixtures in vicinity of the critical point and require a cell with smaller dimensions and fewer components to assemble the equipment. In addition, they may not be recommended for some multicomponent systems, and can present errors related to the preparation of the mixture and to the detection of the phase transition (PEPER et al. 2019).

2.5 THERMODYNAMIC MODELS

Obtaining experimental data on phase behavior becomes a potentially expensive operation for complex multicomponent systems, where there is a need to investigate in detail wide ranges of temperature, pressure and composition, as small

changes in these conditions can be important. Furthermore, available information in the literature is not necessarily within the operational range of an industrial process. Due to these reasons, it becomes necessary to develop and use predictive methods to calculate phase equilibrium and thermophysical properties of components (SHAAHMADI et al., 2023).

In 1983, professor John M. Prausnitz wrote (PRAUSNITZ et al., 1983):

“At present, applied thermodynamics is a tool box with very many tools, each designed for a particular job. I expect that, if current trends continue, in a few years we will have not only better tools but also fewer tools for covering a much wider range of problems.”

Although nearly 40 years have passed, a wide variety of thermodynamic models, called equations of state (EoS), are still used to determine the physico-chemical conditions of systems at equilibrium for a wide variety of industries, such as biochemical, petrochemical, pharmaceutical, and others. The development of a single model with absolute applicability is extremely difficult due to the great diversity of chemical species and their interactions over distinct temperatures, pressures, and concentration. Moreover, this model would lack simplicity, requiring multiple adjustable parameters and probably taking long computational times to converge, which is not desired for simple systems (KONTOGEOORGIS et al., 2020).

The a few examples of equations of state can be divided as following (KONTOGEOORGIS; FOLAS, 2010; KONTOGEOORGIS et al., 2020):

- Virial equation
- Multiparameter Eos
- Cubic EoS
 - Van der Waals
 - Peng-Robinson
 - Soave-Redlich Kwong
- Association models
 - Chemical Theories
 - Associated Perturbed Anisotropic Chain Theory (APACT)
 - Lattice-Fluid Theories
 - Perturbation Theories

- Statistical Associating Fluid Theory (SAFT)
- Elliot-Suresh-Donohue (ESD)
- Cubic Plus Association (CPA)
- Perturbed Chain Statistical Associating Fluid Theory (PC-SAFT)

Each model has its advantages and limitations, which, for cubic equations and for SAFT, will be detailed later. Furthermore, Kontogeorgis et al. (2020) also reminded the quotation from the British statistician George E. P. Box: “Essentially, all models are wrong, but some are useful”.

2.5.1 Cubic equations of state

Polynomial equations that are cubic in molar volume (v) are known as cubic EoS. They are simple and fast methods, applicable over a wide range of temperature and pressure, with a positive performance at predicting phase equilibrium and thermophysical properties. However, these classic models may not be suitable for complicated VLE of polar mixtures, LLE of highly immiscible systems, solid-liquid equilibrium with associating fluids, and equilibrium of complex compounds such as biomolecules and electrolytes (KONTOGEOORGIS; FOLAS, 2010).

The most well-known Eos, which are the van der Waals (vdW), Redlich-Kwong (RK), Soave-Redlich-Kwong (SRK), and Peng-Robinson (PR), can be described by the generic cubic equation of state for pure components at Equations 8-11 (SMITH; VAN NESS; ABBOT, 2018).

$$P = \frac{RT}{v - b} - \frac{a(T)}{(v + \epsilon b)(v + \sigma b)} \quad 8$$

$$a(T) = \Psi \frac{\alpha(T_r; \omega) R^2 T_c^2}{P_c^2} \quad 9$$

$$b = \Omega \frac{RT_c}{P_c} \quad 10$$

$$T_r = \frac{T}{T_c} \quad 11$$

where R is ideal gas constant, $a(T)$ is the attraction term, b is the repulsion term, ϵ , σ , Ψ and Ω are numbers that vary accordingly to the model, and the function $\alpha(T_r; \omega)$ varies with the compound, temperature, and EoS, as indicated in Table 1. ω is the acentric factor of the substance, which represents the non-sphericity of a molecule.

Table 1 – Parameters of cubic EoS.

EoS	$\alpha(T_r; \omega)$	ϵ	σ	Ψ	Ω
vdW	1	0	0	0.42188	0.12500
RK	$T_r^{-1/2}$	0	1	0.42748	0.08664
SRK	$\alpha_{\text{SRK}}(T_r; \omega)^1$	0	1	0.42748	0.08664
PR	$\alpha_{\text{PR}}(T_r; \omega)^2$	$1 + \sqrt{2}$	$1 - \sqrt{2}$	0.45724	0.07780

¹ $\alpha_{\text{SRK}}(T_r; \omega) = [1 + (0.480 + 1.574 \omega - 0,176 \omega^2)(1 - T_r^{1/2})]^2$

² $\alpha_{\text{PR}}(T_r; \omega) = [1 + (0.37464 + 1.54226 \omega - 0,26992 \omega^2)(1 - T_r^{1/2})]^2$

Source: adapted from SMITH; VAN NESS; ABBOT, 2018.

These equations can be further implemented for mixtures with the van der Waals quadratic mixing rule (vdW2), as follows in Equations 12 and 13.

$$\alpha(T) = \sum_{i=1}^n \sum_{j=1}^n x_i x_j \sqrt{a_i(T) a_j(T) (1 - k_{ij})} \quad 12$$

$$b = \sum_{i=1}^n \sum_{j=1}^n x_i x_j \frac{1}{2} (b_i + b_j) (1 - l_{ij}) \quad 13$$

where n is the number of components in the mixture, i indicates the first substance, j indicates the second substance, and k_{ij} and l_{ij} are adjustable binary interaction parameters.

2.5.2 Association models

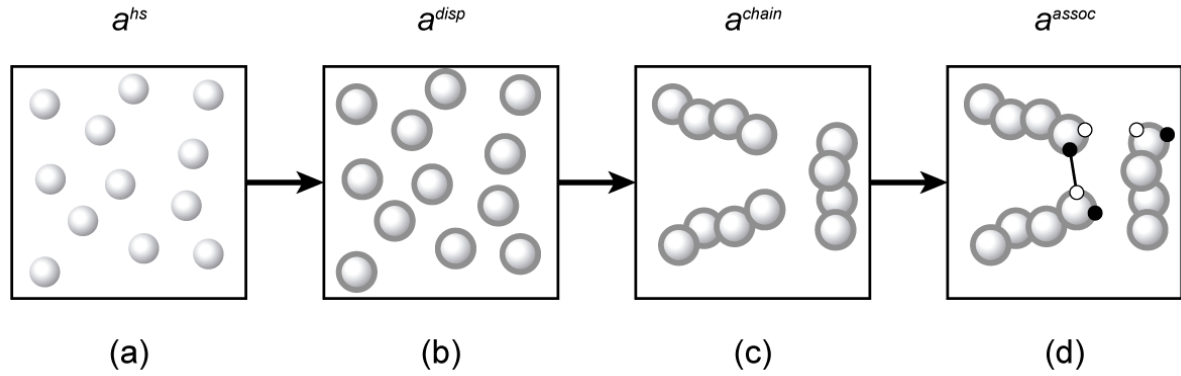
Methods capable of describing the effects of highly polar molecules able to form hydrogen bonds are called association models. They can be classified as chemical, lattice, or perturbation. Chemical theories have the number of oligomers formed in a system as the extent of association, which is a function of composition, density, and temperature. Lattice, or quasi-chemical, theories determine the extent of association as the number of bonds formed by distinct molecules at close proximity sites in the lattice. Lastly, for perturbation theories, statistical mechanics calculations are used to determine the total energy of hydrogen bonding and the number of bonding sites (KONTOGEORGIS; FOLAS, 2010).

2.5.3 The SAFT equations

Statistical associating fluid theory describes a series of models based on the first order perturbation theory of Wertheim and are defined by five parameters for associating fluids, or three for non-associating ones: the number of segments in a molecule (m_i), segment diameter (σ_i), segment energy parameter or depth of potential well (ϵ_i/k), volume of association ($\kappa^{A_iB_j}$), and energy of association ($\epsilon^{A_iB_j}$). Being the last two only required for self-associating fluids like pure water or pure methanol (KONTOGEORGIS; FOLAS, 2010; CHAPMAN, et al., 1989).

Figure 17 shows the steps which contribute to the Helmholtz energy at Equation 14. In Figure 17a a reference fluid is considered to consist of hard spheres with equal diameter σ_i ; Figure 17b has the dispersive potential of magnitude ϵ_i added due to attraction between spheres; shown in Figure 17c is the formation of chain molecule from m_i connected segments; and lastly in Figure 17d chains are able to associate through attractive interaction at certain sites, these associations has an energy $\epsilon^{A_iB_j}$ and are describe in a volume $\kappa^{A_iB_j}$ (KONTOGEORGIS; FOLAS, 2010; SHAAHMADI et al., 2023; CHAPMAN, et al., 1989).

Figure 17 - Procedure to form a molecule in SAFT-framework.



Source: adapted from SHAAHMADI et al., 2023

$$a^{res} = a^{hs} + a^{disp} + a^{chain} + a^{assoc} \quad 14$$

Which can also be represented as:

$$a^{res} = a^{seg} + a^{chain} + a^{assoc} \quad 15$$

where a^{res} is the residual Helmholtz energy, a^{seg} is the Helmholtz energy of the segment that includes the hard-sphere reference a^{hs} and the dispersion term a^{disp} , a^{chain} is the contribution from chain formation, and a^{assoc} is the contribution from association. These terms are given by the equations 16-29.

$$\frac{a^{chain}}{RT} = \sum_i x_i (1 - m_i) \ln(g_{ii}(d_{ii})^{hs}) \quad 16$$

$$\frac{a^{assoc}}{RT} = \sum_i x_i \left[\sum_{A_i} \left(\ln X^{A_i} - \frac{X^{A_i}}{2} \right) + \frac{1}{2} M_i \right] \quad 17$$

$$X^{A_i} = \left[1 + \sum_j \sum_{B_j} \rho_j X^{B_j} \Delta^{A_i B_j} \right] \quad 18$$

$$\Delta^{A_i B_j} = \sigma_{ij}^3 g_{ij}(\sigma_{ij})^{seg} \kappa^{A_i B_j} [\exp(\epsilon^{A_i B_j}/kT) - 1] \quad 19$$

where d_{ii} is the temperature-dependent diameter, g_{ii} is the radial distribution function, X^{A_i} is the fraction of molecules i not bonded at site A , M_i is the number of association sites on molecule i , ρ_j is the molar density of j , and $\Delta^{A_i B_j}$ is the association strength between two sites A and B from molecules i and j .

$$\frac{d}{\sigma} = 1 + \frac{0.2977kT/\epsilon}{1 + 0.33163kT/\epsilon + f(m)(kT/\epsilon)^2} \quad 20$$

$$f(m) = 0.0010477 + 0.025337 \frac{(m-1)}{m} \quad 21$$

$$g_{ij}^{seg}(d_{ij}) \approx g_{ij}^{hs}(d_{ij}^+) = \frac{1}{1 - \xi_3} + \left(\frac{d_i d_j}{d_i + d_j} \right) \frac{3\xi_w}{(1 - \xi_3)^2} + \left(\frac{d_i d_j}{d_i + d_j} \right)^2 \frac{2\xi_w^2}{(1 - \xi_3)^3} \quad 22$$

$$\xi_k = \frac{\pi N_{AV}}{6} \rho \sum_i X_i m_i d_{ii}^k \quad 23$$

Modifications to the original dispersion term of the original SAFT proposed by Chapman et al. (1989) resulted in groups of variations, such as CK-SAFT, simplified SAFT, LJ-SAFT, soft-SAFT, SAFT-VR, GC-SAFT, and the most well-known and used variation PC-SAFT (KONTOGEOORGIS; FOLAS, 2010; KONTOGEOORGIS et al., 2020).

Gross and Sadowski (2001) proposed the following dispersion term for perturbed chain SAFT (PC-SAFT), which uses hard-chain fluids instead of spherical molecules as a reference:

$$\frac{a^{disp}}{kTN} = \frac{A_1}{kTN} + \frac{A_2}{kTN} \quad 24$$

$$\frac{A_1}{kTN} = -2\pi\rho m^2 \left(\frac{\epsilon}{kT} \right) \sigma^3 \sum_{i=0}^6 a_i \eta^i \quad 25$$

$$\frac{A_2}{kTN} = -\pi\rho m^3 \left(1 + m \frac{8\eta - 2\eta^2}{(1-\eta)^4} + (1-m) \frac{20\eta - 27\eta^2 + 12\eta^3 - 2\eta^4}{((1-\eta)(2-\eta))^2} \right) \left(\frac{e}{kT} \right)^2 \sigma^3 \sum_{i=0}^6 b_i \eta^i \quad 26$$

$$\eta = \xi_3 \quad 27$$

$$a_i = a_{0i} + \frac{m-1}{m} a_{1i} + \frac{m-1}{m} \frac{m-2}{m} a_{2i} \quad 28$$

$$b_i = b_{0i} + \frac{m-1}{m} b_{1i} + \frac{m-1}{m} \frac{m-2}{m} b_{2i} \quad 29$$

where the universal model constants are indicated in Table 2.

Table 2- Universal model constants in PC-SAFT EoS.

i	a_{0i}	a_{1i}	a_{2i}	b_{0i}	b_{1i}	b_{2i}
0	0.9105631	-0.3084016	-0.0906148	0.7240946	-0.5755498	0.0976883
1	0.6361281	0.1860531	0.4527842	2.2382791	0.6995095	-0.2557574
2	2.6861347	-2.5030047	0.5962700	-4.0025849	3.8925673	-9.1558561
3	-26.5473624	21.4197936	-1.7241829	-21.0035768	-17.2154716	20.6420759
4	97.7592087	-65.2558853	-4.1302112	26.8556413	192.6722644	-38.8044300
5	-159.5915408	83.3186804	13.7766318	206.5513384	-161.8264616	93.6267740
6	91.2977740	-33.7469229	-8.6728470	-355.6023561	-165.2076934	-29.6669055

Source: Gross and Sadowski (2021).

Among SAFT variants, PC-SAFT has been used to model systems with compounds presenting high asymmetry, polar and associative mixtures, and phase equilibrium for polymers. Although this equation calculates vapor pressure and liquid density with excellent correlation, the vicinity of the critical point is often overestimated. Therefore, it may not be adequate, without additional modifications, to validate with

experimental data from phase equilibrium close to critical conditions (KONTOGEORGIS; FOLAS, 2010; GROSS; SADOWSKI, 2001).

2.6 STATE OF THE ART

Systems containing carbon dioxide and ϵ -Caprolactone, ω -pentadecalactone, or globalide, with or without the presence of a cosolvent, that already had their phase behavior studied are shown in Table 3. Binary mixtures of carbon dioxide and cosolvents used in ternary system studies are also present. This table contains information about temperature and pressure ranges for each referenced work.

As evidenced by the Table 3, data for phase equilibria of all the binary systems of carbon dioxide with a monomer or with a cosolvent have already been reported. Moreover, ternary mixtures of carbon dioxide, a monomer, and the cosolvent chloroform or dichloromethane, also was investigated for both ϵ -caprolactone and ω -pentadecalactone, although, for globalide the only ternary system studied was with dichloromethane as a cosolvent. Therefore, it becomes clear that there is a gap in the literature about phase behavior studies of carbon dioxide, globalide, and chloroform.

Furthermore, usage of the PC-SAFT to fit experimental data for high-pressure phase equilibrium systems containing polymers has shown good performance. In recent works, Mayer et al. (2020) and Nascimento et al. (2020) applied this thermodynamic model in mixtures with ϵ -caprolactone and poly(ϵ -caprolactone), and with ω -pentadecalactone and poly(ω -pentadecalactone), respectively. These works validated experimental data of ϵ -caprolactone or ω -pentadecalactone with SAFT equations, thus, the pure-component parameters m_i , σ_i , and ϵ/k had to be estimated by fitting to density and vapor pressure data. As globalide is a molecule that has recently started to be investigated, no information was found in literature regarding its density and vapor pressure data.

Table 3- Overview of the existing works in the literature about phase equilibrium data of ϵ -caprolactone, ω -pentadecalactone, globalide, chloroform, and dichloromethane in high pressures.

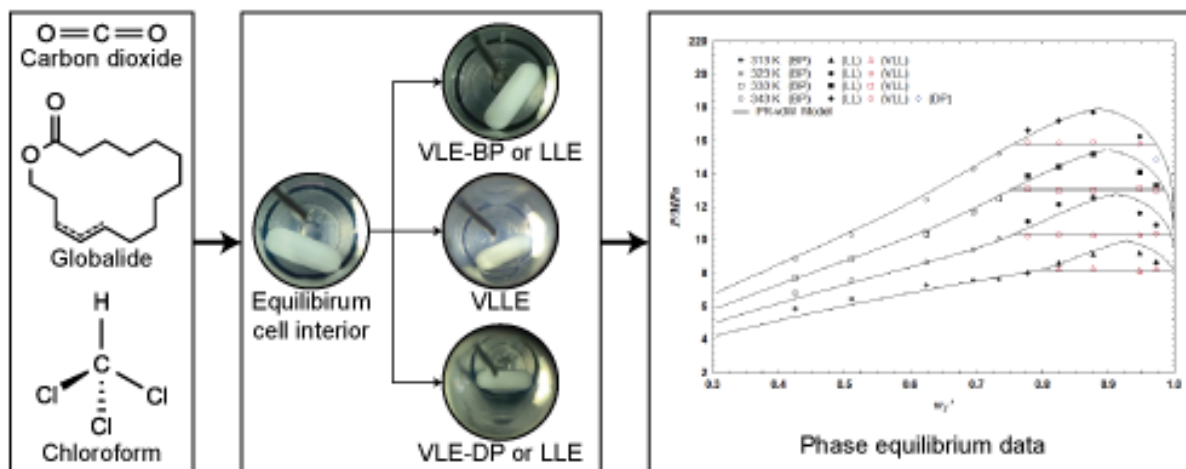
System	T/K	P/MPa	References
	313.15 - 363.15	3.46 - 20.83	Xu et al., 2003
CO ₂ + ϵ -CL	323.15 - 383.15	7.48 - 33.90	Bergeout et al., 2004
	303.15 - 343.15	3.46 - 20.83	Bender et al., 2010
CO ₂ + ω -PDL	303.15 - 343.15	5.40 - 25.43	Rebelatto et al., 2018a
CO ₂ + GL	313.15 - 343.15	6.98 - 25.55	Rebelatto et al., 2020
	303.15 - 333.15	0.03 - 9.84	Scurto et al., 2001
CO ₂ + CHCl ₃	278.30 - 371.25	0.74 - 12.00	Peters; Florusse, 1995
	291.15 - 311.15	1.94 - 5.91	Stievano; Elvassore, 2005
CO ₂ + CH ₂ Cl ₂	308.15 - 328.15	1.49 - 8.85	Tsvintzelis et al., 2004
CO ₂ + ϵ -CL + CHCl ₃	323.15 - 353.15	4.68 - 21.85	Girardi et al., 2021
CO ₂ + ϵ -CL + CH ₂ Cl ₂	323.15 - 353.15	5.05 - 25.75	Mayer et al., 2019
CO ₂ + ω -PDL + CHCl ₃	313.15 - 343.15	5.60 - 21.02	Rebelatto et al., 2018a
CO ₂ + ω -PDL + CH ₂ Cl ₂	313.15 - 343.15	3.62 - 19.46	Rebelatto et al., 2018b
CO ₂ + GL + CH ₂ Cl ₂	313.15 - 343.15	3.55 - 19.36	De Quadros et al., 2022

3 HIGH PRESSURE PHASE EQUILIBRIUM DATA FOR THE TERNARY SYSTEM CONTAINING CARBON DIOXIDE, CHLOROFORM AND GLOBALIDE

Abstract

Clean industrial polymerization for the production of biocompatible and nontoxic polymer has received an increasing interest, and, therefore, research studies into these processes are necessary to accompany this growing demand. Poly(globalide), one of those polymers, is a polyester with an unsaturated main carbon chain that allows a variety of functionalizations to the polymer, which makes this material attractive to biomedical applications. It is synthesized by the ring-opening polymerization reaction of its macrolactone monomer named globalide. An alternative to traditional processes is the employment of greener solvents, such as supercritical carbon dioxide, and the use of enzymes, instead of metal catalysts. Rather than operating exclusively with organic solvents, the use of supercritical carbon dioxide reduces the volume of toxic waste to the environment, and circumvents the need for further purification steps. Nevertheless, small quantities of organic solvents, such as chloroform, are desired to promote a better solubilisation and production of higher molar mass polymers. In order to gather crucial data to conduct polymerization reactions in supercritical medium, the high-pressure phase behavior of the ternary system constituted by carbon dioxide + globalide + chloroform was studied. The experiments were conducted applying the static-synthetic method in a variable-volume view cell at a mass ratios of globalide to chloroform of 0.5:1, 1:1, and 2:1, over a temperature range from 313.15 to 343.15 K, and pressures from 5.17 to 20.25 MPa. Phase transitions of vapor-liquid bubble point (VLE-BP), vapor-liquid dew point (VLE-DP), liquid-liquid (LLE), and vapor-liquid-liquid (VLLE) type were observed. Through the P-w diagram, the phase behavior of the ternary system in chloroform free-basis was analyzed between 42.50% to 97.35% of carbon dioxide mass composition. The data presented in this work provides necessary information for the optimization and improvement of poly(globalide) synthesis in supercritical media.

Graphical abstract



3.1 INTRODUCTION

Recently, regulations worldwide have driven the production of greener plastics and plastic processes. Among biocompatible and biodegradable plastics, in the last few decades, polyesters synthesized from lactones have been used for pharmaceutical and biomedical applications, due to suitable thermal, chemical and mechanical properties (WILSON, et al., 2019). These polymers and copolymers are more commonly applied in drug-delivery devices and in tissue engineering, and have been also implemented for fertilizer, automotive, and packaging applications (TSUTSUMI et al., 2019; BIŃCZAK et al., 2021). It has been reported that both mechanical and thermal properties, and biodegradation rates can be adjusted by modifying the polymer's crystalline phase by copolymerization, which is the reaction between two distinct monomers, and by functionalization with other chemical species. Nevertheless, the production of these polymers must be carefully planned, as incorrect choices of solvents, catalysts, and initiators can impede medical, pharmaceutical, and food application, due to possible toxic components among those options (HEGE et al., 2014; BIŃCZAK et al., 2021).

Globalide (GL) is an unsaturated macrolactone with a 16-membered ring that contains one unsaturated bond. It is a colorless to pale yellow liquid that has a strong odor which is commonly described as sweet musk waxy, woody, or herbal. (TGSC, c2021b; API et al., 2022). Although this non-toxic and biodegradable material can be found in a variety of cleaning and cosmetic products, recent studies have investigated the polymerization (VAN DER MEULEN et al., 2008; CHIARADIA et al., 2018;

POLLONI et al., 2018; GUINDANI et al., 2022) and the copolymerization (GUINDANI et al., 2017; TINAJERO-DÍAZ et al., 2019; TINAJERO-DÍAZ et al., 2019) of the globalide, as well as the functionalization of its polymer poly(globalide) (ATES et al., 2014; CHIARADIA et al., 2019; POLLONI et al., 2020; AMARAL et al., 2020; OLIVEIRA et al., 2022), and of the copolymer poly(globalide-co- ϵ -caprolactone (CLAUDINO et al., 2012; GUINDANI et al., 2019a; GUINDANI et al., 2019b; BELTRAME et al., 2021).

In order to achieve suitable and safe polyesters for biomedical and food applications, the usage of enzymatic catalysts, instead of conventional metallic complexes, has received growing attention. Although most works conducting the polymerization of lactones use toluene as a solvent, recently, the use of supercritical carbon dioxide has been proposed, since it turns possible to recover both the solvent and the enzyme as the process ends (POLLONI, et al., 2017; GUINDANI et al., 2017; GUALANDI et al., 2010).

A reliable supercritical fluid for industrial processes is carbon dioxide (CO_2), as its critical point is easily achievable, having a critical temperature of 31.04 °C and a critical pressure of 7.38 MPa (REBELATTO, 2018). It is a low cost, non-flammable, inert solvent with low toxicity available in high purity that can be easily separated at ambient temperature and pressure from the final reaction product and be recycled in the process (LEITNER, 2000; COMIM et al., 2013). The use of supercritical CO_2 in enzymatic ring-opening polymerization with Globalide and other's lactone as monomers has shown similar results when working with the organic solvent toluene (GUINDANI, 2018; POLLONI, 2018).

Just as the density of a supercritical fluid varies as temperature and pressure change, the solubility of a monomer in supercritical CO_2 can be adjusted as variation on these conditions occurs (TU et al., 2002). Moreover, as the polymerization takes place the chemical composition of the system changes, and higher pressures are needed to solvate the developed polymer and to achieve higher molecular weights (NUNES DA PONTE, 2009; NASCIMENTO, 2019). Therefore, to better comprehend how these properties behave, and to achieve a single phase medium, as multi-phase systems disturbs the efficiency of polymerization through mass transfer interfacial resistance between solvent phases, the study of phase equilibrium of systems containing the reaction compounds becomes indispensable (BENDER, 2008).

Although it may seem contradictory, new studies investigated the effect of toxic organic compounds, such as chloroform and dichloromethane, as cosolvents for polymerization under supercritical CO₂ media. Those cosolvents have lower boiling temperatures than toluene, 61.2 °C and 40.0 °C respectively, thus they can be more easily pulled apart from the polymer as the system depressurizes and CO₂ turns from a supercritical fluid into a gas (REBELATTO, 2018; NASCIMENTO, 2019, MAYER, 2020). Recently, De Quadros et al. (2022) collected phase equilibria data for the system containing carbon dioxide + dichloromethane + globalide in order to compare with the binary data of carbon dioxide + globalide gathered by Rebelatto et al. (2020). Hence, the study of the ternary system containing chloroform as a cosolvent becomes necessary to better evaluate the conditions under which polymerization begins.

According to these remarks, the aim of this work is to study phase equilibria data of the ternary system carbon dioxide + chloroform + globalide. The experimental data was gathered over a temperature range of 313.15 K to 343.15 K with different concentrations of the compounds maintaining the globalide to chloroform mass ratios of 0.5:1, 1:1, and 2:1. Furthermore, the Peng-Robinson equation of state was used with van der Waals mixing rule to compare with the experimental values.

3.2 MATERIAL AND METHODS

3.2.1 Materials

The main solvent for the ternary system, carbon dioxide (0.999 mass fraction purity in liquid phase), was purchased from White Martins S.A. (Brazil). The cosolvent chloroform (0.998 mass fraction purity) was provided by NEON (Brazil). Furthermore, the monomer globalide was purchased from Symrise (Brazil). To achieve the water content in mass fraction of 0.0032 with standard uncertainty of 0.0001, the monomer was dried in a vacuum oven at 373.15 K and 0.01 MPa during 48 h and its water quantity was measured by Karl Fischer Coulometric Titrator (HI-904 – HANNA instruments). Table 4 provides for each compound used in this work the chemical name, molecular formula, CAS Registry Number, provenance, purification method, and minimum mass fraction purity, the last provided by the supplier.

Table 4 - Chemical name, molecular formula, provenance, purification method and purity of the materials.

Chemical name	Molecular formula	CAS Number	Supplier	Purification method	Minimum mass fraction purity
Carbon dioxide	CO ₂	124-38-9	White Martins S.A.	None	0.999
Chloroform	CHCl ₃	67-66-3	NEON	None	0.970
Globalide	C ₁₅ H ₂₆ O ₂	34902-57-3	Symrise	^a Dried	0.998

Caption: ^a The globalide was dried at 373.15 K under a vacuum of 0.01 MPa for 48 h.

Source: Prepared by the authors.

3.2.2 Phase equilibrium apparatus and procedure

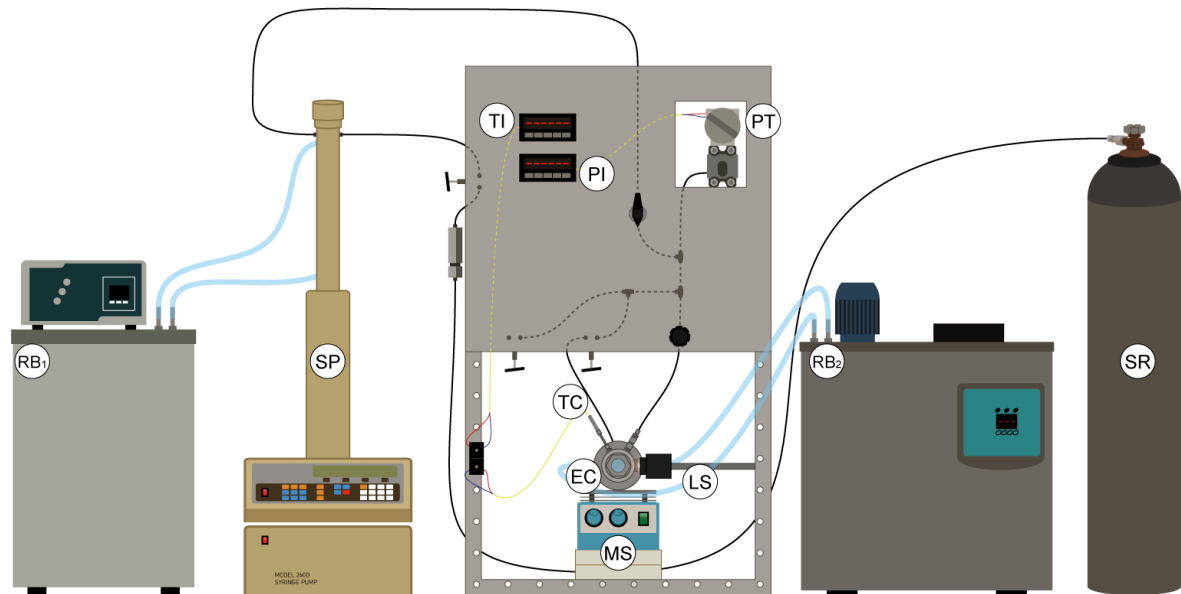
To determine the occurrence of a phase transition, the synthetic-visual method was employed while observing through a high-pressure variable-volume view cell. This method consists of the visual observation of phase transitions in a mixture with a precise known composition. The following experimental apparatus and procedure have also been followed and described in a variety of studies (NASCIMENTO et al., 2020; REBELATTO et al., 2020; GIRARDI et al., 2021; DE QUADROS et al., 2022).

The phase equilibrium apparatus consists of eleven laboratory equipment, as shown in Figure 18, and six valves, represented at Figure 19. A scheme of the unassembled variable-volume view cell is shown in Figure 20.

Carbon dioxide is stored in the solvent reservoir (SR), which is connected to the syringe pump (SP). This pump allows a controlled volume feed of solvent inside the equilibrium variable-volume view cell (EC), and the further control of pressure as the experiments take place. To ensure a constant temperature as the equilibrium cell is fed with carbon dioxide, a recirculation bath (RB₂) is maintained at a fixed temperature of 280.15 K. A pressure transistor (PT) measures the pressure applied to the cylindrical piston inside the cell, this pressure can be visualized by the pressure indicator (PI). The equilibrium cell is supported by a magnetic stirrer (MS), which induces movement to the magnetic bar that is inside the cell and promotes the system homogenization. Controlling the temperature of the system is done by connecting the cell's jacket to another recirculation bath (RB₁). As heat is lost from the bath to the

jacket, a thermocouple (TC) is fitted inside the cell to measure the system's temperature precisely, this temperature is displayed by the temperature indicator (TI). At last, to facilitate the visualization of the phase transition, a light source (LS) is placed by a lateral sapphire window at the cell.

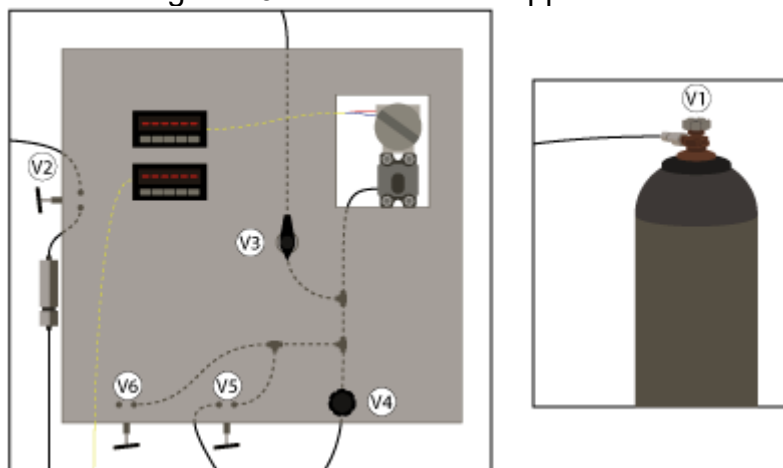
Figure 18 – High-pressure phase equilibrium apparatus.



Source: the author.

The six valves are installed to ensure control and safety procedures. A ball valve (V1) connected to the solvent reservoir is used to carry carbon dioxide to the syringe pump and to guarantee that solvent is not wasted. A check valve (V2) is attached to the syringe pump and secures the unidirectional flow of the solvent. Another ball valve (V3) is installed at the center of the workbench board, this is a safety measure that must be closed to separate the syringe pump in case of gas leakage in the cell. The micrometric valve (V4) allows the flow of solvent inside the cell, which is controllable through the volume display of the syringe pump. Carbon dioxide can exert pressure to the cell's piston by the opening of a ball valve (V5). Furthermore, a fourth ball valve (V6) is used to depressurize the system as the experiments conclude.

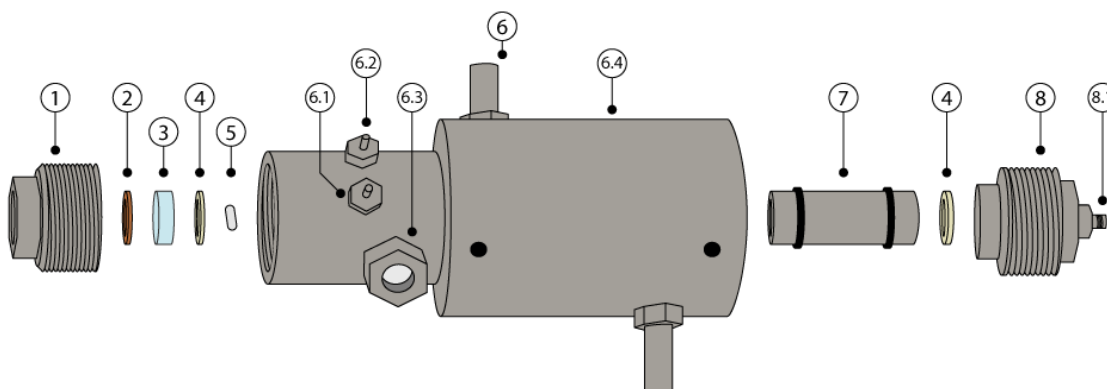
Figure 19 – Valves of the Apparatus.



Source: the author.

The variable-volume view cell (no. 6) must be assembled for each different composition of the system. Before inserting the chemical compounds in the cell, the piston (no. 7) must be put together and placed at the back end of the equipment. A sealing ring (no. 4) is positioned between the cell's back end and the back thread (no. 8). As the synthetic visual method determines, accurate masses of globalide, followed by carefully measured masses of chloroform, were weighted on a precision scale balance (Shimadzu, Model AY220 with 0.0001 g accuracy) and placed inside the equilibrium cell, by the front end. The magnetic bar (no. 5) is also put in the front of the cell, followed by another sealing ring (no. 4), the carefully placed sapphire window (no. 3), a copper ring (no. 2), and then the front thread (no. 1).

Figure 20 – Unassembled equilibrium cell.



Source: the author.

The assembled cell is settled at the magnetic stirrer and attached to the micrometric valve (V4) through the feeding connection (no. 6.1) and to the thermocouple through the thermocouple connection (no. 6.2). Under constant pressure and temperature of 10.0 MPa and 280.15 K, carbon dioxide is allowed to flow through the micrometric valve (V4) with a precision of 0.01 mL. The solvent's density value under the feeding conditions is estimated through the Peng-Robinson equation of state, therefore the volume to mass conversion was performed. Lastly, the equilibrium cell is attached to the ball valve (V5) through the back thread connection (no. 8.1), the equipment jacket (no. 6.4) is connected to the recirculation bath (RB₂) through hoses, and the light source was placed by the lateral sapphire window (no. 6.3).

For each composition, the phase behavior was determined under fixed temperatures of 313.15, 323.15, 333.15, and 343.15 K. At said conditions, the system was homogenized through increases in pressure and through magnetic stirring, achieving a single-phase. Hereafter, the system would be exposed to a small negative pressure gradient, maintaining a constant temperature, so that a phase transition could be visualized in the imminence of its appearance. The transition pressure was observed in triplicate for each temperature and composition.

Figure 21- Synthetic-visual method.



Source: the author.

Figure 21 shows the inside of the equilibrium cell at a single phase region and the visual determination of transitions threshold. Vapor-liquid equilibrium bubble point (VLE-BP) and dew point (VLE-DP) are characterized by the appearance of a small bubble at the top, or droplets at the bottom, of the visualization chamber, respectively. The emergence of a non-bubble misty phase stretching at the top of the cell characterize a liquid-liquid equilibrium (LLE) and can be confirmed if followed, as

pressure values decreases, by a second meniscus formation at the bottom, which characterize a vapor-liquid-liquid equilibrium (VLLE).

Under the temperature range of 313.15 K to 343.15 K and pressures spanning from 5.14 MPa to 20.25 MPa, phase equilibrium data of the ternary system {carbon-dioxide (1) + chloroform (2) + globalide (3)} were obtained for the globalide to chloroform mass ratios of 0.5:1, 1:1, and 2:1. Carbon dioxide mass fractions varied from 0.2593 to 0.9608.

3.2.3 Thermodynamic models

The Peng-Robinson equation of state (PENG; ROBINSON, 1976) with the van der Waals quadratic mixing rule (PR-vdW2), equations 30 to 35 was employed to validate the obtained experimental data. The required characteristics of the pure compounds, molar mass $M(\text{g}\cdot\text{mol}^{-1})$ critical temperature T_c (K), critical pressure P_c (MPa) and acentric factor ω , are shown in Table 5.

$$P = \frac{RT}{v - b} - \frac{a(T)}{v(v + b) + b(b - v)} \quad 30$$

$$a = \sum_{i=1}^n \sum_{j=1}^n x_i x_j \sqrt{a_i a_j} (1 - k_{ij}) \quad 31$$

$$b = \sum_{i=1}^n \sum_{j=1}^n x_i x_j \frac{1}{2} (b_i + b_j) (1 - l_{ij}) \quad 32$$

$$a_i = 0.45724 \left[1 + (0.37464 + 1.5422\omega - 0.26992\omega^2) (1 - R_r^{1/2}) \right] \frac{RT_c^2}{P_c^2} \quad 33$$

$$b_i = 0.07780 \frac{RT_c}{P_c} \quad 34$$

$$T_r = \frac{T}{T_c} \quad 35$$

Table 5 - Characteristics of pure compounds.

Compound	M/(g·mol ⁻¹)	Tc/K	Pc/MPa	ω
Carbon dioxide	44.01	304.12 ^a	7.37 ^a	0.2250 ^a
Chloroform	119.38	536.40 ^b	5.47 ^b	0.2220 ^b
Globalide	238.37	840.33 ^c	2.44 ^c	0.5876 ^c

Source: ^a POLING; PRAUSNITZ; O'CONNELL, 2001

^b SMITH; VAN NESS; ABBOTT, 2018

^c REBELATTO et al., 2020

The model was conducted using a FORTRAN code implemented by Ferrari et al. (2009), which estimated the binary interaction parameters k_{ij} and l_{ij} using the Simplex method to minimize the objective function (OF) shown in equation 36. The generated residues are computed by absolute deviation (AD) and root-mean-square deviation (rmsd), equations 37 and 38, respectively.

$$OF = \sum_{i=1}^{nobs} (P_i^{cal} - P_i^{exp}) \quad 36$$

$$AD = \sum_{i=1}^{nobs} \frac{|P_i^{cal} - P_i^{exp}|}{nobs} \quad 37$$

$$rmsd = \sqrt{\sum_{i=1}^{nobs} \frac{(P_i^{cal} - P_i^{exp})^2}{nobs}} \quad 38$$

where $nobs$ is the number experimental observations, P_i^{exp} is the arithmetic mean of three transition pressure measurements, P_i^{cal} denotes the calculated pressure by the model.

3.3 RESULTS AND DISCUSSION

In order to investigate the effects of adding chloroform in a system containing carbon dioxide and globalide, the experimental results are presented in cosolvent free-basis. Representing data this way allows direct comparison between the binary system [CO₂ (1) + GL (2)] and the ternary system [CO₂ (1) + GL (2) + CHCl₃ (3)], and facilitates the graphical visualization through pseudobinary diagrams. Moreover, this representation has been largely reported in other works (ZHANG et al., 2013; MAYER et al., 2019; GIRARDI et al., 2021; DE QUADROS et al., 2022). Table 6 shows both the cosolvent free-basis composition, w'_1 and w'_2 , and the overall composition, w_1 , w_2 and w_3 , of the ternary system.

The experimental phase transition data of the systems at globalide to chloroform mass ratio of 0.5:1, 1:1, and 2:1 are respectively presented in Table 7, Table 8, and Table 9. These tables contain information about the cosolvent free-basis composition w'_1 and w'_2 , the temperature T , and the pressure P at the threshold of the phase transition, as well as the type of the transition. For vapor-liquid equilibrium, both bubble point (VLE-BP) and dew point (VLE-DP) were observed at distinct conditions. Liquid-liquid equilibrium (LLE) and vapor-liquid-liquid (VLLE) were reported at different pressures for the same composition and temperature. Furthermore, as the experiments were conducted in triplicate, the standard deviation of pressure (sd) is also shown.

The data at Table 7, Table 8, and Table 9 are used to create a Pw -diagrams for the system at distinct globalide to chloroform mass ratios. These diagrams are presented in Figure 22, Figure 23, and Figure 24, which also show the calculated phase equilibrium data as continuous lines.

For the proportion of 0.5:1, shown in Table 7 and Figure 22, higher concentrations of cosolvents are found, which leads to lower transition pressures as the chloroform promotes the solubilization of the medium. As the pressure decreases, it approaches the operational limit of the equipment, close to the conditions of vaporization of the pressurizing fluid, therefore it was not possible to carry experiments at fractions smaller than $w'_1 = 0.5122$. For all temperatures, vapor-liquid equilibrium bubble point was observed within the composition range from $w'_1 = 0.5122$ to $w'_1 = 0.8776$, although this transition was noticed as well for all mass fractions at 313.15 K. Except for the 313.15 K isotherm, the other showed behavior of vapor-liquid equilibrium dew point at concentrations of $w'_1 = 0.9294$ to $w'_1 = 0.9734$.

Table 6 - Cosolvent free-basis mass fractions and overall mass fraction.

W'1	W'2	W1	W2	W3
Globalide to chloroform mass ratio of 0.5:1				
0.5122	0.4878	0.2593	0.2469	0.4938
0.6234	0.3766	0.3557	0.2148	0.4295
0.6948	0.3052	0.4314	0.1895	0.3791
0.7347	0.2653	0.4799	0.1733	0.3469
0.7774	0.2226	0.5382	0.1541	0.3078
0.8256	0.1744	0.6121	0.1293	0.2586
0.8776	0.1224	0.7045	0.0983	0.1972
0.9294	0.0706	0.8588	0.0469	0.0943
0.9734	0.0266	0.9240	0.0252	0.0508
Globalide to chloroform mass ratio of 1:1				
0.4254	0.5746	0.2705	0.3653	0.3642
0.5113	0.4887	0.3435	0.3283	0.3282
0.6242	0.3758	0.4538	0.2732	0.2730
0.6949	0.3051	0.5327	0.2338	0.2335
0.7344	0.2656	0.5800	0.2098	0.2102
0.7782	0.2218	0.6364	0.1814	0.1821
0.8256	0.1744	0.7032	0.1485	0.1483
0.8776	0.1224	0.7825	0.1091	0.1084
0.9480	0.0520	0.9016	0.0494	0.0490
0.9734	0.0266	0.9482	0.0259	0.0258
Globalide to chloroform mass ratio of 2:1				
0.4249	0.5751	0.3301	0.4467	0.2232
0.5131	0.4869	0.4126	0.3916	0.1958
0.6243	0.3757	0.5255	0.3163	0.1582
0.6940	0.306	0.6035	0.2642	0.1322
0.7353	0.2647	0.6477	0.2348	0.1175
0.7782	0.2218	0.7000	0.2002	0.0998
0.8251	0.1749	0.7588	0.1610	0.0801
0.8602	0.1398	0.8276	0.1151	0.0573
0.9481	0.0519	0.9239	0.0506	0.0255
0.9734	0.0266	0.9608	0.0262	0.0130

Table 7- Phase equilibrium results for the system [CO₂ (1) + GL (2) + CHCl₃ (3)], in chloroform free-basis, at globalide to chloroform mass ratio of 0.5:1.

T/K	P/MPa	sd/MPa	Transition Type	T/K	P/MPa	sd/MPa	Transition Type
$w'_1 = 0.5122$ ($w'_2 = 0.4878$)				$w'_1 = 0.8256$ ($w'_2 = 0.1744$)			
313.15	5.17	0.02	VLE-BP	313.15	7.37	0.03	VLE-BP
323.15	6.19	0.01	VLE-BP	323.15	9.07	0.03	VLE-BP
333.15	6.99	0.03	VLE-BP	333.15	10.89	0.02	VLE-BP
343.15	7.92	0.03	VLE-BP	343.15	13.36	0.02	VLE-BP
$w'_1 = 0.6234$ ($w'_2 = 0.3766$)				$w'_1 = 0.8776$ ($w'_2 = 0.1224$)			
313.15	5.89	0.02	VLE-BP	313.15	7.67	0.02	VLE-BP
323.15	6.94	0.03	VLE-BP	323.15	9.62	0.03	VLE-BP
333.15	8.24	0.03	VLE-BP	333.15	12.14	0.03	VLE-BP
343.15	9.65	0.03	VLE-BP	343.15	14.63	0.04	VLE-BP
$w'_1 = 0.6948$ ($w'_2 = 0.3052$)				$w'_1 = 0.9294$ ($w'_2 = 0.0706$)			
313.15	6.40	0.01	VLE-BP	313.15	8.25	0.02	VLE-BP
323.15	7.62	0.03	VLE-BP	323.15	9.84	0.05	VLE-DP
333.15	9.08	0.04	VLE-BP	333.15	12.32	0.02	VLE-DP
343.15	10.75	0.03	VLE-BP	343.15	14.53	0.03	VLE-DP
$w'_1 = 0.7347$ ($w'_2 = 0.2653$)				$w'_1 = 0.9734$ ($w'_2 = 0.0266$)			
313.15	6.78	0.02	VLE-BP	313.15	8.43	0.03	VLE-BP
323.15	8.12	0.02	VLE-BP	323.15	9.64	0.05	VLE-DP
333.15	9.82	0.03	VLE-BP	333.15	11.96	0.06	VLE-DP
343.15	11.40	0.02	VLE-BP	343.15	13.85	0.06	VLE-DP
$w'_1 = 0.7774$ ($w'_2 = 0.2226$)							
313.15	6.91	0.03	VLE-BP				
323.15	8.45	0.01	VLE-BP				
333.15	10.29	0.02	VLE-BP				
343.15	12.43	0.04	VLE-BP				

w'_1 denotes mass fraction of carbon dioxide on a chloroform free-basis; w'_2 denotes the mass fraction of globalide on a chloroform free-basis; VLE-BP, vapor-liquid-equilibrium type bubble point; VLE-DP, vapor-liquid equilibrium type dew point; LLE, liquid-liquid-equilibrium; VLLE, vapor-liquid-liquid-equilibrium; T , system temperature; P , system pressure; sd, standard deviation. Variable expanded uncertainties with 95% of confidence level: $U(T) = 0.50$ K; $U(P) = 0.10$ MPa; $U(w_1) = 0.0163$; $U(w_2) = 0.0054$; $U(w_3) = 0.0108$.]

Table 8 - Phase equilibrium results for the system [CO₂ (1) + GL (2) + CHCl₃ (3)], in chloroform free-basis, at globalide to chloroform mass ratio of 1:1.

T/K	P/MPa	sd/MPa	Transition Type	T/K	P/MPa	sd/MPa	Transition Type
$w'_1 = 0.4254$ ($w'_2 = 0.5746$)				$w'_1 = 0.8256$ ($w'_2 = 0.1744$)			
313.15	5.84	0.03	VLE-BP	313.15	8.58	0.04	LLE
323.15	6.80	0.03	VLE-BP	313.15	8.22	0.06	VLLE
333.15	7.72	0.05	VLE-BP	323.15	12.17	0.06	LLE
343.15	8.84	0.05	VLE-BP	323.15	10.33	0.07	VLLE
$w'_1 = 0.5113$ ($w'_2 = 0.4887$)				333.15	14.44	0.06	LLE
313.15	6.44	0.06	VLE-BP	333.15	12.97	0.08	VLLE
323.15	7.57	0.06	VLE-BP	343.15	17.19	0.05	LLE
333.15	8.85	0.03	VLE-BP	343.15	15.83	0.09	VLLE
343.15	10.34	0.02	VLE-BP	$w'_1 = 0.8776$ ($w'_2 = 0.1224$)			
$w'_1 = 0.6242$ ($w'_2 = 0.3758$)				313.15	9.11	0.04	LLE
313.15	7.25	0.03	VLE-BP	313.15	8.31	0.05	VLLE
323.15	8.66	0.04	VLE-BP	323.15	12.57	0.04	LLE
333.15	10.38	0.02	VLE-BP	323.15	10.30	0.05	VLLE
343.15	12.44	0.05	VLE-BP	333.15	15.19	0.06	LLE
$w'_1 = 0.6949$ ($w'_2 = 0.3051$)				333.15	13.02	0.07	VLLE
313.15	7.57	0.01	VLE-BP	343.15	17.69	0.03	LLE
323.15	9.42	0.01	VLE-BP	343.15	15.91	0.06	VLLE
333.15	11.71	0.03	VLE-BP	$w'_1 = 0.9480$ ($w'_2 = 0.0520$)			
343.15	14.26	0.04	VLE-BP	313.15	9.23	0.01	LLE
$w'_1 = 0.7344$ ($w'_2 = 0.2656$)				313.15	8.19	0.07	VLLE
313.15	7.64	0.03	VLE-BP	323.15	11.63	0.01	LLE
323.15	10.10	0.04	VLE-BP	323.15	10.27	0.06	VLLE
333.15	12.49	0.03	VLE-BP	333.15	14.08	0.03	LLE
343.15	15.23	0.05	VLE-BP	333.15	12.10	0.09	VLLE
$w'_1 = 0.7782$ ($w'_2 = 0.2218$)				343.15	16.27	0.02	LLE
313.15	8.00	0.04	VLE-BP	343.15	15.79	0.10	VLLE
323.15	11.12	0.06	LLE	$w'_1 = 0.9734$ ($w'_2 = 0.0266$)			
323.15	10.26	0.05	VLLE	313.15	8.66	0.02	LLE
333.15	13.83	0.04	LLE	313.15	8.26	0.02	VLLE
333.15	13.07	0.04	VLLE	323.15	10.90	0.04	LLE
343.15	16.62	0.05	LLE	323.15	10.38	0.06	VLLE
343.15	15.88	0.06	VLLE	333.15	13.28	0.07	LLE
				333.15	13.03	0.07	VLLE
				343.15	14.83	0.07	VLE-DP

w'_1 denotes mass fraction of carbon dioxide on a chloroform free-basis; w'_2 denotes the mass fraction of globalide on a chloroform free-basis; VLE-BP, vapor-liquid-equilibrium type bubble point; VLE-DP, vapor-liquid equilibrium type dew point; LLE, liquid-liquid-equilibrium; VLLE, vapor-liquid-liquid-equilibrium; T , system temperature; P , system pressure; sd, standard deviation. Variable expanded uncertainties with 95% of confidence level: $U(T) = 0.50$ K; $U(P) = 0.10$ MPa; $U(w_1) = 0.0155$; $U(w_2) = 0.0078$; $U(w_3) = 0.0078$.)

Table 9 - Phase equilibrium results for the system [CO₂ (1) + GL (2) + CHCl₃ (3)], in chloroform free-basis, at globalide to chloroform mass ratio of 2:1.

continues

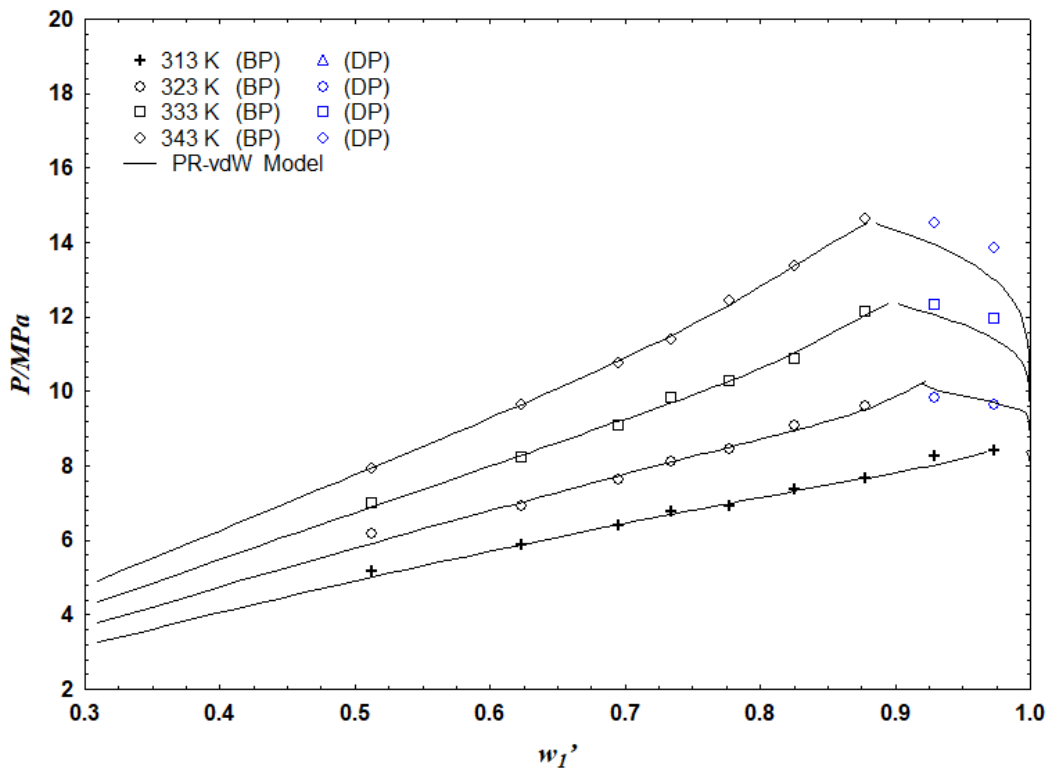
T/K	P/MPa	sd/MPa	Transition Type	T/K	P/MPa	sd/MPa	Transition Type
$w'_1 = 0.4249$ ($w'_2 = 0.5751$)				$w'_1 = 0.8251$ ($w'_2 = 0.1749$)			
313.15	7.16	0.04	VLE-BP	313.15	11.97	0.04	LLE
323.15	8.50	0.04	VLE-BP	313.15	10.08	0.07	VLLE
333.15	9.70	0.05	VLE-BP	323.15	14.72	0.03	LLE
343.15	11.81	0.05	VLE-BP	323.16	12.77	0.08	VLLE
$w'_1 = 0.5131$ ($w'_2 = 0.4869$)				333.13	17.64	0.08	LLE
313.15	7.57	0.01	VLE-BP	333.14	15.45	0.06	VLLE
323.15	9.25	0.07	VLE-BP	343.14	20.24	0.04	LLE
333.15	11.05	0.03	VLE-BP	343.15	18.00	0.07	VLLE
343.15	13.46	0.06	VLE-BP	$w'_1 = 0.8602$ ($w'_2 = 0.1398$)			
$w'_1 = 0.6243$ ($w'_2 = 0.3757$)				313.15	11.92	0.03	LLE
313.15	8.58	0.03	VLE-BP	313.15	10.23	0.05	VLLE
323.15	11.21	0.02	VLE-BP	323.15	14.69	0.03	LLE
333.15	14.13	0.03	VLE-BP	323.16	12.63	0.08	VLLE
343.15	16.86	0.05	VLE-BP	333.13	17.44	0.01	LLE
$w'_1 = 0.6940$ ($w'_2 = 0.3060$)				333.14	15.48	0.08	VLLE
313.15	9.93	0.03	VLE-BP	343.14	20.25	0.05	LLE
323.15	12.74	0.05	LLE	343.15	17.92	0.06	VLLE
323.15	12.56	0.06	VLLE	$w'_1 = 0.9481$ ($w'_2 = 0.0519$)			
333.15	15.49	0.03	LLE	313.15	10.63	0.02	LLE
333.15	15.34	0.04	VLLE	313.15	10.15	0.09	VLLE

continued

343.15	18.26	0.03	LLE	323.15	13.38	0.05	LLE
343.15	17.84	0.05	VLLE	323.16	12.75	0.04	VLLE
$w'_1 = 0.7353$ ($w'_2 = 0.2647$)				333.13	15.61	0.03	LLE
313.15	10.56	0.06	LLE	333.14	15.46	0.05	VLLE
313.15	10.13	0.06	VLLE	343.14	18.34	0.05	LLE
323.15	13.17	0.01	LLE	343.15	17.87	0.06	VLLE
323.15	12.83	0.04	VLLE	$w'_1 = 0.9734$ ($w'_2 = 0.0266$)			
333.15	15.98	0.04	LLE	313.15	9.90	0.05	VLE-DP
333.15	15.41	0.04	VLLE	323.15	11.97	0.01	VLE-DP
343.15	19.01	0.04	LLE	333.15	14.31	0.04	VLE-DP
343.15	17.93	0.07	VLLE	343.15	16.27	0.02	VLE-DP
$w'_1 = 0.7782$ ($w'_2 = 0.2218$)							
313.15	11.19	0.05	LLE				
313.15	10.18	0.05	VLLE				
323.15	14.36	0.07	LLE				
323.15	12.68	0.10	VLLE				
333.15	17.49	0.04	LLE				
333.15	15.39	0.04	VLLE				
343.15	19.88	0.03	LLE				
343.15	17.96	0.03	VLLE				

w'_1 denotes mass fraction of carbon dioxide on a chloroform free-basis; w'_2 denotes the mass fraction of globalide on a chloroform free-basis; VLE-BP, vapor-liquid-equilibrium type bubble point; VLE-DP, vapor-liquid equilibrium type dew point; LLE, liquid-liquid-equilibrium; VLLE, vapor-liquid-liquid-equilibrium; T , system temperature; P , system pressure; sd, standard deviation. Variable expanded uncertainties with 95% of confidence level: $U(T) = 0.50$ K; $U(P) = 0.10$ MPa; $U(w_1) = 0.0148$; $U(w_2) = 0.0099$; $U(w_3) = 0.0049$.

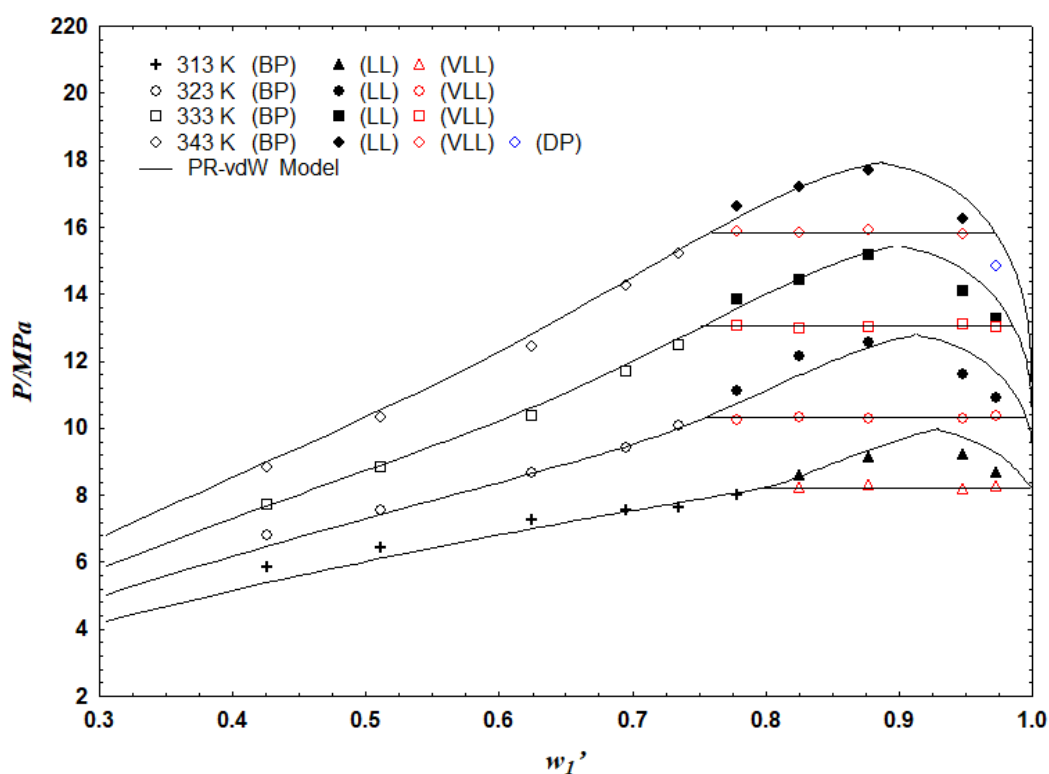
Figure 22 - Pressure - mass composition diagram for the system [CO₂ (1) + GL (2) + CHCl₃ (3)], in chloroform free-basis, at globalide to chloroform mass ratio of 0.5:1.



Source: the author.

At globalide to chloroform mass proportion of 1:1, results are shown in Table 8 and Figure 23. The increase in the globalide fraction, when compared with the previous concentration, causes an increase in pressure, allowing experimental data collection from $w_1' = 0.4254$ to $w_1' = 0.9734$. For these compositions liquid-liquid and vapor-liquid-liquid transitions were observed in the vicinity of the critical point. VLE-BP was found in fractions up to $w_1' = 0.7782$ and a single VLE-DP was encountered at $w_1' = 0.9734$ and temperature of 343.15 K.

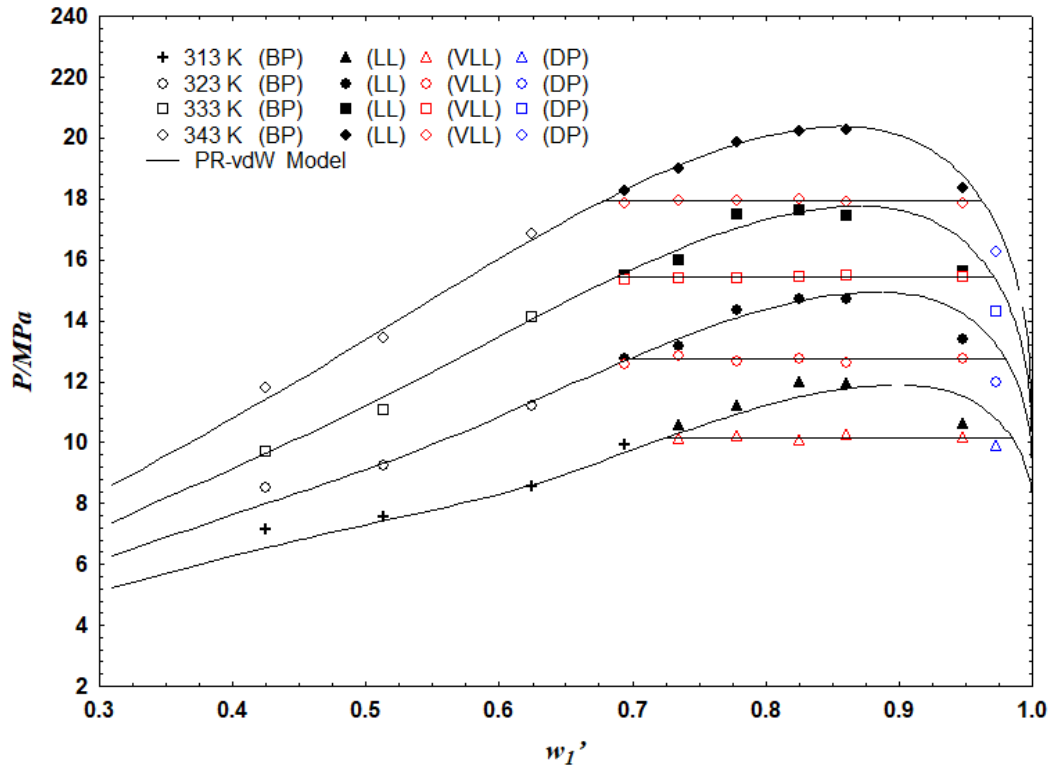
Figure 23 - Pressure - mass composition diagram for the system [CO₂ (1) + GL (2) + CHCl₃ (3)], in chloroform free-basis, at globalide to chloroform mass ratio of 1:1.



Source: the author.

Figure 24 represents the data shown in Table 9, associated with the globalide to chloroform mass ratio of 2:1. Due to the low concentration of cosolvent, the transition pressure at these compositions are the highest collected, reaching values up to 20.25 MPa. It is also notable a greater immiscibility between the liquid phases as liquid-liquid equilibrium transitions span into a wider range of concentrations. VLE-BP was collected between $w_1' = 0.4249$ to $w_1' = 0.6243$ for all isotherms, and also at 313.15 K for the fraction of $w_1' = 0.6940$. VLE-DP was observed for each temperature in composition higher than $w_1' = 0.9481$.

Figure 24 - Pressure - mass composition diagram for the system [CO₂ (1) + GL (2) + CHCL₃ (3)], in chloroform free-basis, at globalide to chloroform mass ratio of 2:1.



Source: the author.

The PR-vdW2 model was used, for each distinct mass ratio (0.5:1, 1:1, and 2:1), to estimate binary interactions parameters k_{ij} and l_{ij} with absolute deviation and root mean square deviation as fitted variables; results are shown in Table 10. For a few isotherms, in the vicinity of the critical point, the model was not able to converge, creating a short discontinuity in the Pw-diagrams. Nevertheless, the positive performance of these calculations can be verified, not only by graphical visualization, but also by the low values of the fitted parameters AD and RMSD. The continuous line for the triphasic transition VLLE were obtained through the average value of the experimental results.

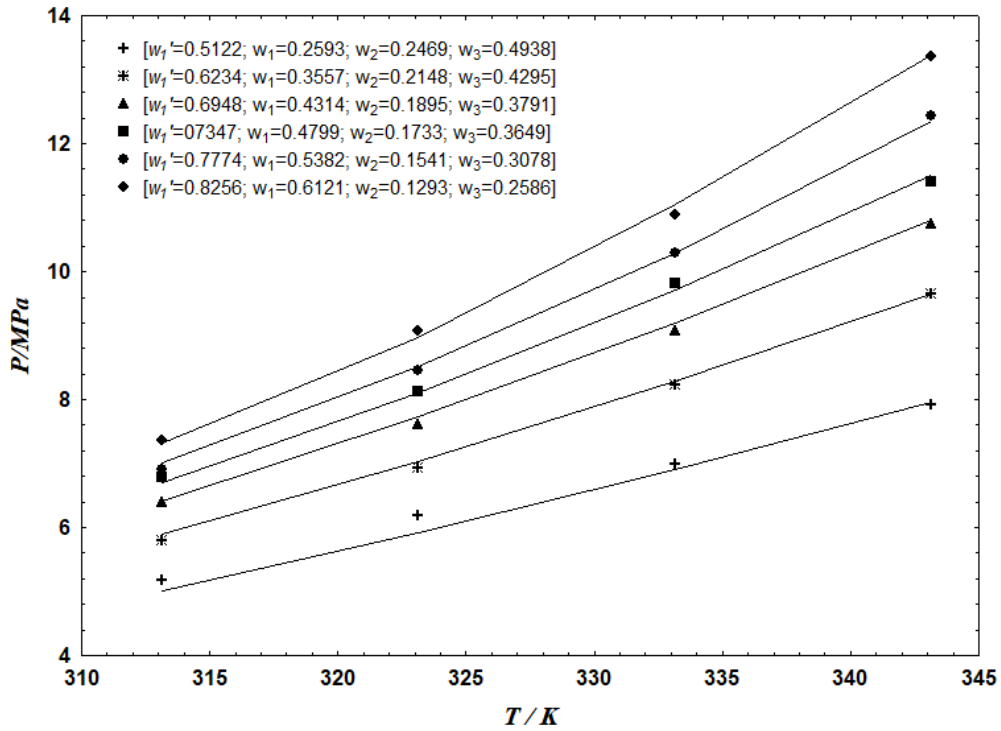
Figure 25, Figure 26, and Figure 27 illustrate the PT-diagram for some of the observed fractions of the system at globalide to chloroform mass ratios of 0.5:1, 1:1, and 2:1, as the graphical representation of all experimental data would be convoluted to display in single graphs for each mass proportion. The increase in pressure to achieve a single phase medium as temperature rises characterize the lower critical solution temperature behavior (LCST), which can also be perceived in Figure 23 and Figure 24, for the compositions of $w'_1 = 0.7782$ and $w'_1 = 0.6940$, respectively. At the

isotherm of 313.15 K the three components are more miscible, forming a weak complex that breaks up in two phases (VLE-BP), while at higher temperatures up to three-phase transitions (VLLE) can be visualized. This behavior has also been reported for the binary system carbon dioxide and globalide (REBELATTO et al., 2020) and for the ternary system carbon dioxide, globalide, and dichloromethane (DE QUADROS et al., 2022).

Table 10 – Estimated binary interaction parameters.

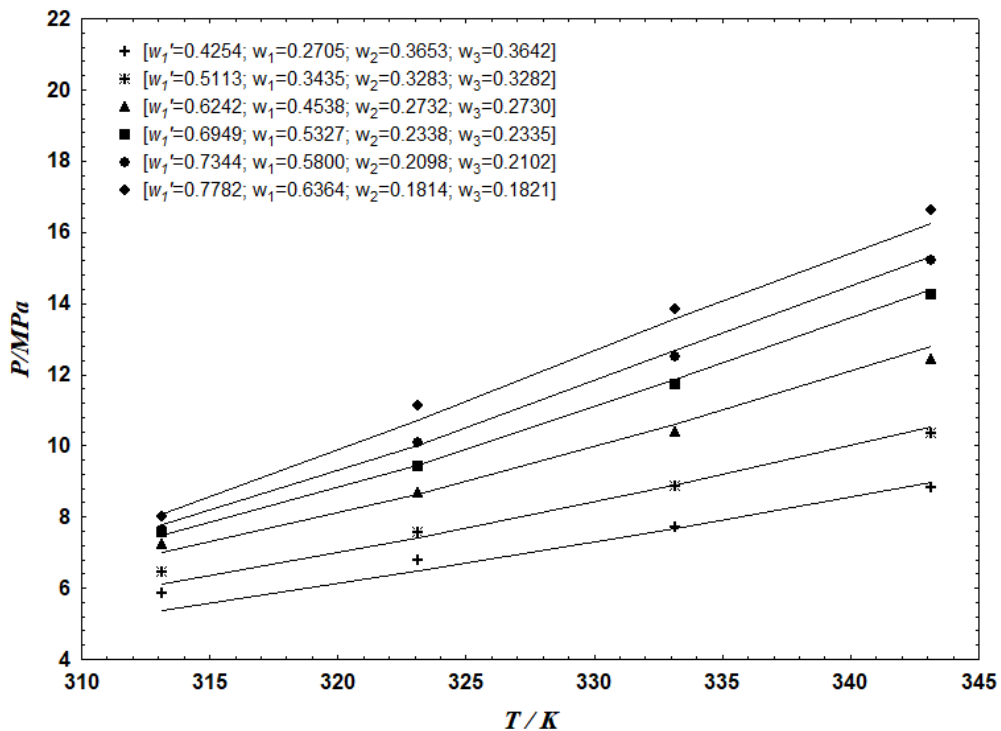
T/K	i-j	k_{ij}	l_{ij}	rmsd/MPa	AD/MPa
CO ₂ (1) + GL (2) + CHCL ₃ (3) mass ratio of 0.5:1					
313 - 343	1-2	-0.0385	0.0667	0.254	0.205
	1-3	0.1843	-0.2203		
	2-3	-0.0784	0.0008		
CO ₂ (1) + GL (2) + CHCL ₃ (3) mass ratio of 1:1					
313 - 343	1-2	-0.0507	0.0335	0.229	0.182
	1-3	0.0487	0.0009		
	2-3	-0.0737	0.1095		
CO ₂ (1) + GL (2) + CHCL ₃ (3) mass ratio of 2:1					
313 - 343	1-2	0.0183	-0.0703	0.079	0.098
	1-3	0.0186	-0.0107		
	2-3	-0.0745	-0.0147		

Figure 25 – PT-diagram for the system [CO₂ (1) + GL (2) + CHCl₃ (3)], in chloroform free-basis, at globalide to chloroform mass ratio of 0.5:1.



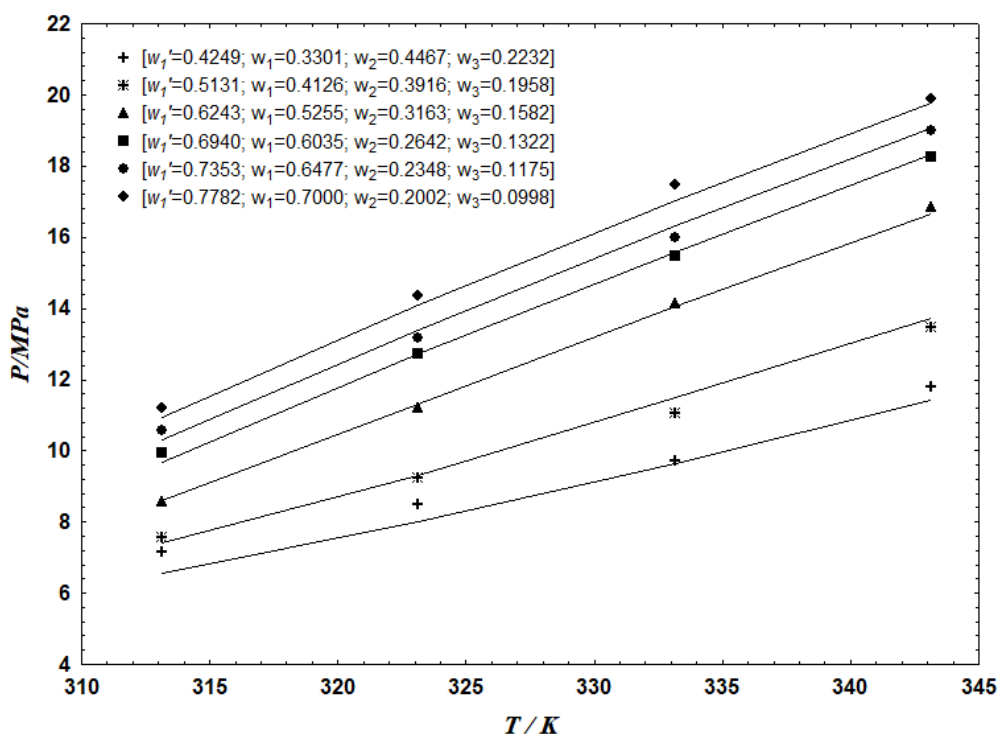
Source: the author.

Figure 26 – PT-diagram for the system [CO₂ (1) + GL (2) + CHCl₃ (3)], in chloroform free-basis, at globalide to chloroform mass ratio of 1:1.



Source: the author.

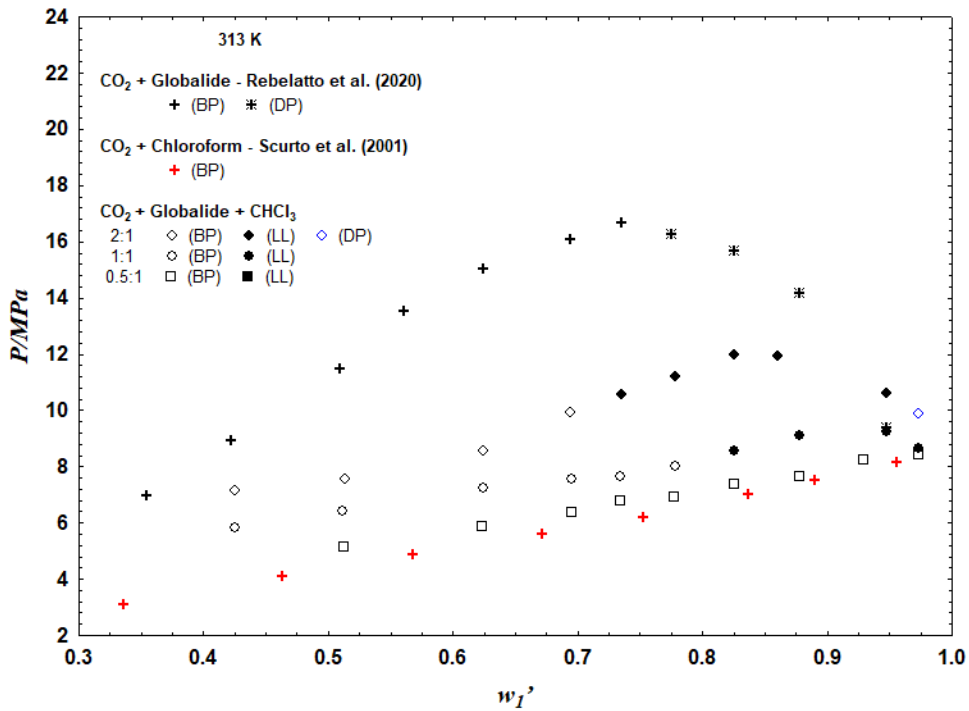
Figure 27 – PT-diagram for the system [CO₂ (1) + GL (2) + CHCl₃ (3)], in chloroform free-basis, at globalide to chloroform mass ratio of 2:1.



Source: the author.

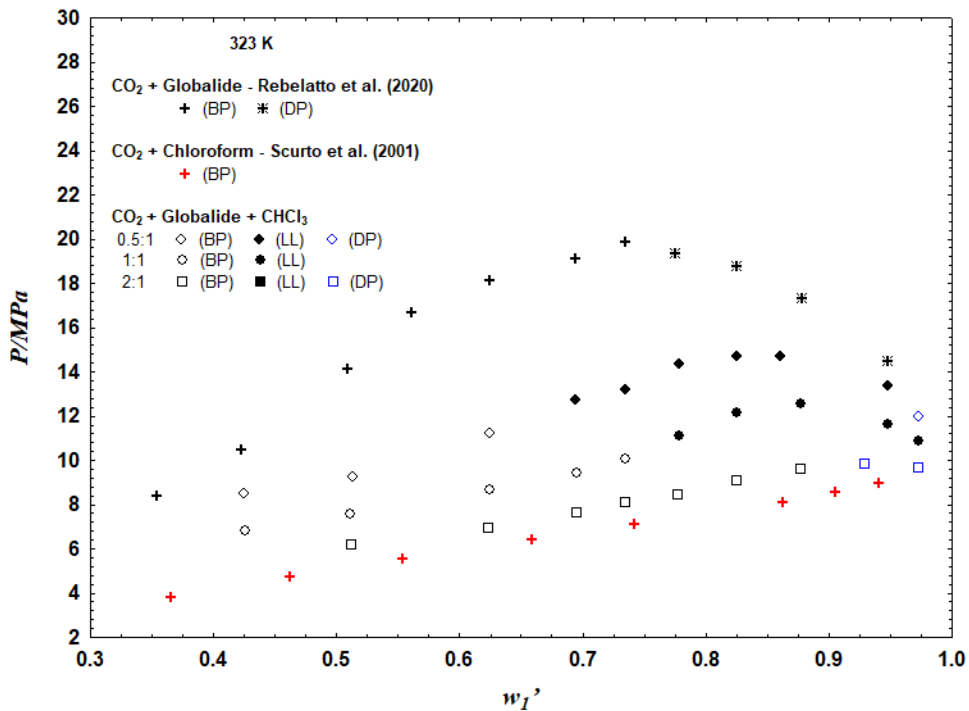
As shown in Figure 28, Figure 29, Figure 30, Figure 31, the experimental data for the ternary system containing [carbon dioxide (1) + globalide (2) + chloroform (3)] collected in this work was compared with the results at same temperatures reported by Rebelatto et al. (2020) and Scurto et al. (2001), corresponding to the binary systems [carbon dioxide (1) + globalide (2)] and [carbon dioxide (1) + chloroform (2)], respectively. It is noticed that as the globalide concentration increases, the transition pressures approach those of the chloroform-free binary system. The same is observed as the cosolvent concentration is high, reaching pressure values close to the globalide absent system. Scurto et al. (2001) did not report phase transitions at 343.15 K, therefore, only the results from Rebelatto et al. (2020) are shown for this isotherm in Figure 31.

Figure 28 – Pw' -diagram at 313.15 for the comparison between the ternary system $[\text{CO}_2 (1) + \text{GL} (2) + \text{CHCl}_3 (3)]$, in chloroform free-basis, the pseudobinary system $[\text{CO}_2 (1) + \text{GL} (2)]$, and the binary system $[\text{CO}_2 (1) + \text{CHCl}_3 (2)]$.



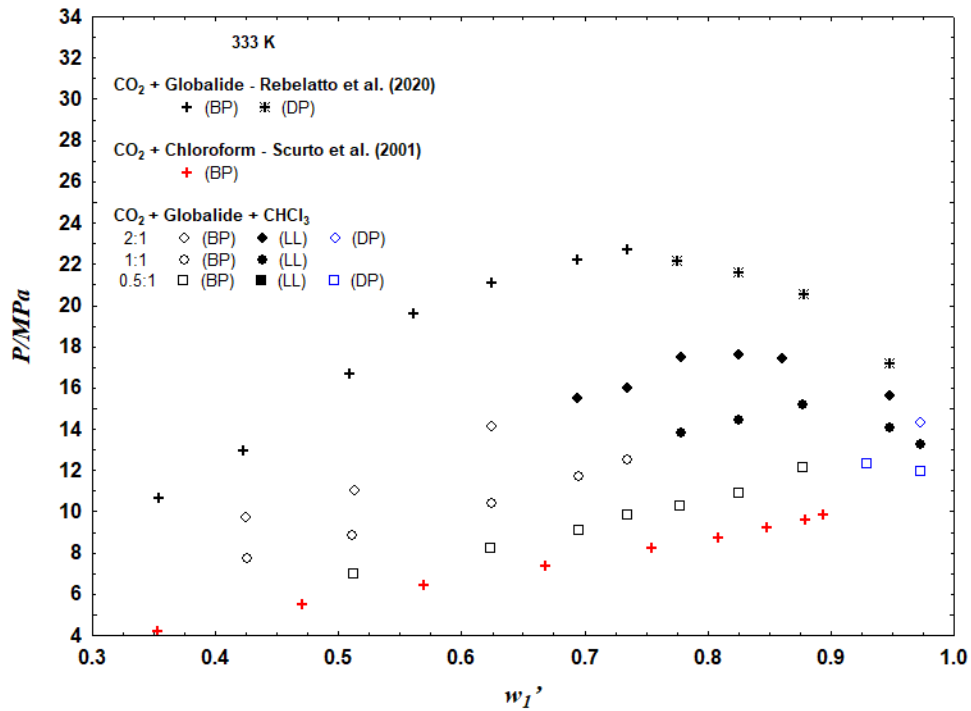
Source: the author.

Figure 29 - Pw' -diagram at 323.15 for the comparison between the ternary system $[\text{CO}_2 (1) + \text{GL} (2) + \text{CHCl}_3 (3)]$, in chloroform free-basis, the pseudobinary system $[\text{CO}_2 (1) + \text{GL} (2)]$, and the binary system $[\text{CO}_2 (1) + \text{CHCl}_3 (2)]$.



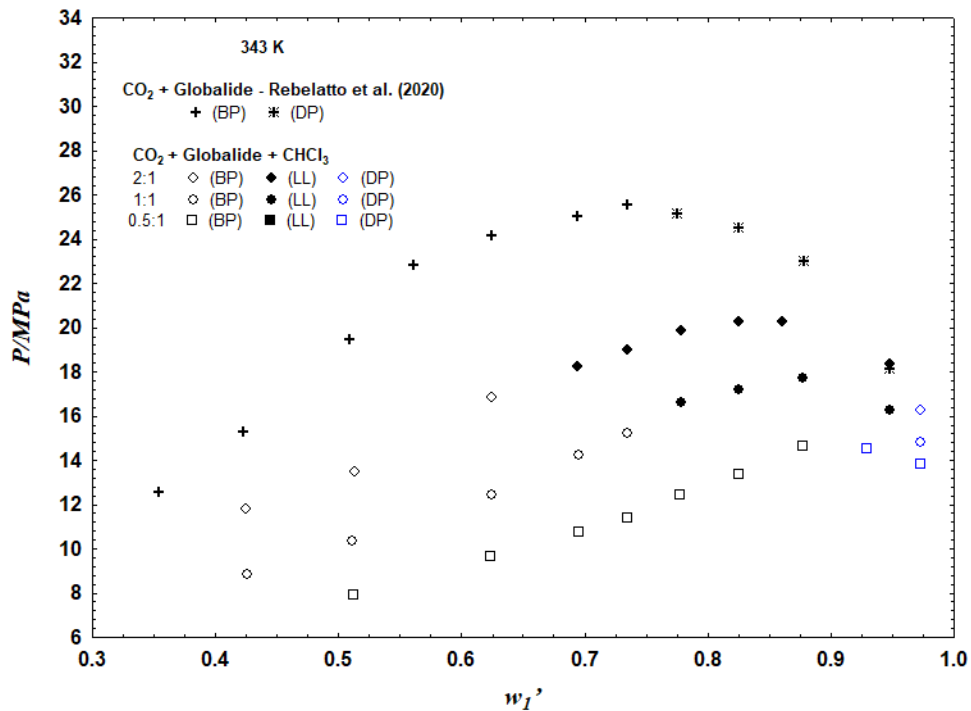
Source: the author.

Figure 30 – Pw' -diagram at 333.15 for the comparison between the ternary system $[\text{CO}_2 (1) + \text{GL} (2) + \text{CHCl}_3 (3)]$, in chloroform free-basis, the pseudobinary system $[\text{CO}_2 (1) + \text{GL} (2)]$, and the binary system $[\text{CO}_2 (1) + \text{CHCl}_3 (2)]$



Source: the author.

Figure 31 – Pw' -diagram at 343.15 for the comparison between the ternary system $[\text{CO}_2 (1) + \text{GL} (2) + \text{CHCl}_3 (3)]$, in chloroform free-basis, and the pseudobinary system $[\text{CO}_2 (1) + \text{GL} (2)]$.



Source: the author.

3.4 PARTIAL CONCLUSIONS

High pressure phase equilibrium data of the ternary system {carbon dioxide (1) + chloroform (2) + globalide (3)} at globalide to chloroform mass ratios of 0.5:1, 1:1, and 2:1 were experimentally collected under a temperature range of 315.15 K to 343.15 K, as carbon dioxide fractions varied from 0.4249 to 0.9734 in phase transition pressures spanning from 5.14 MPa to 20.25 MPa. The use of chloroform as a cosolvent showed to be effective since it is noticeable that as the globalide to chloroform mass ratio reduced, the phase transition pressure decreased. Among phase transitions, VLE-BP, VLE-DP, LLE, and VLLE were visualized. Furthermore, the data gathered experimentally had a satisfactory representation by the PR-vdW model. The results of this work are valuable for estimating optimal conditions for the polymerization of globalide with carbon dioxide and chloroform as solvent and cosolvent, respectively.

4 EXPERIMENTAL VAPOR PRESSURE DATA FOR ϵ -CAPROLACTONE, ω -PENTADECALACTONE, AND GLOBALIDE, AND PREDICT PC-SAFT PARAMETERS

Abstract

The study of pure component parameters of SAFT equations of state, for lactones that are used as monomers for the polymerization of biodegradable and biocompatible materials, is essential to the design and operation of these processes. These parameters can be calculated from experimental vapor pressure data, which are scarce for lactones. Therefore, this work reports new vapor pressure measurements of ϵ -caprolactone, ω -pentadecalactone, and globalide. The experiments were carried out at temperatures ranging from 297.8 to 333.7 K using a static method. Vapor pressures varied from 0.169 to 0.789 for ϵ -caprolactone, from 0.174 to 0.445 for ω -pentadecalactone, and from 0.174 to 0.847 for globalide. Furthermore, these results were used to estimate the Antoine correlation parameters and the pure component parameters of the PC-SAFT equation.

4.1 INTRODUCTION

Lactone-based polymers have received a growing interest since the resorbable-polymer-boom in the 1970s, the development of tissue engineering in the 1990s, and recently as new breakthroughs in the biomedical, food packaging, and pharmaceutical industries are being made (THAKUR et al., 2021). These biocompatible and biodegradable materials, can have their suitable thermal, chemical, and mechanical properties adjusted by modifying the polymer's crystalline phase by copolymerization and functionalization (WILSON, et al., 2019; HEGE et al., 2014). Furthermore, new polymerization techniques at mild temperatures have been proposed through the usage of the enzyme *Candida Antarctica Lipase B* as a catalyst for the reaction, and through the usage of supercritical carbon dioxide as a solvent (BIŃCZAK et al., 2021; POLLONI, et al., 2017; GUALANDI et al., 2010).

In order to design and operate polymerization processes with supercritical carbon dioxide as a reaction media, adequate models should be able to predict the correct operational conditions of temperature, pressure, and compositions. Equations

of state such as SAFT and its variations have shown a positive correlation between experimental data and calculated results. Among the modifications to the SAFT model, PC-SAFT excels at describing systems containing polymers. Moreover, these equations require pure components parameters to be applied in mixture systems, which can be estimated from vapor pressure data (KONTOGEORGIS et al., 2020; KONTOGEORGIS; FOLAS, 2010; GROSS; SADOWSKI, 2002).

Few studies have reported the vapor pressure of ϵ -Caprolactone (BIAZUS et al., 2008; EMEL'YANENKO et al., 2010), and ω -pentadecalactone (EMEL'YANENKO et al., 2011), and none was found in the literature for globalide. Globalide is a non-toxic and biodegradable lactone that can be found in a variety of cleaning and cosmetic products. It is present in small amounts in baby oil, body lotions, face moisturizers, fine fragrances, hand creams, lipsticks, shampoos, and tampons, and in slightly higher concentrations in aerosol air fresheners, hand dishwashing detergents, and soaps (TGSC, c2021b; API et al., 2022). Moreover, it has received recent attention as a monomer for polymerization due to its unsaturated bond, which allows the final polymer to be functionalized through thiol-ene reactions (GUINDANI et al., 2019a).

In this context, the aim of this work is to investigate experimental vapor pressure data for ϵ -caprolactone, ω -pentadecalactone, and globalide at temperature ranges of 297.8 - 333.7 K, and to estimate the pure components parameters for these lactones using the PC-SAFT equation of state.

4.2 MATERIAL AND METHODS

4.2.1 Materials

ϵ -Caprolactone and ω -pentadecalactone, both with 0.970 mass fraction purity, were purchased from Sigma-Aldrich. Globalide, with 0.998 mass fraction purity, was provided by Symrise. Furthermore, decane used to check the accuracy of the experimental procedure was purchased from Sigma-Aldrich. Materials were used without further purifications, as sample degassing is a step in the method. Table 11 provides the molecular formula, CAS Registry Number, provenance, and minimum mass fraction purity (provided by the supplier) for each compound used in this work.

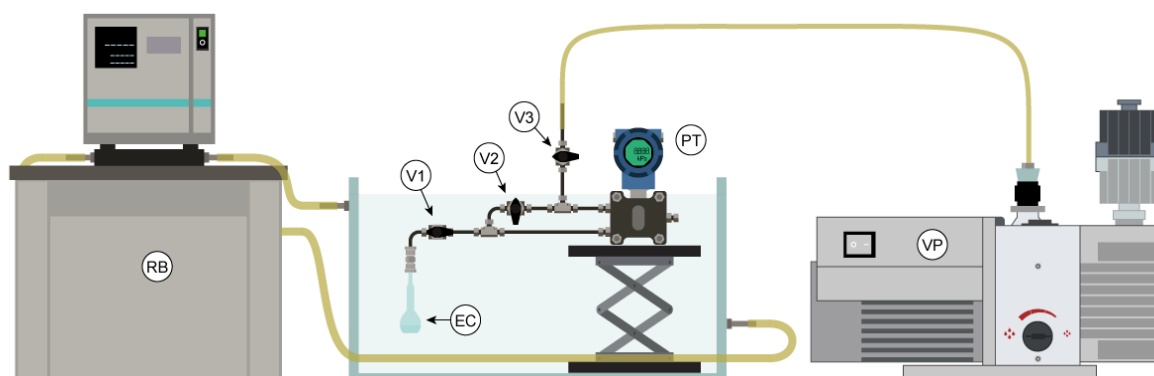
4.2.2 Apparatus and experimental procedure

Experiments were conducted on equipment similar to those used by Biazus et al. (2008) and Ndiaye et al. (2005). The equilibrium cell (EC) was made from a modified 25 mL Pyrex glass volumetric flask to fit precisely with the rest of the equipment. A NP860 HRT Novus model differential pressure transducer (PT), calibrated in the operation range of 0.075 kPa to 6.890 kPa, was connected by two ¼ inches stainless steel lines that were separated by a Swagelok stainless steel ball valve SS-43GS4 model (V2). One of these lines was further attached to the equilibrium cell, while the other was assembled to a Edwards RV8 model high-performance vacuum pump (VP). Both the cell and the pump can be isolated from the respective lines by closing another two Swagelok stainless steel ball valves SS-43GS4 model (V1 and V3, respectively). The apparatus is represented in Figure 32.

Table 11 - Chemical name, molecular formula, provenance, purification method and purity of the materials.

Chemical name	Molecular formula	CAS Number	Supplier	Minimum mass fraction purity
Decane	$C_{10}H_{22}$	124-18-5	Sigma-Aldrich	0.990
ϵ -Caprolactone	$C_6H_{10}O_2$	502-44-3	Sigma-Aldrich	0.970
ω -Pentadecalactone	$C_{15}H_{28}O_2$	106-02-5	Sigma-Aldrich	0.970
Globalide	$C_{15}H_{26}O_2$	34902-57-3	Symrise	0.998

Figure 32 - Vapor pressure apparatus scheme.



Source: the author.

Approximately 12.5 g of sample was weighted on a precision scale balance and inserted into the equilibrium cell, which was further attached to the apparatus. To ensure a minimal temperature difference between the equilibrium cell, the connecting lines, and the sockets in the differential pressure transducer, and to minimize the occurrence of thermal transpiration, these parts of the apparatus were immersed in a water bath connected to a recirculation bath (RB) with controlled temperature.

At temperatures close to 333.15 K, degassing was performed by exposure of the sample to gradually increased vacuum over a period of 5 h. With the ball valve V1 closed and the other two opened, moderate vacuum would be applied to both pressure transducer sockets for at least ten minutes. After that, the ball valve V3 was closed, and, subsequently, the valve V1 was opened to submit the sample to moderated pressure changes during two minutes. Then, these two valves were returned to the initial position. This procedure was repeated at least 25 times to ensure the complete gas removal from the sample, detected by no changes in pressure between the degassing steps. For each sample the mass lost during the overall procedure was lower than 0.012 g.

Each measurement was conducted by exposing both sockets of the pressure transducer to vacuum, with valve V1 closed and the others opened, and then changing the position of each valve in the exact order from V3 to V1, this configuration is shown in Figure 32. One socket of the pressure transducer was under vacuum, while the other was under the vapor pressure of the sample. This procedure was repeated three times with ten minutes between each measure to ensure repeatability.

4.2.3 Thermodynamic model

The perturbed chain SAFT (PC-SAFT) equation of state developed by Gross and Sadowski (2001) was employed to estimate the pure component parameters segment diameter σ ; number of segments m , and segment energy ϵ/k . Details about the equation can be found in Gross and Sadowski (2001). An MATLAB 2013a algorithm with the *fmincon* sub-routine developed by Mayer et al. (2020) was used to minimize the objective function at Equation 39. The generated residues are computed by absolute deviation (AD) and root-mean-square deviation (rmsd), equations 40 and 41, respectively.

$$OF = \sum_{i=1}^{nobs} (P_i^{cal} - P_i^{exp}) \quad 39$$

$$AD = \sum_{i=1}^{nobs} \frac{|P_i^{cal} - P_i^{exp}|}{nobs} \quad 40$$

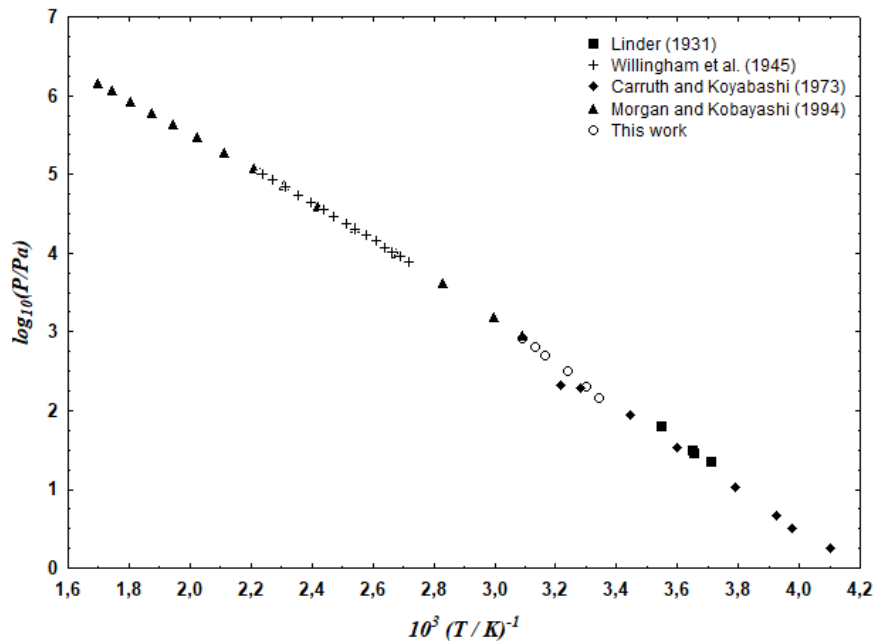
$$rmsd = \sqrt{\sum_{i=1}^{nobs} \frac{(P_i^{cal} - P_i^{exp})^2}{nobs}} \quad 41$$

where *nobs* is the number experimental observations, P_i^{exp} is the arithmetic mean of three transition pressure measurements, P_i^{cal} denotes the calculated pressure by the model.

4.3 RESULTS AND DISCUSSION

The accuracy of the experimental procedure was checked by the vapor pressure measurement of decane and by the comparison with the data from Linder (1931), Willingham et al. (1945), Carruth and Kobayashi (1973), and Morgan and Kobayashi (1994), as indicated in Figure 33. The data reported in this work presented a positive agreement with the literature.

Figure 33 - Vapor pressure of decane comparison with literature.



Source: the author.

The experimental vapor pressure measurement for the three studied lactones, and for decane is presented in Table 12, as well as the standard deviation of temperature and pressure. Positive repeatability was achieved by conducting the experiments in triplicate, with standard deviations for pressure less than 0.007 kPa, and a positive reproducibility was established by conducting the experiment for three different weighted samples of ϵ -caprolactone at 318.15 K, with a standard deviation for pressure smaller than 0.004 kPa.

Table 12 - Experimental vapor pressure data for decane, ϵ -caprolactone, ω -pentadecalactone, and globalide.

decane				ϵ -caprolactone			
T/K	sd/K	P/kPa	sd/kPa	T/K	sd/K	P/kPa	sd/kPa
299.1	0.1	0.141	0.006	298.2	0.1	0.169	0.001
302.8	0.1	0.199	0.001	303.2	0.2	0.213	0.003
308.3	0.3	0.316	0.003	307.5	0.1	0.261	0.001
313.5	0.1	0.501	0.002	313.7	0.1	0.335	0.001
318.9	0.3	0.630	0.002	318.4	0.1	0.421	0.003
323.4	0.1	0.794	0.004	323.2	0.1	0.514	0.004
				328.1	0.2	0.581	0.003
				332.9	0.3	0.798	0.004

ω -pentadecalactone				globalide			
T/K	sd/K	P/kPa	sd/kPa	T/K	sd/K	P/kPa	sd/kPa
298.4	0.1	0.174	0.001	297.8	0.1	0.152	0.001
302.6	0.1	0.183	0.000	302.3	0.1	0.206	0.003
308.1	0.2	0.219	0.002	308.0	0.1	0.261	0.002
312.9	0.1	0.246	0.002	313.3	0.2	0.346	0.003
317.9	0.0	0.285	0.003	318.5	0.2	0.432	0.006
322.8	0.0	0.329	0.003	323.4	0.0	0.615	0.007
327.9	0.1	0.382	0.002	328.6	0.1	0.810	0.006
333.6	0.1	0.445	0.001	333.7	0.1	1.147	0.005

With the experimental data, Antoine correlation parameters, at equation 42, were calculated. The constants A, B, and C were obtained by minimizing the equation 43, and are shown in Table 13, with each respective correlation coefficient (R), absolute deviation (AD) and root-mean-square deviation (rmsd).

$$\log_{10} P = A - \frac{B}{C + T} \quad 42$$

$$OF = \sum_{i=1}^{nobs} (P_i^{cal} - P_i^{exp}) \quad 43$$

Table 13 - Constants for the Antoine Equation.

Compound	A	B	C	R ²
ϵ -Caprolactone	9.62271	2586.085	50.870	0.9955
ω -Pentadecalactone	7.30191	1910.481	76.383	0.9939
Globalide	12.01822	3382.177	43.372	0.9914

Figure 34 shows the vapor pressure for ϵ -caprolactone results determined in this work, the Antoine correlation and data reported from Emel'yanenko et al. (2010) and from Biazus et al. (2008). The noticeable distinction between the results from Emel'yanenko and the other data could be explained by the use of a different procedure, as it employs the transpiration method, and Biazus and this work uses a

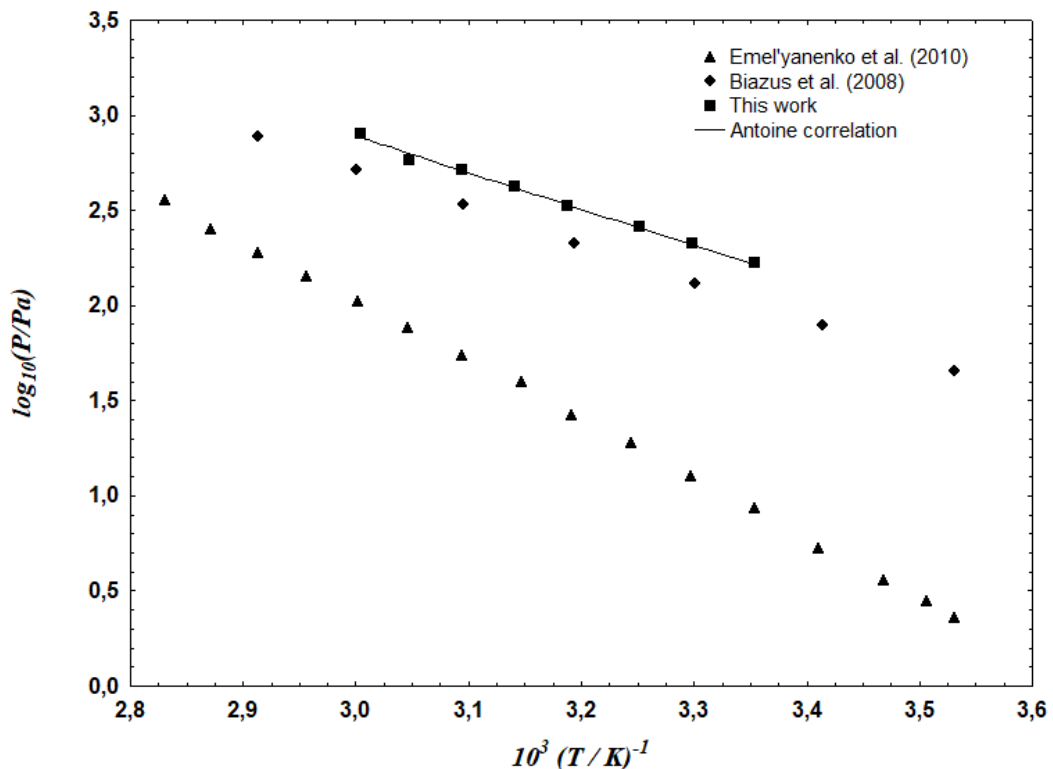
static method. Another explanation could be the presence of oligomers or impurities in the materials used.

Furthermore, shown in Figure 35 is the vapor pressure data for ω -pentadecalactone, the Antoine correlation, and results from Emel'yanenko (2011). Similarly to the ϵ -caprolactone differences, the methodology used for each work could be responsible for this divergence, as well as the possible presence of contaminants.

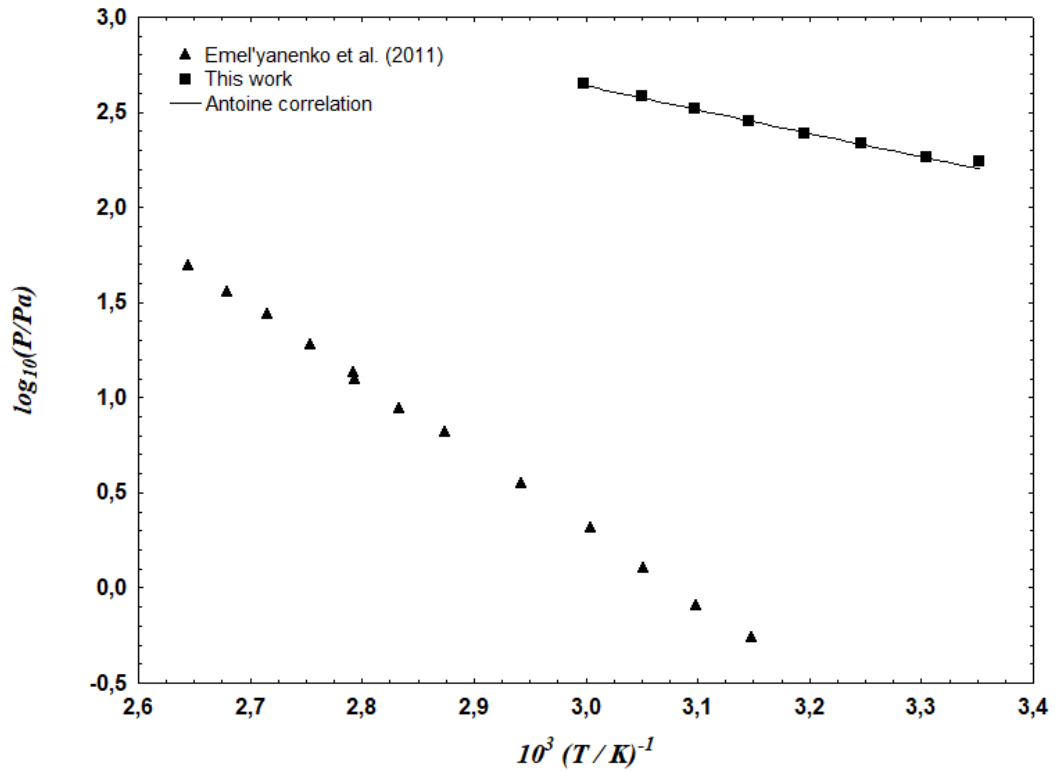
Vapor pressure results for globalide are shown in Figure 36, as well as the Antoine correlation.

Lastly, the calculated PC-SAFT parameters for pure compounds are indicated in Table 14. Vapor pressure was estimated and plotted in Figure 37, Figure 38 and Figure 39. Although the results may not seem to present a positive graphical resemblance, the smalls AD and rmsd corroborate with the performed calculations.

Figure 34 - Vapor pressure of ϵ -caprolactone and comparison with literature.

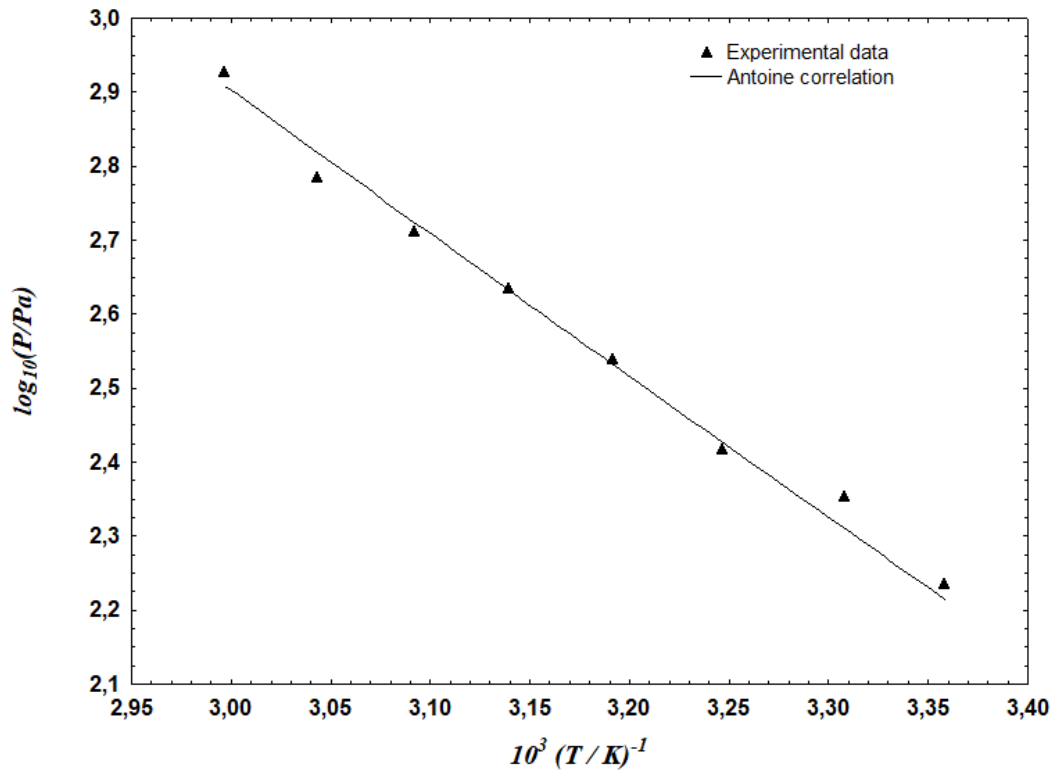


Source: the author.

Figure 35 - Vapor pressure of ω -pentadecalactone and comparison with literature.

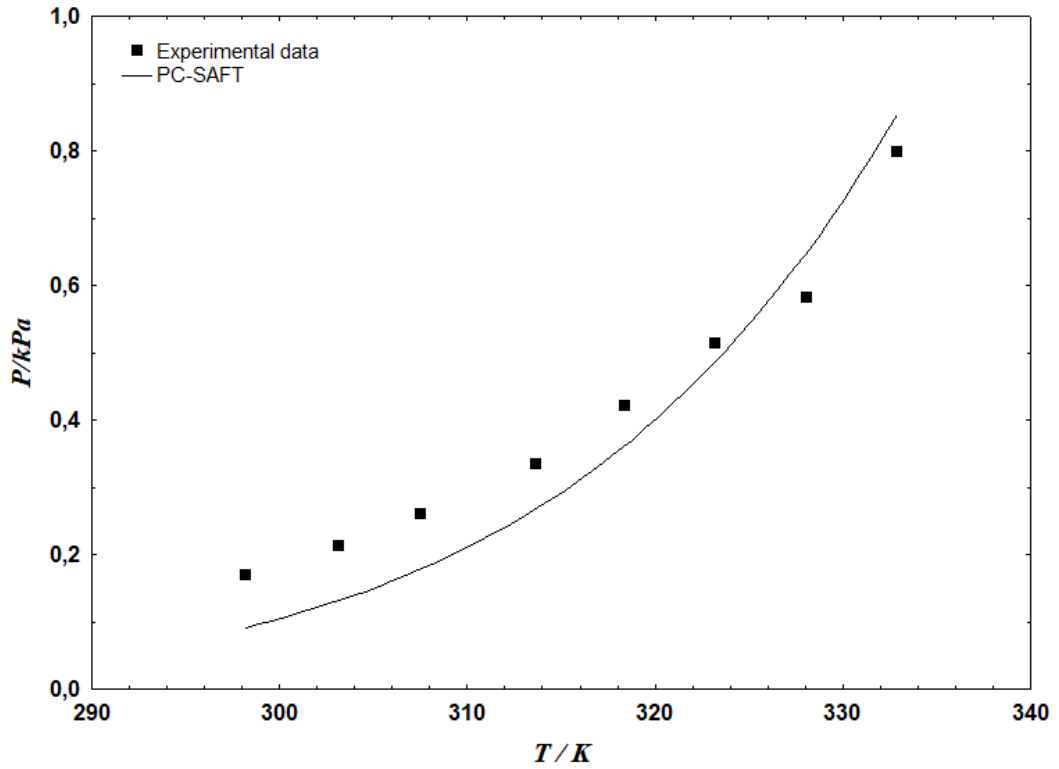
Source: the author.

Figure 36 - Vapor pressure of globalide.



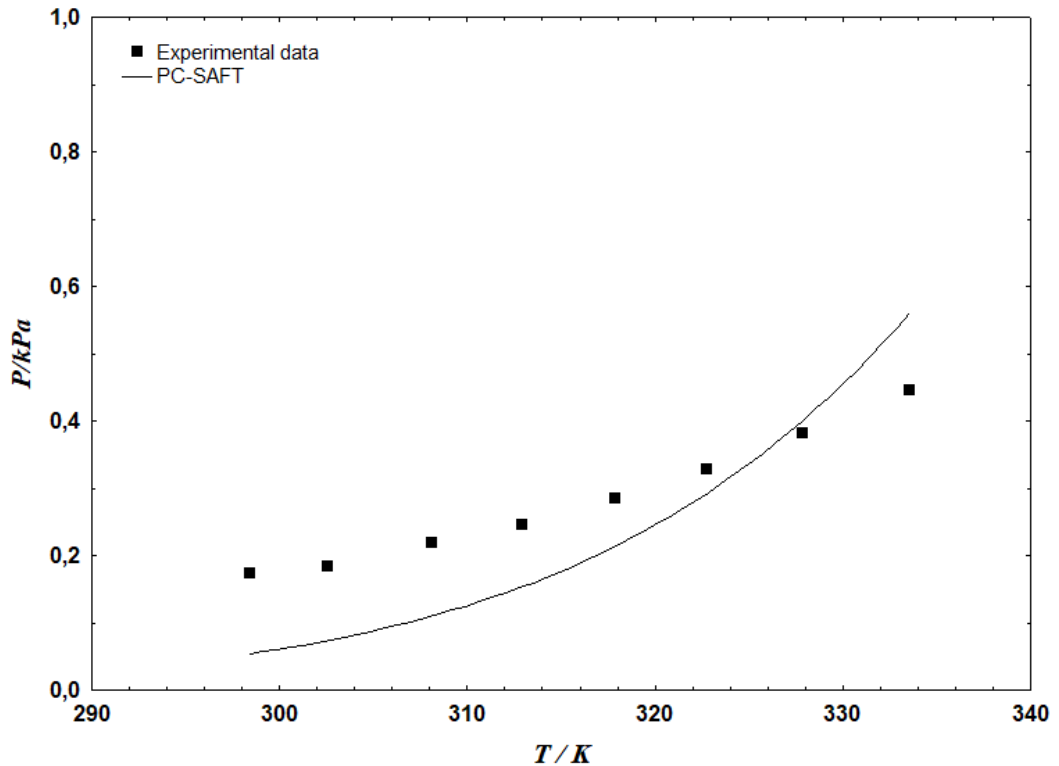
Source: the author.

Figure 37 - Experimental vapor pressure of ϵ -caprolactone and calculated vapor pressure with PC-SAFT.



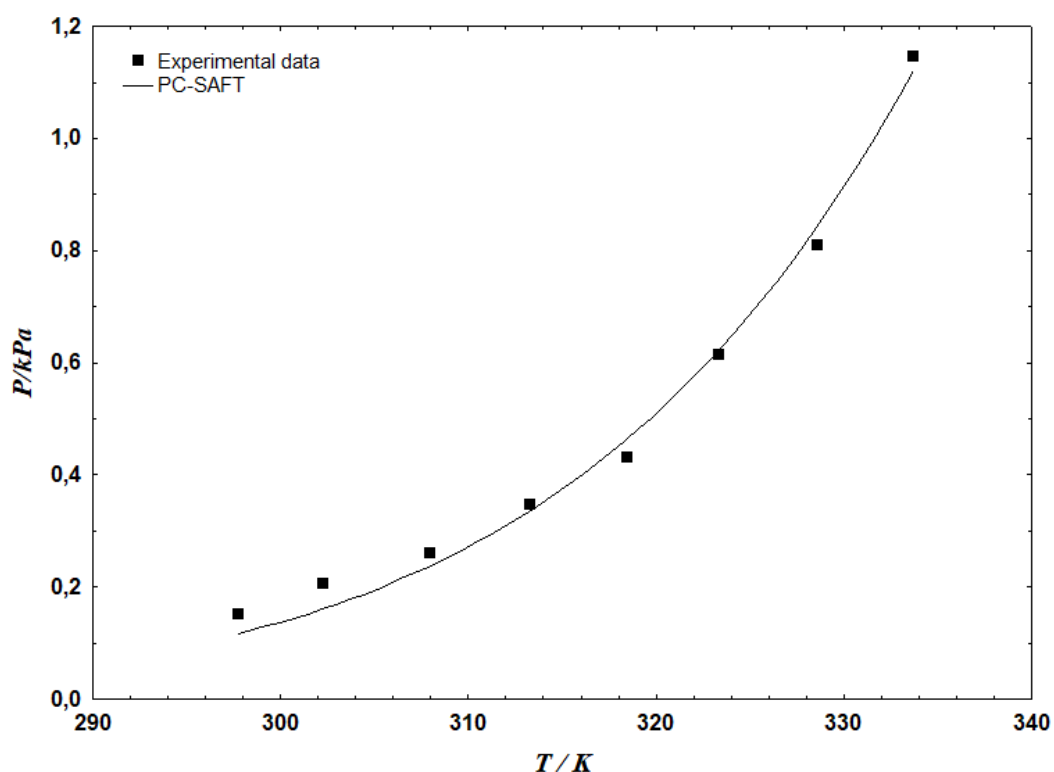
Source: the author.

Figure 38- Experimental vapor pressure of ω -pentadecalactone and calculated vapor pressure with PC-SAFT.



Source: the author.

Figure 39 - Experimental vapor pressure of globalide and calculated vapor pressure with PC-SAFT.



Source: the author.

Table 14 - Characteristics of pure compounds for PC-SAFT calculated from the collected vapor pressure data.

Compound	m_i	$\sigma_i / \text{\AA}$	$(\varepsilon/k) / \text{K}$	rmsd/kPa	AD/kPa
ε -Caprolactone	4.7374	3.8001	252.1207	4.495×10^{-5}	6.487×10^{-2}
ω -Pentadecalactone	4.9149	3.8651	251.0259	8.389×10^{-5}	8.420×10^{-2}
Globalide	4.3973	3.6765	260.0103	8.636×10^{-6}	2.700×10^{-2}

4.4 PARTIAL CONCLUSIONS

Vapor pressure data for ε -caprolactone, ω -pentadecalactone, and globalide at a temperature range from 297.8 to 333.7 K are presented in this work. The accurate experimental procedure secured a positive repeatability and reproducibility of the measurements. Furthermore, the experimental data were correlated using the Antoine equation and were used to estimate the pure component parameters for the PC-SAFT equation of state, with small deviations. Results obtained in this work may be useful for processes containing the studied lactones.

5 CONCLUSION REMARKS

In this work, high-pressure phase equilibrium of the ternary system {carbon dioxide + chloroform + globalide}, and vapor pressure experiments for ϵ -caprolactone, ω -pentadecalactone, and globalide were conducted.

The ternary system {carbon dioxide + chloroform + globalide} was studied at three different mass ratios of globalide to chloroform over a wide composition range of carbon dioxide. These experiments reported phase transition at temperatures of 315.15 K to 343.15 K and pressures spanning from 5.14 MPa to 20.25 MPa. The observed phase transitions were vapor-liquid-equilibrium bubble point, vapor-liquid equilibrium dew point, liquid-liquid equilibrium, and vapor-liquid-liquid equilibrium. Furthermore, chloroform has shown to be an effective cosolvent for the ternary system, as evident by the comparison with the binary systems {carbon dioxide + globalide} and {carbon dioxide + chloroform}. Lastly the thermodynamic model PR-vdW2 applied satisfactorily represented the gathered data.

Vapor pressure data for the three lactones was investigated at temperatures of 297.8 to 333.7 K with good repeatability and reproducibility. The gathered data were used to estimate the Antoine correlation parameters and the pure components parameters for the PC-SAFT equation of state.

Both studies are important for the development of polymerization of lactones in a supercritical carbon dioxide solution. Not only by providing valuable data to estimate optimal initial conditions for poly(globalide) synthesis, but also by determining essential parameters for the process simulation and control of systems containing ϵ -caprolactone, ω -pentadecalactone, and globalide.

5.1 SUGGESTIONS FOR FUTURE RESEARCHES

- Investigate the high pressure phase behavior of the quaternary system {carbon dioxide + chloroform + globalide + poly(globalide)}.
- Study the phase equilibrium of the ternary systems {carbon dioxide + chloroform + poly(globalide)} and {carbon dioxide + globalide + poly(globalide)}.
- Investigate the high pressure phase behavior of systems containing other promising lactones in carbon dioxide solution, such as β -

butyrolactone, ϵ -decalactone, β -malolactone, γ -butyrolactone, and δ -valerolactone.

- Perform the synthesis of poly(globalide) in supercritical carbon dioxide media, with or without the addition of co-solvents.

REFERENCES

ALBERTSSON, Ann-Christine; VARMA, Indra K. Recent Developments in Ring Opening Polymerization of Lactones for Biomedical Applications. **Biomacromolecules**, v. 4, n. 6, p. 1466–1486, 2003.

ALONSO, David Martin; WETTSTEIN, Stephanie G.; DUMESIC, James A. Gamma-valerolactone, a sustainable platform molecule derived from lignocellulosic biomass. **Green Chemistry**, v. 15, n. 3, p. 584, 2013.

AMARAL, Heliane R.; WILSON, James A.; DO AMARAL, Ronaldo J.F.C.; *et al.* Synthesis of bilayer films from regenerated cellulose nanofibers and poly(globalide) for skin tissue engineering applications. **Carbohydrate Polymers**, v. 252, p. 117201, 2021.

API, A.M.; BELSITO, D.; BISERTA, S.; *et al.* RIFM fragrance ingredient safety assessment, ω -pentadecalactone, CAS Registry Number 106-02-5. **Food and Chemical Toxicology**, v. 146, p. 111762, 2020.

API, A.M.; BELSITO, D.; BOTELHO, D.; *et al.* RIFM fragrance ingredient safety assessment, oxacyclohexadecen-2-one, CAS registry number 34902-57-3. **Food and Chemical Toxicology**, v. 164, p. 113088, 2022.

ATES, Zeliha; AUDOUIN, Fabrice; HARRINGTON, Amy; *et al.* Functional Brush-Decorated Poly(globalide) Films by ARGET-ATRP for Bioconjugation: Functional Brush-Decorated Poly(globalide) Films **Macromolecular Bioscience**, v. 14, n. 11, p. 1600–1608, 2014.

ATKINS, P. W.; DE PAULA, Julio. **Atkins' Physical chemistry**. 8th ed. Oxford ; New York: Oxford University Press, 2006.

BELTRAME, Jeovandro Maria; GUINDANI, Camila; NOVY, Mara Gabriela; *et al.* Covalently Bonded *N*-Acetylcysteine-polyester Loaded in PCL Scaffolds for Enhanced Interactions with Fibroblasts. **ACS Applied Bio Materials**, v. 4, n. 2, p. 1552–1562, 2021.

BENDER, João P.; FEITEIN, Mirian; FRANCESCHI, Elton; *et al.* Phase behaviour of binary systems of lactones in carbon dioxide. **The Journal of Chemical Thermodynamics**, v. 42, n. 1, p. 48–53, 2010.

BENDER, João Paulo. **EQUILÍBRIO DE FASES DE POLÍMEROS BIOCAMPATÍVEIS E MONÔMEROS: DADOS EXPERIMENTAIS E MODELAGEM**. Dissertação (Mestrado), Universidade Regional Integrada do Alto Uruguai e das Missões, Campus de Erechim, Programa de Mestrado em Engenharia de Alimentos, Erechim, 2008.

BERGEOT, Vincent; TASSAING, Thierry; BESNARD, Marcel; *et al.* Anionic ring-opening polymerization of ϵ -caprolactone in supercritical carbon dioxide: parameters influencing the reactivity. **The Journal of Supercritical Fluids**, v. 28, n. 2–3, p. 249–261, 2004.

BIAZUS, Taline F.; CEZARO, Alana M.; BORGES, Gustavo R.; *et al.* Vapour pressure data of ϵ -caprolactone, δ -hexalactone, and γ -caprolactone. **The Journal of Chemical Thermodynamics**, v. 40, n. 3, p. 437–441, 2008.

BIŃCZAK, Jakub; DZIUBA, Krzysztof; CHROBOK, Anna. Recent Developments in Lactone Monomers and Polymer Synthesis and Application. **Materials**, v. 14, n. 11, p. 2881, 2021.

BISHT, Kirpal S.; HENDERSON, Lori A.; GROSS, Richard A.; *et al.* Enzyme-Catalyzed Ring-Opening Polymerization of ω -Pentadecalactone. **Macromolecules**, v. 30, n. 9, p. 2705–2711, 1997.

BURDOCK, George A. **Fenaroli's Handbook of Flavor Ingredients**. 0. ed. [s.l.]: CRC Press, 2016.

CAI, Jiali; LIU, Chen; CAI, Minmin; *et al.* Effects of molecular weight on poly(ω -pentadecalactone) mechanical and thermal properties. **Polymer**, v. 51, n. 5, p. 1088–1099, 2010.

CARRUTH, Grant F.; KOBAYASHI, Riki. Vapor pressure of normal paraffins ethane through n-decane from their triple points to about 10 mm mercury. **Journal of Chemical & Engineering Data**, v. 18, n. 2, p. 115–126, 1973.

CAS COMMON CHEMISTRY. ϵ -Caprolactone. c2022. Disponível em: <https://commonchemistry.cas.org/detail?cas_rn=502-44-3>. Acesso em: 12 nov. 2022.

CHAPMAN, W.G.; GUBBINS, K.E.; JACKSON, G.; *et al.* SAFT: Equation-of-state solution model for associating fluids. **Fluid Phase Equilibria**, v. 52, p. 31–38, 1989.

CHEN, Biqiong; EVANS, Julian R. G. Poly(ϵ -caprolactone)–Clay Nanocomposites: Structure and Mechanical Properties. **Macromolecules**, v. 39, n. 2, p. 747–754, 2006.

CHIARADIA, Viviane; HANAY, Saltuk B.; KIMMINS, Scott D.; *et al.* Crosslinking of Electrospun Fibres from Unsaturated Polyesters by Bis-Triazolinediones (TAD). **Polymers**, v. 11, n. 11, p. 1808, 2019.

CHIARADIA, Viviane; POLLONI, André E.; DE OLIVEIRA, Débora; *et al.* Polyester nanoparticles from macrolactones via miniemulsion enzymatic ring-opening polymerization. **Colloid and Polymer Science**, v. 296, n. 5, p. 861–869, 2018.

CHRISTOV, M; DOHRN, R. High-pressure fluid phase equilibria. **Fluid Phase Equilibria**, v. 202, n. 1, p. 153–218, 2002.

CLAUDINO, Mauro; VAN DER MEULEN, Inge; TREY, Stacy; *et al.* Photoinduced thiol-ene crosslinking of globalide/ ϵ -caprolactone copolymers: Curing performance and resulting thermoset properties. **Journal of Polymer Science Part A: Polymer Chemistry**, v. 50, n. 1, p. 16–24, 2012.

COMIM ROSSO, Sibebe R.; BIANCHIN, Emanuel; DE OLIVEIRA, Débora; *et al.* Enzymatic synthesis of poly(ϵ -caprolactone) in supercritical carbon dioxide medium by means of a variable-volume view reactor. **The Journal of Supercritical Fluids**, v. 79, p. 133–141, 2013.

COOPER, Andrew I. Polymer synthesis and processing using supercritical carbon dioxide. **Journal of Materials Chemistry**, v. 10, n. 2, p. 207–234, 2000.

DASTAGER, Syed G. Aroma Compounds. *In*: SINGH NEE' NIGAM, Poonam; PANDEY, Ashok (Orgs.). **Biotechnology for Agro-Industrial Residues Utilisation**. Dordrecht: Springer Netherlands, 2009, p. 105–127.

DE GEUS, Matthijs; VAN DER MEULEN, Inge; GODERIS, Bart; *et al.* Performance polymers from renewable monomers: high molecular weight poly(pentadecalactone) for fiber applications. **Polymer Chemistry**, v. 1, n. 4, p. 525–533, 2010.

DE QUADROS, Sabrina. **EQUILÍBRIO DE FASES A ALTAS PRESSÕES DO SISTEMA CONTENDO DIÓXIDO DE CARBONO, GLOBALIDE E DICLOROMETANO**. Dissertação (Mestrado), Universidade Federal de Santa Catarina, Centro Tecnológico, Programa de Pós-Graduação em Engenharia Química, Florianópolis, 2022.

DE QUADROS, Sabrina; REBELATTO, Evertan A.; GUINDANI, Camila; *et al.* High pressure phase behavior of ternary system (carbon dioxide + globalide + dichloromethane) at different dichloromethane to globalide mass ratios. **The Journal of Chemical Thermodynamics**, v. 176, p. 106911, 2023.

DEITERS, U.K.; SCHNEIDER, G.M. High pressure phase equilibria: experimental methods. **Fluid Phase Equilibria**, v. 29, p. 145–160, 1986.

DOHRN, Ralf; BRUNNER, Gerd. High-pressure fluid-phase equilibria: Experimental methods and systems investigated (1988–1993). **Fluid Phase Equilibria**, v. 106, n. 1–2, p. 213–282, 1995.

DOHRN, Ralf; FONSECA, José M.S.; PEPER, Stephanie. Experimental Methods for Phase Equilibria at High Pressures. **Annual Review of Chemical and Biomolecular Engineering**, v. 3, n. 1, p. 343–367, 2012.

DOHRN, Ralf; PEPER, Stephanie; FONSECA, José M.S. High-pressure fluid-phase equilibria: Experimental methods and systems investigated (2000–2004).

EMEL'YANENKO, V. N.; VEREVKIN, S. P.; STEPURKO, E. N.; *et al.* The thermodynamic characteristics of 15-pentadecanolide and 16-hexadecanolide. **Russian Journal of Physical Chemistry A**, v. 85, n. 3, p. 348–356, 2011.

EMEL'YANENKO, V. N.; VEREVKIN, S. P.; STEPURKO, E. N.; *et al.* Thermodynamical properties of ϵ -caprolactone. **Russian Journal of Physical Chemistry A**, v. 84, n. 3, p. 356–363, 2010.

FERRARI, Jarbas C.; NAGATANI, Gabriel; CORAZZA, Fernanda C.; *et al.* Application of stochastic algorithms for parameter estimation in the liquid–liquid phase equilibrium modeling. **Fluid Phase Equilibria**, v. 280, n. 1–2, p. 110–119, 2009.

FLORY, Paul J. Fundamental Principles of Condensation Polymerization. **Chemical Reviews**, v. 39, n. 1, p. 137–197, 1946.

FONSECA, José M.S.; DOHRN, Ralf; PEPER, Stephanie. High-pressure fluid-phase equilibria: Experimental methods and systems investigated (2005–2008). **Fluid Phase Equilibria**, v. 300, n. 1–2, p. 1–69, 2011.

FORNARI, Rosa E.; ALESSI, Paolo; KIKIC, Ireneo. High pressure fluid phase equilibria: experimental methods and systems investigated (1978–1987). **Fluid Phase Equilibria**, v. 57, n. 1–2, p. 1–33, 1990.

GIRARDI, Davi G.L.; MAYER, Diego A.; REBELATTO, Evertan A.; *et al.* Phase behaviour and thermodynamic modelling of the ternary system (carbon dioxide + ϵ -caprolactone + chloroform). **The Journal of Chemical Thermodynamics**, v. 155, p. 106381, 2021.

GOLD, Victor (Org.). **The IUPAC Compendium of Chemical Terminology: The Gold Book**. 4. ed. Research Triangle Park, NC: International Union of Pure and Applied Chemistry (IUPAC), 2019.

GOOGLE SCHOLAR. “globalide” - Google Scholar. c2022. Disponível em: <https://scholar.google.com/scholar?lr=&q=%22globalide%22&hl=pt-BR&scisbd=2&as_sdt=0,5&as_vis=1>. Acesso em: 11 nov. 2022.

GROSS, Joachim; SADOWSKI, Gabriele. Modeling Polymer Systems Using the Perturbed-Chain Statistical Associating Fluid Theory Equation of State. **Industrial & Engineering Chemistry Research**, v. 41, n. 5, p. 1084–1093, 2002.

GROSS, Joachim; SADOWSKI, Gabriele. Perturbed-Chain SAFT: An Equation of State Based on a Perturbation Theory for Chain Molecules. **Industrial & Engineering Chemistry Research**, v. 40, n. 4, p. 1244–1260, 2001.

GUALANDI, Chiara; WHITE, Lisa J.; CHEN, Liu; *et al.* Scaffold for tissue engineering fabricated by non-isothermal supercritical carbon dioxide foaming of a highly crystalline polyester. **Acta Biomaterialia**, v. 6, n. 1, p. 130–136, 2010.

GUINDANI, Camila. **ENZYMATIC RING OPENING POLYMERIZATION OF POLY(GLOBALIDE-CO- ϵ -CAPROLACTONE) BY MEANS OF SUPERCRITICAL TECHNOLOGY AND POST FUNCTIONALIZATION BY THIOL-ENE REACTIONS**. Tese (Doutorado), Universidade Federal de Santa Catarina, Centro Tecnológico, Programa de Pós-Graduação em Engenharia Química, Florianópolis, 2018.

GUINDANI, Camila; CANDIOTTO, Graziâni; ARAÚJO, Pedro H.H.; *et al.* Controlling the biodegradation rates of poly(globalide-co- ϵ -caprolactone) copolymers by post polymerization modification. **Polymer Degradation and Stability**, v. 179, p. 109287, 2020.

GUINDANI, Camila; DOZORETZ, Pablo; ARAÚJO, Pedro H.H.; *et al.* N-acetylcysteine side-chain functionalization of poly(globalide-co- ϵ -caprolactone) through thiol-ene reaction. **Materials Science and Engineering: C**, v. 94, p. 477–483, 2019a.

GUINDANI, Camila; DOZORETZ, Pablo; VENERAL, Josamaique G.; *et al.* Enzymatic ring opening copolymerization of globalide and ϵ -caprolactone under supercritical conditions. **The Journal of Supercritical Fluids**, v. 128, p. 404–411, 2017.

GUINDANI, Camila; FREY, Marie-Luise; SIMON, Johanna; *et al.* Covalently Binding of Bovine Serum Albumin to Unsaturated Poly(Globalide-Co- ϵ -Caprolactone) Nanoparticles by Thiol-Ene Reactions. **Macromolecular Bioscience**, v. 19, n. 10, p. 1900145, 2019b.

GUINDANI, Camila; JARAMILLO, Wilfred A.G.; CANDIOTTO, Graziâni; *et al.* Synthesis of polyglobalide by enzymatic ring opening polymerization using pressurized fluids. **The Journal of Supercritical Fluids**, v. 186, p. 105588, 2022.

HEGE, Cordula S.; SCHILLER, Stefan M. Non-toxic catalysts for ring-opening polymerizations of biodegradable polymers at room temperature for biohybrid materials. **Green Chemistry**, v. 16, n. 3, p. 1410–1416, 2014.

KONTOGEORGIS, Georgios M.; FOLAS, Georgios K. **Thermodynamic Models for Industrial Applications**. Chichester, UK: John Wiley & Sons, Ltd, 2010.

KONTOGEORGIS, Georgios M.; LIANG, Xiaodong; ARYA, Alay; *et al.* Equations of state in three centuries. Are we closer to arriving to a single model for all applications? **Chemical Engineering Science: X**, v. 7, p. 100060, 2020.

KOURIST, Robert; HILTERHAUS, Lutz. Microbial Lactone Synthesis Based on Renewable Resources. *In*: KAMM, Birgit (Org.). **Microorganisms in Biorefineries**. Berlin, Heidelberg: Springer Berlin Heidelberg, 2015, v. 26, p. 275–301.

KUNDYS, Anna; BIAŁECKA-FLORJAŃCZYK, Ewa; FABISZEWSKA, Agata; *et al.* Candida antarctica Lipase B as Catalyst for Cyclic Esters Synthesis, Their Polymerization and Degradation of Aliphatic Polyesters. **Journal of Polymers and the Environment**, v. 26, n. 1, p. 396–407, 2018.

LARRAÑAGA, Michael D.; LEWIS, Richard J.; LEWIS, Robert A. **Hawley's Condensed Chemical Dictionary, Sixteenth Edition**. Hoboken, NJ, USA: John Wiley & Sons, Inc., 2016.

LEBEDEV, Boris; YEVSTROPOV, Alexei. [No title found]. **Die Makromolekulare Chemie**, v. 185, n. 6, p. 1235–1253, 1984.

LEITNER, Walter. Homogeneous catalysts for application in supercritical carbon dioxide as a 'green' solvent. **Comptes Rendus de l'Académie des Sciences - Series IIC - Chemistry**, v. 3, n. 7, p. 595–600, 2000.

LIN, Wen-Jen. Comparison of thermal characteristics and degradation properties of ϵ -caprolactone copolymers. **Journal of Biomedical Materials Research**, v. 47, n. 3, p. 420–423, 1999.

LINDER, E. G. Vapor Pressures of Some Hydrocarbons. **The Journal of Physical Chemistry**, v. 35, n. 2, p. 531–535, 1931.

MAŁAJOWICZ, Jolanta; NOWAK, Dorota; FABISZEWSKA, Agata; *et al.* Comparison of gamma-decalactone biosynthesis by yeast *Yarrowia lipolytica* MTLY40-2p and W29 in batch-cultures. **Biotechnology & Biotechnological Equipment**, v. 34, n. 1, p. 330–340, 2020.

MAYER, Diego A.; REBELATTO, Evertan A.; GIRARDI, Davi G.L.; *et al.* Effect of different polymer molar mass on the phase behavior of carbon dioxide + dichloromethane + ϵ -caprolactone + poly(ϵ -caprolactone) system. **Fluid Phase Equilibria**, v. 521, p. 112687, 2020.

MAYER, Diego Alex. **Phase equilibrium data and thermodynamic modeling of ϵ -caprolactone and poly(ϵ -caprolactone) systems at high pressures**. Tese (Doutorado), Universidade Federal de Santa Catarina, Centro Tecnológico, Programa de Pós-Graduação em Engenharia de Alimentos, Florianópolis, 2020.

MAYER, Diego Alex; REBELATTO, Evertan Antonio; NDIAYE, Papa Matar; *et al.* High Pressure Phase Equilibrium Data for the Ternary System Containing Carbon Dioxide, Dichloromethane, and ϵ -Caprolactone. **Journal of Chemical & Engineering Data**, v. 64, n. 5, p. 2036–2044, 2019.

MCGINTY, D.; LETIZIA, C.S.; API, A.M. Fragrance material review on ω -pentadecalactone. **Food and Chemical Toxicology**, v. 49, p. S193–S201, 2011.

MOHAMED, Rabiatul Manisah; YUSOH, Kamal. A Review on the Recent Research of Polycaprolactone (PCL). **Advanced Materials Research**, v. 1134, p. 249–255, 2015.

MORGAN, David L.; KOBAYASHI, Riki. Direct vapor pressure measurements of ten n-alkanes in the 10-C28 range. **Fluid Phase Equilibria**, v. 97, p. 211–242, 1994.

NASCIMENTO, Juliane C.; REBELATTO, Evertan A.; MAYER, Diego A.; *et al.* Phase behavior of carbon dioxide + chloroform + ω -pentadecalactone + poly(ω -pentadecalactone) system: Experimental data and PC-SAFT modeling. **Fluid Phase Equilibria**, v. 521, p. 112736, 2020.

NASCIMENTO, Juliane Costa. **Determinação experimental de dados de equilíbrio de fases da reação de polimerização da poli(ω - pentadecalactona) a altas pressões**. Dissertação (Mestrado), Universidade Federal de Santa Catarina, Centro Tecnológico, Programa de Pós- Graduação em Engenharia de Alimentos, Florianópolis, 2019.

NDIAYE, Papa M.; TAVARES, Frederico W.; DALMOLIN, Irede; *et al.* Vapor Pressure Data of Soybean Oil, Castor Oil, and Their Fatty Acid Ethyl Ester Derivatives. **Journal of Chemical & Engineering Data**, v. 50, n. 2, p. 330–333, 2005.

NIST. Carbon dioxide. c2021. Disponível em:

<<https://webbook.nist.gov/cgi/cbook.cgi?ID=C124389&Mask=4#Thermo-Phase>>.

Acesso em: 11 nov. 2022.

NOGUEIRA, Juliete Pedreira; SOUZA, Iago Hudson da Silva; ANDRADE, Julianna Karla Santana; *et al.* Status of research on lactones used as aroma: A bibliometric review. **Food Bioscience**, v. 50, p. 102004, 2022.

NUNES DA PONTE, Manuel. Phase equilibrium-controlled chemical reaction kinetics in high pressure carbon dioxide. **The Journal of Supercritical Fluids**, v. 47, n. 3, p. 344–350, 2009.

OEC - THE OBSERVATORY OF ECONOMIC COMPLEXITY. Lactones, other than coumarins. Trade, complexity, and rankings update to 2020. Disponível em: <<https://oec.world/en/profile/hs/lactones-other-than-coumarins>>. Acesso em: 11 nov. 2022.

OECD. SIDS Initial Assessment Report for SIAM 19. 2005. Disponível em: <<https://hpcvchemicals.oecd.org/UI/handler.axd?id=2ccdc186-93a9-47cd-b91d-26789738233d>>. Acesso em: 11 nov. 2022.

OLIVEIRA, Fernando Cabral Sales; AMARAL, Ronaldo Jose Farias Correa; SANTOS, Luiza Erthal Cardoso; *et al.* Versatility of unsaturated polyesters from electrospun macrolactones: RGD immobilization to increase cell attachment. **Journal of Biomedical Materials Research Part A**, v. 110, n. 2, p. 257–265, 2022.

PANTEN, Johannes; SURBURG, Horst; HÖLSCHER, Bernd. New Oxa-Bridged Macrocycles. **Chemistry & Biodiversity**, v. 5, n. 6, p. 1011–1022, 2008.

PENG, Ding-Yu; ROBINSON, Donald B. A New Two-Constant Equation of State. **Industrial & Engineering Chemistry Fundamentals**, v. 15, n. 1, p. 59–64, 1976.

PEPER, Stephanie; FONSECA, José M.S.; DOHRN, Ralf. High-pressure fluid-phase equilibria: Trends, recent developments, and systems investigated (2009–2012). **Fluid Phase Equilibria**, v. 484, p. 126–224, 2019.

PÉREZ DE DIEGO, Y.; WUBBOLTS, F.E.; WITKAMP, G.J.; *et al.* Measurements of the phase behaviour of the system dextran/DMSO/CO₂ at high pressures. **The Journal of Supercritical Fluids**, v. 35, n. 1, p. 1–9, 2005.

PETERS, Cor J.; FLORUSSE, Louw J. Experimental Determination of Vapor-Liquid Equilibria in Binary Mixtures of Carbon Dioxide + Chloroform. **Journal of Chemical & Engineering Data**, v. 40, n. 4, p. 948–949, 1995.

POLING, Bruce E.; PRAUSNITZ, John M.; O'CONNELL, John P. **The Properties of Gases and Liquids**. 5th. ed. [s.l.]: McGraw-Hill: New York, 2001.

POLLONI, André E.; CHIARADIA, Viviane; DO AMARAL, Ronaldo José F. C.; *et al.* Polyesters with main and side chain phosphoesters as structural motives for biocompatible electrospun fibres. **Polymer Chemistry**, v. 11, n. 12, p. 2157–2165, 2020.

POLLONI, André E.; REBELATTO, Evertan A.; VENERAL, Josamaique G.; *et al.* Enzymatic ring opening polymerization of ω -Pentadecalactone in different solvents in a variable-volume view reactor. **Journal of Polymer Science Part A: Polymer Chemistry**, v. 55, n. 7, p. 1219–1227, 2017.

POLLONI, André Eliezer. **Polimerização de ω -Pentadecalactona e Funcionalização para Conjugação com Poli(tioéter-fosfoéster)**. Tese (Doutorado), Universidade Federal de Santa Catarina, Centro Tecnológico, Programa de Pós-Graduação em Engenharia Química, Florianópolis, 2018.

POLLONI, André Eliezer; CHIARADIA, Viviane; FIGURA, Eduardo Moresco; *et al.* Polyesters from Macrolactones Using Commercial Lipase NS 88011 and Novozym 435 as Biocatalysts. **Applied Biochemistry and Biotechnology**, v. 184, n. 2, p. 659–672, 2018.

PRAUSNITZ, John M. ; KROLIKONSKI BUCK, Theresa; FREDENSLUND, Aage; *et al.* Current Trends in research and development. **Fluid Phase Equilibria**, v. 14, p. 403–408, 1983.

PRAUSNITZ, John M.; LICHTENTHALER, Rüdiger N.; AZEVEDO, Edmundo Comes de. **Molecular thermodynamics of fluid-phase equilibria** . 3rd. ed. Upper-Saddle River, New Jersey: Prentice Hall PTR, 1999.

REBELATTO, Evertan A.; GUINDANI, Camila; DE AZEVEDO, Evelin C.; *et al.* Determination of high-pressure phase equilibrium data of systems containing supercritical carbon dioxide and globalide. **The Journal of Supercritical Fluids**, v. 166, p. 104996, 2020.

REBELATTO, Evertan A.; POLLONI, André E.; ANDRADE, Kátia S.; *et al.* High-pressure phase equilibrium data for systems containing carbon dioxide, ω -pentadecalactone, chloroform and water. **The Journal of Chemical Thermodynamics**, v. 122, p. 125–132, 2018a.

REBELATTO, Evertan A.; POLLONI, André E.; ANDRADE, Kátia S.; *et al.* Phase behaviour of pseudoternary system (carbon dioxide + ω -pentadecalactone + dichloromethane) at different dichloromethane to ω -pentadecalactone mass ratios. **The Journal of Chemical Thermodynamics**, v. 126, p. 55–62, 2018b.

REBELATTO, Evertan Antonio. **Equilíbrio de Fases de Sistemas contendo Dióxido de Carbono, ω -pentadecalatona e cossolventes em Altas Pressões: Dados Experimentais e Modelagem Termodinâmica**. Tese (Doutorado), Universidade Federal de Santa Catarina, Centro Tecnológico, Programa de Pós- Graduação em Engenharia de Alimentos, Florianópolis, 2018.

REDDY, Yarram Narasimha; KUMARI, Tenkayala Navya; THOTA, Pradeepkumar; *et al.* Chemoenzymatic total synthesis of cryptocaryalactone natural products. **Tetrahedron Letters**, v. 59, n. 2, p. 160–162, 2018.

RODRIGUEZ-REARTES, S.B.; CISMONTI, M.; FRANCESCHI, E.; *et al.* High-pressure phase equilibria of systems carbon dioxide+n-eicosane and propane+n-eicosane. **The Journal of Supercritical Fluids**, v. 50, n. 3, p. 193–202, 2009.

SANDLER, Stanley I.; SANDLER, Stanley I. **Chemical, biochemical, and engineering thermodynamics**. 4th ed. Hoboken, N.J: John Wiley, 2006.

SARTORI, Suélen Karine; DIAZ, Marisa Alves Nogueira; DIAZ-MUÑOZ, Gaspar. Lactones: Classification, synthesis, biological activities, and industrial applications. **Tetrahedron**, v. 84, p. 132001, 2021.

SCOPUS. Scopus - Document search results. c2022. Disponível em: <https://id.elsevier.com/as/authorization.oauth2?platSite=SC%2Fscopus&ui_locales=en-US&scope=openid+profile+email+els_auth_info+els_analytics_info+urn%3Acom%3Aelsevier%3Aidp%3Apolicy%3Aproduct%3Aindv_identity&response_type=code&redirect_uri=https%3A%2F%2Fwww.scopus.com%2Fauthredirect.uri%3FtxGid%3D2352cec958ee1a3a239b3399>

4f25b39e&state=forceLogin%7Ct%3D5D23723B587367053F6BAEE23267FA25.i-0862be1c2907d127a%3A4&authType=SINGLE_SIGN_IN&prompt=login&client_id=SCOPUS&isValidNewDocSearchRedirection=true>. Acesso em: 12 nov. 2022.

SCURTO, Aaron M; LUBBERS, Christopher M; XU, Gang; *et al.* Experimental measurement and modeling of the vapor–liquid equilibrium of carbon dioxide + chloroform. **Fluid Phase Equilibria**, v. 190, n. 1–2, p. 135–147, 2001.

SEMANTHIC SCHOLAR. globalide | Semantic Scholar. c2021. Disponível em: <<https://www.semanticscholar.org/search?q=globalide&sort=relevance>>. Acesso em: 12 nov. 2022.

SHAAHMADI, Fariborz; SMITH, Sonja AM; SCHWARZ, Cara E; *et al.* Group-contribution SAFT equations of state: A review. **Fluid Phase Equilibria**, v. 565, p. 113674, 2023.

SILVA, Rui; COELHO, Eduardo; AGUIAR, Tatiana Q.; *et al.* Microbial Biosynthesis of Lactones: Gaps and Opportunities towards Sustainable Production. **Applied Sciences**, v. 11, n. 18, p. 8500, 2021.

SINHA, V.R.; BANSAL, K.; KAUSHIK, R.; *et al.* Poly- ϵ -caprolactone microspheres and nanospheres: an overview. **International Journal of Pharmaceutics**, v. 278, n. 1, p. 1–23, 2004.

SMITH, J. M.; VAN NESS, H. C.; ABBOTT, Michael M.; *et al.* **Introduction to chemical engineering thermodynamics**. Eighth edition. New York, NY: McGraw-Hill Education, 2018.

STIEVANO, Matteo; ELVASSORE, Nicola. High-pressure density and vapor–liquid equilibrium for the binary systems carbon dioxide–ethanol, carbon dioxide–acetone and carbon dioxide–dichloromethane. **The Journal of Supercritical Fluids**, v. 33, n. 1, p. 7–14, 2005.

SZELWICKA, Anna; KOLANOWSKA, Anna; LATOS, Piotr; *et al.* Carbon nanotube/PTFE as a hybrid platform for lipase B from *Candida antarctica* in transformation of α -angelica lactone into alkyl levulinates. **Catalysis Science & Technology**, v. 10, n. 10, p. 3255–3264, 2020.

TAKAMURA, Hiroyoshi. Recent topics of the stereodivergent synthesis of natural products. **Tetrahedron Letters**, v. 59, n. 11, p. 955–966, 2018.

TGSC - THE GOOD SCENTS COMPANY. ω -pentadecalactone, 106-02-5. c2021a. Disponível em: <<http://www.thegoodscentscopy.com/data/rw1004211.html>>. Acesso em: 12 nov. 2022.

TGSC - THE GOOD SCENTS COMPANY. musk decenone, 34902-57-3. c2021b. Disponível em: <<http://www.thegoodscentscopy.com/data/rw1016021.html>>. Acesso em: 12 nov. 2022.

TGSC - THE GOOD SCENTS COMPANY. epsilon-caprolactone, 502-44-3. c2021c. Disponível em: <<http://www.thegoodscentscopy.com/data/rw1242691.html>>. Acesso em: 12 nov. 2022.

THAKUR, Mamta; MAJID, Ishrat; HUSSAIN, Shafat; *et al.* Poly(ϵ -caprolactone): A potential polymer for biodegradable food packaging applications. **Packaging Technology and Science**, v. 34, n. 8, p. 449–461, 2021.

TINAJERO-DÍAZ, Ernesto; MARTÍNEZ DE ILARDUYA, Antxon; MUÑOZ-GUERRA, Sebastián. Block and Graft Copolymers Made of 16-Membered Macrolactones and L-Alanine: A Comparative Study. **Macromolecular Chemistry and Physics**, v. 220, n. 17, p. 1900214, 2019.

TINAJERO-DÍAZ, Ernesto; MARTÍNEZ DE ILARDUYA, Antxon; MUÑOZ-GUERRA, Sebastián. Copolymacrolactones Grafted with L-Glutamic Acid: Synthesis, Structure, and Nanocarrier Properties. **Polymers**, v. 12, n. 4, p. 995, 2020.

TSIVINTZELIS, I.; MISSOPOLINO, D.; KALOGIANNIS, K.; *et al.* Phase compositions and saturated densities for the binary systems of carbon dioxide with ethanol and dichloromethane. **Fluid Phase Equilibria**, v. 224, n. 1, p. 89–96, 2004.

TSUTSUMI, Chikara; MANABE, Souta; NAKAYAMA, Susumu; *et al.* Impregnation of poly(L-lactide-ran- δ -valerolactone) with essential bark oil using supercritical carbon dioxide. **Scientific Reports**, v. 9, n. 1, p. 16326, 2019.

TU, L.Sze; DEGHANI, F; FOSTER, N.R. Micronisation and microencapsulation of pharmaceuticals using a carbon dioxide antisolvent. **Powder Technology**, v. 126, n. 2, p. 134–149, 2002.

VAN DER MEULEN, Inge; DE GEUS, Matthijs; ANTHEUNIS, Harro; *et al.* Polymers from Functional Macrolactones as Potential Biomaterials: Enzymatic Ring Opening Polymerization, Biodegradation, and Biocompatibility. **Biomacromolecules**, v. 9, n. 12, p. 3404–3410, 2008.

WILBERTH, Herrera-Kao; MANUEL, Cervantes-Uc J.; TANIA, Lara-Ceniceros; *et al.* Effect of reaction temperature on the physicochemical properties of poly(pentadecanolide) obtained by enzyme-catalyzed ring-opening polymerization. **Polymer Bulletin**, v. 72, n. 3, p. 441–452, 2015.

WILLINGHAM, C.B.; TAYLOR, W.J.; PIGNOCCO, J.M.; *et al.* Vapor pressures and boiling points of some paraffin, alkylcyclopentane, alkylcyclohexane, and alkylbenzene hydrocarbons. **Journal of Research of the National Bureau of Standards**, v. 35, n. 3, p. 219, 1945.

WILSON, James A.; ATES, Zeliha; PFLUGHAUPT, Robin L.; *et al.* Polymers from macrolactones: From pheromones to functional materials. **Progress in Polymer Science**, v. 91, p. 29–50, 2019.

WIN-SHWE, Tin-Tin; FUJIMAKI, Hidekazu. Neurotoxicity of toluene. **Toxicology Letters**, v. 198, n. 2, p. 93–99, 2010.

WOODRUFF, Maria Ann; HUTMACHER, Dietmar Werner. The return of a forgotten polymer—Polycaprolactone in the 21st century. **Progress in Polymer Science**, v. 35, n. 10, p. 1217–1256, 2010.

XU, Qun; WAGNER, Klaus-D.; DAHMEN, Nicolaus. Vapor–liquid equilibria of different lactones in supercritical carbon dioxide. **The Journal of Supercritical Fluids**, v. 26, n. 2, p. 83–93, 2003.

ZHANG, Lianzhong; GUO, Yuanyue; DENG, Dongshun; *et al.* Experimental Measurement and Modeling of Ternary Vapor–Liquid Equilibrium for Water + 1-Propanol + 1-Butyl-3-methylimidazolium Chloride. **Journal of Chemical & Engineering Data**, v. 58, n. 1, p. 43–47, 2013.